THE ROLE OF THE N-TERMINUS OF THE $Ca_V2.2$ VOLTAGE-DEPENDENT CALCIUM CHANNEL IN THE INHIBITION BY G-PROTEINS

LOLA WHEAT

A THESIS SUBMITTED IN FULFILLMENT OF THE
REQUIREMENTS FOR THE DEGREE OF
DOCTOR OF PHILOSOPHY
AT THE UNIVERSITY OF LONDON

DEPARTMENT OF PHARMACOLOGY
UNIVERSITY COLLEGE LONDON
LONDON, UK

SEPTEMBER 2006

ProQuest LLC
789 East Eisenhower Parkway
P.O. Box 1346
Ann Arbor, MI 48106-1346

Abstract

The neuronal $Ca_V2.2$ calcium channel is inhibited by $G\beta\gamma$ subunits of heterotrimeric G-proteins in a voltage-dependent manner. It has been shown previously that an 11 amino acid motif (44-55) in the intracellular N-terminus of $Ca_V2.2\alpha1$ (α_1B) is essential for G-protein modulation of currents. Mutation of 2 amino acids, R52 and R54, in this region completely abolishes G-protein inhibition. They may form part of the $G\beta\gamma$ binding site, or translate binding into a functional response.

To investigate the role of the N-terminus of the $Ca_V2.2\alpha_1$ subunit I have expressed functional channels in *Xenopus* oocytes and recorded currents using the two-electrode voltage-clamp technique. To examine further the role of the N-terminus I have tethered it to the membrane via an N-terminal palmitoylation motif and I have also used an isolated N-terminus. The palmitoylation motif $Ca_V2.2\alpha_1$ showed reduced modulation by $G\beta\gamma$ (lower facilitation ratio and reduced GPCR activated inhibition). Other additions on the N-terminus such as GFP or a HA-tag, also reduced modulation. However, only the palmitoylation motif $Ca_V2.2\alpha_1$ showed an increase in the rate of loss of G-protein modulation during depolarisation (faster facilitation rate). This increase in facilitation rate is unique to the palmitoylation motif $Ca_V2.2\alpha_1$. The increased facilitation rate may be due to a reduction in the affinity of the channel for $G\beta\gamma$ because of the reduced mobility of the N-terminus.

Contents

Title 1

Abstract 2

Contents 4

List of Figures and Tables 13

List of Abbreviations 18

Chapter 1 Introduction 23

1.1 Classical Biophysics 23

1.1.1 The Nernst Equation 23

1.1.2 The Ionic Theory 24

1.1.3 The Sodium Hypothesis 25

1.1.4 Ion Channels 26

1.2 The History of Calcium Channel Discovery 28

1.2.1 There Are Different Types of Calcium Current 28

1.2.2 L-Type, T-type and N-type Calcium Currents 30

1.2.3 P/Q-Type Calcium Currents 31

1.3 The Molecular Structure of Voltage-Dependent Calcium Channels 33

1.3.1 Protein Subunits 33

1.3.2 The α_1-Subunits 36

1.3.4 Activation and Gating 37

1.3.5 Inactivation 37

1.3.6 Voltage-Dependent Inactivation 38

1.3.7 Calcium-Dependent Inactivation 40

1.3.8 Ca_V2 Family Channels and Ca^{2+}/Calmodulin 40

1.3.9 Splice Variants of $Ca_V2.2$ 41

1.3.10 Functional Effects of the Auxiliary Subunits 42

1.3.11 β-Subunits 43

1.3.12 β-Subunit Functional Effects 44

1.3.13 The β-Subunits and Biophysical Properties of the Channel 46

1.3.14 Functional Effects of the α_2-δ-Subunit 50

1.3.15 Functional Effects of the γ-Subunits 50

1.4 Physiological Function of Voltage-Gated Calcium Channels 51

1.4.1 Regenerative Electrical Excitability 51

1.4.2 Intracellular Calcium Ion Concentration 52

1.4.3 Excitation-Contraction Coupling 53

1.4.4 Excitation-secretion coupling 54

1.4.5 Synaptic Proteins 55

1.4.6 Phosphorylation of Calcium Channels 57

1.4.7 $PI(4,5)P_2$ Modulates Voltage-Dependent Calcium Channels 58

1.4.7 G-Proteins Modulate Voltage-Dependent Calcium Channels 58

1.5 Heterotrimetric G-Proteins 58

1.5.1 GPCRs are Cell Surface Receptors 59

1.5.2 GPCRs Provide an Activation Pathway for Heterotrimeric G-Proteins 60

1.5.3 Gα Effectors 61

1.5.4 Gβγ Effectors 62

1.6 G-Protein Modulation of Voltage-Gated Calcium Channels 63

1.6.1 G-Protein Activation Reduces Calcium Currents 63

1.6.2 G-Protein Modulation is Voltage-Dependent and Membrane-Delimited 65

1.6.3 Modulation is via a $G\alpha_{i/o}$ Pathway 67

1.6.4 Gβγ Mediates the Modulation, Not Gα 68

1.6.5 Which Gβγ-Subtypes? 69

1.7 Molecular Mechanisms of G-Protein Modulation 72

1.7.1 Gβγ Interacts Directly with the Channel 72

1.7.2 Facilitation and Reinhibition 74

1.7.3 The Site of Interaction 75

1.7.4 The I-II Loop 76

1.7.5 Calcium Channel β-Subunits and Gβγ Modulation 78

1.7.6 The C-Terminus 80

1.7.7 The N-Terminus 82

1.7.8 Crosstalk 83

1.7.9 PKC and Gβγ Crosstalk 83

1.7.9 Syntaxin and Gβγ Crosstalk 84

Chapter 2 Methods 86

2.1 Molecular biology methods 86

2.2 The *Xenopus* Oocyte Expression System 89

2.2.1 Oocyte Collection 90

2.2.2 cDNA Injection 90

2.2.3 BAPTA Injection 92

2.3 Electrophysiology Methods 92

2.3.1 The Voltage-Clamp Technique 92

2.3.2 Electrophysiological Recording Equipment 95

2.3.3 Perfusion System 96

2.3.4 Recording of Currents through Voltage-Dependent Calcium Channels in *Xenopus* Oocytes 97

2.3.5 Leak Subtraction P/4 protocol 98

2.3.6 Filtering and Sampling 98

2.4 Analysis of currents 98

Chapter 3 Results 1 100

3.1 The Current-Voltage Relationship 100

3.2 Over-expressing $G\beta_1\gamma_2$ 102

3.2.1 $Ca_V2.2$(R52,54A) does not display pre-pulse facilitation when $G\beta_1\gamma_2$ is over-expressed 104

3.2.2 Isolated N-terminus 106

3.2.3 Co-expressing the isolated N-terminus has no effect on pre-pulse facilitation when $G\beta_1\gamma_2$ is over-expressed 106

3.2.4 Co-expressing the isolated N-terminus in a higher ratio had no effect on pre-pulse facilitation when $G\beta_1\gamma_2$ was over-expressed 108

3.2.5 Palmitoylation motif $Ca_V2.2$(R52,54A) did not display pre-pulse facilitation when $G\beta_1\gamma_2$ over-expressed 109

3.2.6 Palmitoylation motif $Ca_V2.2$(R52,54A) did not display pre-pulse facilitation when $G\beta_1\gamma_2$ was over-expressed 110

3.2.7 Palmitoylation motif $Ca_V2.2$ showed reduced pre-pulse facilitation ratio when $G\beta_1\gamma_2$ over-expressed 111

3.2.8 The mutated palmitoylation motif $Ca_V2.2$ showed reduced pre-pulse facilitation ratio when $G\beta_1\gamma_2$ over-expressed 113

3.2.9 Haemagglutinin tagged $Ca_V2.2$ had reduced pre-pulse facilitation when $G\beta_1\gamma_2$ was over-expressed 114

3.2.10 GFP tagged $Ca_V2.2$ had reduced pre-pulse facilitation when $G\beta_1\gamma_2$ was over-expressed 115

3.2.11 Co-expressing the isolated N-terminus with palmitoylation motif $Ca_V2.2$ or mutated palmitoylation motif $Ca_V2.2$ had no effect on pre-pulse facilitation when $G\beta_1\gamma_2$ was over-expressed 116

3.3 Clonidine mediated inhibition 119

3.4 Pre-pulse facilitation in the presence of clonidine 122

3.4.1 Pre-pulse causes facilitation when α_2A-Gαo is over-expressed and clonidine is applied 122

3.5 Clonidine mediated inhibition is reversible and repeatable 124

3.6 Clonidine Mediated Modulation 125

3.6.1 Palmitoylation motif Ca_V2.2 has reduced clonidine mediated inhibition when α_2A-Gαo is over-expressed 125

3.6.2 Palmitoylation motif Ca_V2.2 has reduced pre-pulse facilitation when α_2A-Gαo is over-expressed and clonidine is applied 126

3.6.3 Mutated palmitoylation motif Ca_V2.2 has reduced clonidine mediated inhibition when α_2A-Gαo is over-expressed 127

3.6.4 Mutated palmitoylation motif Ca_V2.2 has reduced pre-pulse facilitation when α_2A-Gαo is over-expressed and clonidine is applied 128

3.6.5 HA tagged Ca_V2.2 has reduced clonidine mediated inhibition when α_2A-Gαo is over-expressed 129

3.6.6 HA tagged Ca_V2.2 has reduced pre-pulse facilitation when α_2A-Gαo is over-expressed and clonidine is applied 131

3.6.7 Over-expressing an isolated N-terminus had no effect on clonidine mediated inhibition of wild type $Ca_V2.2$ when α_2A-Gαo is over-expressed 132

3.6.8 Over-expressing an isolated N-terminus had no effect on pre-pulse facilitation of wild type $Ca_V2.2$ when α_2A-Gαo is over-expressed and clonidine is applied 133

Chapter 4. Results 2 135

4.1 Facilitation Rate 135

4.1.1 Palmitoylation motif $Ca_V2.2$ had a higher rate of facilitation than wild type $Ca_V2.2$ when α_2A-Gαo over-expressed and clonidine applied 137

4.1.2 Mutated palmitoylation motif $Ca_V2.2$ had a similar rate of facilitation to wild type $Ca_V2.2$ when α_2A-Gαo was over-expressed and clonidine applied 138

4.2 Facilitation rate when $G\beta_1\gamma_2$ was over-expressed 139

4.2.1 Palmitoylation motif $Ca_V2.2$ had a faster rate of facilitation than wild type $Ca_V2.2$ when $G\beta_1\gamma_2$ was over-expressed 139

4.2.2 Including cDNA coding for the isolated N-terminus in the injection mixture had no effect on facilitation rate of $Ca_V2.2$ when $G\beta_1\gamma_2$ was over-expressed 140

4.2.3 Including cDNA coding for the isolated N-terminus in the injection mixture had no effect on facilitation rate of palmitoylation motif $Ca_V2.2$ when $G\beta_1\gamma_2$ was over-expressed ...141

4.2.4 Including cDNA coding for the isolated N-terminus in the injection mixture had no effect on facilitation rate of mutated palmitoylation motif $Ca_V2.2$ when $G\beta_1\gamma_2$ was over-expressed 142

4.3 Re-inhibition Rate 144

4.3.1 Palmitoylation motif $Ca_V2.2$ had the same rate of re-inhibition as wild type $Ca_V2.2$ when $G\beta_1\gamma_2$ was over-expressed 145

4.3.2 Palmitoylation motif $Ca_V2.2$ and mutated palmitoylation motif $Ca_V2.2$ had the same rate of re-inhibition as wild type $Ca_V2.2$ when α_2A-Gαo was over-expressed and clonidine applied 146

4.4 Voltage-Dependence of Facilitation 148

4.4.1 There was no difference in the voltage-dependence of facilitation for wild type $Ca_V2.2$, palmitoylation motif $Ca_V2.2$ and mutated palmitoylation motif $Ca_V2.2$ when α_2A-Gαo was over-expressed and clonidine applied 149

Chapter 5. Results 3. Activation and Inactivation 150

5.1 Activation 150

5.1.1 Voltage-dependence of activation 150

5.1.2 Voltage dependence of activation was the same for wild type $Ca_V2.2$ and palmitoylation motif $Ca_V2.2$ when α_2A-$G\alpha o$ was over-expressed 151

5.1.3 Over-expression of $G\beta\gamma$ 153

5.1.4 Kinetics of activation 154

5.2 Inactivation 156

5.2.1 Voltage-dependence of inactivation 156

5.2.2 Kinetics of inactivation 158

Chapter 6. Results 4. Inhibiting Palmitoylation 160

6.1 Inhibiting Palmitoylation Methods 161

6.2 Inhibiting Palmitoylation Results 161

6.2.1 2BP did not affect $Ca_V2.2$ current-voltage relationships when $G\beta_1\gamma_2$ was over-expressed 162

6.2.2 Injection of 2BP did not affect palmitoylation motif $Ca_V2.2$ current-voltage relationships when $G\beta_1\gamma_2$ was over-expressed ..163

6.2.3 Injection of 2BP increased the facilitation ratio of $Ca_V2.2$ and palmitoylation motif $Ca_V2.2$ when $G\beta_1\gamma_2$ was over-expressed....164

6.2.4 Injection of 2BP had no effect on the facilitation rates of either $Ca_V2.2$ currents or palmitoylation motif $Ca_V2.2$ currents 165

Chapter 7. Discussion 166

References.....180

Appendix.....215

List of Figures and Tables

Table 1.1 Types of voltage-gated calcium conductances 33

Figure 1.1 Subunits of voltage-gated calcium channels 35

Figure 1.2 Voltage-dependent calcium channel subunits are classified into 3 families 36

Figure 1.3 Low intracellular calcium ion concentration is maintained 53

Figure 1.4 Voltage-gated calcium channel and the vesicle release machinery 56

Figure 1.5 G-protein coupled receptors act via heterotrimeric G-proteins 60

Figure 1.6 Gα activates intracellular signalling cascades 62

Figure 1.7 Several sites on the Ca_V2 family α_1-subunits are implicated in Gβγ interaction with the channel 83

Figure 1.8 Crosstalk affects Gβγ modulation of the channel 85

Figure 2.1 The Xenopus oocytes expression system 89

Figure 2.2 The Oocyte Injection Apparatus 91

Figure 2.3 The membrane can be viewed as a simple electrical circuit 93

Figure 2.4 The two-electrode voltage-clamp circuit 94

Figure 2.5 The recording chamber and simplified voltage-clamp circuit 96

Figure 2.6 Mean currents were measured between 10 and 15 ms into test pulse 99

Figure 3.1 current-voltage relationship of $Ca_V2.2/\beta_1b/\alpha_2\delta$-2 101

Figure 3.2 When $G\beta_1\gamma_2$ is over-expressed a depolarising pre-pulse effects facilitation.....103

Figure 3.3 $Ca_V2.2$(R52,54A) does not display pre-pulse facilitation when Gβγ over-expressed 105

Figure 3.4 Co-expressing the isolated n-terminus has no effect on pre-pulse facilitation when Gβγ over-expressed 107

Figure 3.5 Co-expressing a higher ratio of the isolated N-terminus had no effect on pre-pulse facilitation when Gβγ over-expressed 108

Figure 3.6 Palmitoylation motif $Ca_V2.2$(R52,54A) did not display pre-pulse facilitation when Gβγ over-expressed 110

Figure 3.7 Palmitoylation motif $Ca_V2.2$ displays reduced pre-pulse facilitation when Gβγ over-expressed 112

Figure 3.8 Mutated palmitoylation motif $Ca_V2.2$displays reduced pre-pulse facilitation when Gβγ over-expressed 113

Figure 3.9 HA $Ca_V2.2$ displays reduced pre-pulse facilitation when Gβγ over-expressed 115

Figure 3.10 GFP $Ca_V2.2$ displays reduced pre-pulse facilitation when Gβγ over-expressed 116

Figure 3.11 Co-expressing the isolated N-terminus had no effect on pre-pulse facilitation of palmitoylation motif $Ca_V2.2$ when Gβγ over-expressed 118

Figure 3.12 Co-expressing the isolated N-terminus had no effect on pre-pulse facilitation of mutated palmitoylation motif $Ca_V2.2$ when Gβγ over-expressed 118

Figure 3.13 Application of clonidine in the perfusate mediates channel inhibition 121

Figure 3.14 When α_2A-Gαo is over-expressed and in the presence of clonidine, pre-pulse facilitation is displayed by $Ca_V2.2$ channels 123

Figure 3.15 Repeated applications of clonidine when α_2A-Gαo is over-expressed show that the effect is reversible and repeatable 125

Figure 3.16 Clonidine mediates inhibition of palmitoylation motif $Ca_V2.2$ when α_2A-Gαo is over-expressed 126

Figure 3.17 Pre-pulse facilitation of palmitoylation motif $Ca_V2.2$ is displayed when α_2A-Gαo is over-expressed and clonidine applied 127

Figure 3.18 Clonidine mediates inhibition of mutated palmitoylation motif $Ca_V2.2$ when α_2A-Gαo is over-expressed 128

Figure 3.19 Pre-pulse facilitation of mutated palmitoylation motif $Ca_V2.2$ is displayed when α_2A-Gαo is over-expressed 129

Figure 3.20 Clonidine mediates inhibition of HA $Ca_V2.2$ when α_2A-Gαo is over-expressed 130

Figure 3.21 Pre-pulse facilitation of HA $Ca_V2.2$ is displayed when α_2A-Gαo is over-expressed and clonidine applied 131

Figure 3.22 Clonidine mediates inhibition of $Ca_V2.2$ with the isolated N-terminus co-expressed when α_2A-Gαo is over-expressed 133

Figure 3.23 Pre-pulse facilitation of $Ca_V2.2$ with the isolated N-terminus co-expressed is displayed when α_2A-Gαo is over-expressed and clonidine applied ...134

Figure 4.1 Facilitation rate of $Ca_V2.2$ when α_2A-Gαo over-expressed and clonidine applied 135

Figure 4.2 Facilitation rate of $Ca_V2.2$ when α_2A-Gαo over-expressed and clonidine applied 136

Figure 4.3 Facilitation rate of palmitoylation motif $Ca_V2.2$ when α_2A-Gαo over-expressed and clonidine applied 137

Figure 4.4 Palmitoylation motif $Ca_V2.2$ had a faster rate of facilitation than wild type $Ca_V2.2$ and mutated palmitoylation motif $Ca_V2.2$ when α_2A-Gαo over-expressed and clonidine applied 137

Figure 4.5 Palmitoylation motif $Ca_V2.2$ had a faster rate of facilitation than wild type $Ca_V2.2$ and mutated palmitoylation motif $Ca_V2.2$ when G$\beta\gamma$ over-expressed 140

Figure 4.6 Over-expression of an isolated N-terminus had no effect on facilitation rate of wild type $Ca_V2.2$ when G$\beta\gamma$ over-expressed 141

Figure 4.7 Over-expression of an isolated N-terminus had no effect on facilitation rate of palmitoylation motif $Ca_V2.2$ when G$\beta\gamma$ over-expressed 142

Figure 4.8 Over-expression of an isolated N-terminus had no effect on facilitation rate of mutated palmitoylation motif $Ca_V2.2$ when G$\beta\gamma$ over-expressed 142

Figure 4.9 Re-inhibition rate of $Ca_V2.2$ when α_2A-Gαo over-expressed and clonidine applied 144

Figure 4.10 Re-inhibition rate of $Ca_V2.2$ when G$\beta\gamma$ over-expressed 145

Figure 4.11 There was no difference in re-inhibition rates of $Ca_V2.2$ and palmitoylation motif $Ca_V2.2$ when G$\beta\gamma$ over-expressed 146

Figure 4.12 Re-inhibition rate of $Ca_V2.2$, palmitoylation motif $Ca_V2.2$ and mutated palmitoylation motif $Ca_V2.2$ when α_2A-Gαo over-expressed and in the presence of clonidine 147

Figure 4.13 Voltage-dependence of facilitation 148

Figure 4.14 Voltage-dependence of facilitation of $Ca_V2.2$ when α_2A-Gαo over-expressed and clonidine applied 149

Figure 4.15 Voltage-dependence of facilitation of $Ca_V2.2$, palmitoylation motif $Ca_V2.2$ and mutated palmitoylation motif $Ca_V2.2$ when α_2A-Gαo and clonidine applied 150

Figure 5.1 There was no difference in activation phase of the IV of $Ca_V2.2$ and palmitoylation motif $Ca_V2.2$ when α_2A-Gαo over-expressed 152

Figure 5.2 There was no difference in activation phase of the IV of $Ca_V2.2$ and mutated palmitoylation motif $Ca_V2.2$ when α_2A-Gαo over-expressed 153

Figure 5.3 The activation phases of the IVs of palmitoylation motif $Ca_V2.2$ and mutated palmitoylation motif $Ca_V2.2$ are depolarised compared to wild type $Ca_V2.2$ when G$\beta\gamma$ over-expressed 154

Figure 5.4 There was no difference in the activation kinetics of $Ca_V2.2$, palmitoylation motif $Ca_V2.2$ and mutated palmitoylation motif $Ca_V2.2$ in absence of G$\beta\gamma$ modulation 155

Figure 5.5 There was no difference in the activation kinetics of $Ca_V2.2$, palmitoylation motif $Ca_V2.2$ and mutated palmitoylation motif $Ca_V2.2$ when G$\beta\gamma$ over-expressed 156

Figure 5.6 Steady-state inactivation of $Ca_V2.2$ and palmitoylation motif $Ca_V2.2$ ...157

Figure 5.7 Kinetics of inactivation of $Ca_V2.2$, palmitoylation motif $Ca_V2.2$ and mutated palmitoylation motif $Ca_V2.2$ 159

Figure 5.8 Maximum whole cell currents 160

Figure 6.1 2BP had no effect on the current-voltage relationship of $Ca_V2.2$ when $G\beta\gamma$ over-expressed 162

Figure 6.2 2BP had no effect on the current-voltage relationship of palmitoylation motif $Ca_V2.2$ when $G\beta\gamma$ 163

Figure 6.3 Facilitation ratio of $Ca_V2.2$ and palmitoylation motif $Ca_V2.2$ increased after 2BP injection 164

Figure 6.4 Injection of 2BP did not affect facilitation rate of $Ca_V2.2$ or palmitoylation motif $Ca_V2.2$ 165

Figure 7.1 Proposed model of $G\beta\gamma$ interaction with the N-terminal tail and the I-II loop of the $Ca_V2.2$ channel 178

List of Abbreviations

2BP	2-bromohexadecanoic palmitate
5-HT	5-hydroxytriptamine
α_2A	α_2A type adrenoceptor
$\alpha_2\delta$-1/2	$\alpha_2\delta$ subunit, type 1 or 2
AC	adenylate cyclase
AID	alpha interaction domain
ATP	adenosine triphosphate
β_{1-4}	beta subunit, type 1-4

Ba^{2+}	barium ions
BAPTA	K3-1,2-bis(aminophenoxy)ethane-N,N,N',N'-tetra-acetic acid
βARK	β-adrenoceptor kinase
C	capacitance
Ca^{2+}	calcium ions
CaMKII	calmoduline dependent kinase type II
cAMP	cyclic adenosine monophosphate
$Ca_V\alpha_1$	calcium channel alpha 1 subunit
cDNA	complementary DNA
CGβγ	Gβγ bound calcium channel
cGMP	cyclic guanine monophosphate
D_2 receptor	dopamine receptor type 2
DAG	diacycl glycerol
dB	decibels
DHP	dihydropyridine
DMSO	dimethyl sulphonic acid
DNA	deoxyribonucleic acid
DRG	dorsal root ganglion
EDTA	ethylene-diamine-tetra-acetic acid
EPSC	excitatory post-synaptic current
ER	endoplasmic reticulum
FRET	fluorescence resonance energy transfer
G	conductance

Gα	alpha subunit of hetreotrimeric G-protein
GABA	gamma aminobutyric acid
$GABA_B$	GABA receptor type B
Gβγ	G-protein βγ-subunit dimer
GDP	guanine diphosphate
GFP	green fluorescent protein
GIRK	G-protein activated potassium channel
G-protein	GTP-binding protein
GPCR	G-protein coupled receptor
GST	glutathione S-transferase
GTP	guanine triphosphate
HA	haemagglutinin
HEPES	N-[2-hydroxyethyl]piperazine-N'[2-ethanesulphonic acid]
HVA	high voltage activated
Hz	Hertz
I-II loop	cytoplasmic loop connecting domains I and II of CaVa1
IP_3	inositol triphosphate
IV	current/voltage relationship
K^+	potassium ions
k_1	association rate constant
k_{-1}	dissociation rate constant
kDa	kilodalton
k_{off}	dissociation rate constant

LVA	low voltage activated
M_2R	muscarinic receptor type 2
MAPK	mitogen-activated protein kinase
mGluR	metabotropic glutamate receptor
mRNA	messenger RNA
ms	miliseconds
mV	milivolts
Na^{2+}	sodium ions
NSF	N-ethylmaleimide sensitive fusion protein
NPY	neuropeptide Y
P1	test pulse 1
P2	test pulse 2
PCR	polymerase chain reaction
PI(4,5)P2	phosphoinositol diphosphate
PI3-K	phosphoinositol 3 kinase
PIP2	phosphoinositol diphosphate
PKA	protein kinase A
PKC	protein kinase B
PLCb2	phospolipase C type β2
P-loop	pore lining loop of $Ca_V\alpha_1$
PTX	pertussis toxin
RNA	ribonucleic acid
S1-S6	transmembrane segments 1-6

SCG	superior cevical ganglion
SEM	standard error of the mean
SH3	src homology domain
SNAP-25	synaptosomal-associated protein of 25kDa
SNARE	soluble NSF attachment receptor
SR	sarcoplasmic reticulum
synprint	synaptic protein interaction
t	time
TE	Tris EDTA buffer
TTX	tetrodotoxin
V_{50}	potential at which 50% maximum current is activated
VAMP	vesicle associated membrane protein

Chapter 1 Introduction

1.1 Classical Biophysics

1.1.1 The Nernst Equation

In 1888 a German chemist, Walther Nernst, developed a theory that could be applied to explain the origin of bioelectric potentials (Nernst, 1888). He noticed that electrical potentials could arise from diffusion of electrolytes in solution. This led him to describe how the equilibrium potential for a particular ion, that is the potential at which the electrochemical gradient for the ion in the solution is 1, is the electromotive force that drives the movement of ions in the solution. For example, applied to biological membranes, if a membrane is at the equilibrium potential for sodium ions, there will be no net flux of sodium ions across the membrane. This form of the Nernst Equation is found below (Equation 1.1).

$$E_{Na} = RT/Z_{Na}F * \ln([Na]_{out}/[Na]_{in}) \qquad \text{Equation 1.1}$$

Where E_{Na} is the equilibrium potential for Na^+ ions, R is the gas constant, T is the absolute temperature, Z_{Na} is the charge on a Na^+ ion, F is the Faraday constant, $[Na]_{out}$ is the extracellular concentration of Na^+ ions and $[Na]_{in}$ is the intracellular concentration of Na^+ ions.

1.1.2 The Ionic Theory

Some years later, Julius Bernstein (Bernstein, 1902; Bernstein, 1912) developed the "membrane hypothesis" of electrical excitability. He noticed that membranes of excitable cells were selectively permeable to K^+ ions and that an electrical potential was set up by K^+ ions diffusing down their concentration gradient from inside the cell to the extracellular medium. He suggested that during an action potential, membrane integrity is lost and cations other than K^+ are able to diffuse into the cell, driven by the potential set up by the diffusion of K^+ during rest, and this causes a loss of the cells internal negative potential. This became known as the ionic theory of membrane excitation.

Hermann (Hermann, 1899; Hermann, 1905a; Hermann, 1905b) suggested that the membrane formed part of an electrical circuit, with currents passing through excited regions of the membrane during action potentials. He also suggested that the self propagation was electrical self-stimulation. By this was meant that small currents that are generated, are due to potential differences between excited and unexcited parts of the membrane.

Empirical evidence for the ionic theory started to be acquired by Cole, who measured the electrical impedance of cell suspensions and single cells, to measure membrane properties. The results of these studies are described in his book (Cole, 1968). These observations found that cells had a cytoplasm of high electrical conductivity, surrounded by a membrane of low conductivity and high electrical capacitance.

Hodgkin demonstrated further evidence for Hermann's theory that electrical self-stimulation was the basis of action potential propagation. He blocked a nerve locally with cold and observed that the action potential depolarised the nerve for a short stretch beyond the block (Hodgkin, 1937a;Hodgkin, 1937b). From this he concluded that the electrically propagated spread of action potentials was due to the passive spread of depolarisation of the membrane.

1.1.3 The Sodium Hypothesis

The total membrane "breakdown", suggested by Bernstein, was clearly not quite accurate. Electrical impedance measurements of the squid giant axon revealed that during an action potential, the membrane conductance was still only a fraction of that of the cytoplasm (Cole and Curtis, 1939). This was explained by the assumption that only a very small area of membrane underwent "breakdown" during an action potential.

However, more questions about the theory were raised when measurements of full action potentials were taken from the squid giant axon using micropipettes. The membrane potential did not drop to 0mV, as expected, but overshot to around +40mV (Hodgkin and Huxley, 1945).

The basis of the overshoot became the sodium hypothesis: the explanation was found by replacing sodium ions in the recording solution with choline ions and showing a reduction in the overshoot of the membrane potential. The new hypothesis

was that during an action potential, the membrane becomes selectively permeable to sodium ions and the magnitude of the overshoot is consistent with this theory; at the peak of the action potential the membrane potential corresponds to the equilibrium potential for sodium, predicted using the Nernst equation. The sodium equilibrium potential is the electromotive force, not zero potential difference, as would be the case if the permeability were non-selective.

Experiments performed on the squid giant axon revealed both sodium and potassium ion selective permeability changes underlie the action potential. The kinetics of these permeability changes were described in a series of papers (Hodgkin and Huxley, 1952a; Hodgkin and Huxley, 1952b; Hodgkin and Huxley, 1952c; Hodgkin et al., 1952; Hodgkin and Huxley, 1952d), but evidence for the mechanism for these changes in selective permeability had not yet been ascertained.

1.1.4 Ion Channels

In the 1960s and 1970s however, the concept of ion channels that had first been suggested in the Hodgkin and Huxley papers (Hodgkin and Huxley, 1952a; Hodgkin and Huxley, 1952b; Hodgkin and Huxley, 1952c; Hodgkin and Huxley, 1952d): The idea that water-filled pores in the membrane could allow ions to enter and exit cells, began to be supported empirically. Ion channel theory began to explain the molecular mechanism for ions to flow across biological membranes in the selective and controlled manner that would be required for the potassium and sodium permeability changes that had been observed. Using pharmacological tools, sodium

and potassium currents could be separated, providing evidence that these ions used distinct pathways to cross cell membranes.

A major advance in electrophysiology came with the invention of the patch-clamp technique (Neher and Sakmann, 1976). A polished micropipette tip can be pushed against the cell membrane and application of light suction to the pipette allows a tight seal of Gigaohm resistance, a Gigaseal, to form between the pipette and the membrane. This allows recordings to be made from single channels and thus gating can now be used to describe activation, deactivation, and inactivation of single ion channels as well as activation, deactivation, and inactivation of currents.

Advances in molecular biology and protein chemistry have led to discoveries of membrane protein subunits that form ion selective pores in the membrane. One superfamily of genes discovered forms pores with an intrinsic voltage sensor, and this includes the sodium and potassium channels that were responsible for the regenerative electrical excitability that Hodgkin and Huxley recorded, these have become known as the Voltage-Gated Ion Channels.

1.2 The History of Calcium Channel Discovery

In studies of the elementary properties of the membrane of crustacean muscle fibres using intracellular recording electrodes, it was noted that action potentials persisted in the absence of Na^+ ions in the extracellular medium. It was suggested that the basis of this Na^+ ion-independent action potential could be that influx of other cations, such as Ca^{2+} ions, was responsible for the transfer of charge (Fatt and Katz, 1953).

Recordings from crayfish muscle fibres showed that during an action potential the membrane was permeable to Ba^{2+}, Sr^{2+} and Ca^{2+} ions. The Ca^{2+} dependent action potential was termed a "calcium spike" (Fatt and Ginsborg, 1958). Recording from Purkinje fibres in Na^+-free medium identified current that was dependent on extracellular calcium concentration. It was suggested that the Ca^{2+} ions responsible for this current could be involved in excitation-contraction coupling (Reuter, 1967).

1.2.1 There Are Different Types of Calcium Current

Multiple types of calcium current were identified using pharmacological and physiological criteria. The calcium currents, responsible for the upstroke of the calcium dependent action potential, could be recorded from cardiac and smooth muscle. The gating of these currents was found to be sensitive to dihydropyridine

(DHP) agonists and antagonists (Hess and Tsien, 1984). The currents were activated by strong membrane depolarisation, had high single channel conductance and little voltage-dependent inactivation, and were regulated by cAMP-dependent phosphorylation (Reuter, 1983).

A new calcium current was discovered when two distinct types of Ca^{2+} currents were recorded from voltage-clamped starfish eggs. One type had characteristics of previously recorded calcium currents, but a fraction of the calcium current showed different pharmacological and biophysical characteristics, for example it was not sensitive to DHPs (Hagiwara et al., 1975).

Further evidence of different calcium currents was found in recordings from mammalian neurons. A low threshold calcium conductance was found addition to the more commonly seen high threshold conductance. The characteristics of the current were compatible with the observations of the after-depolarising potential seen in the neurons (Llinas and Yarom, 1981). These two different calcium conductances were characterised by patch-clamp recording from cultured dorsal root ganglion cells (DRG). A fully inactivating, low threshold current was found to co-exist with the high threshold current in isolated membrane patches in rat and chick dorsal root ganglion neurons. These two calcium conductances were named low-voltage activated (LVA) and high-voltage activated (HVA) (Carbone and Lux, 1984;Fedulova et al., 1985).

1.2.2 L-Type, T-type and N-type Calcium Currents

In a more thorough examination of the calcium currents of dorsal root ganglion neurons, three distinct types of calcium current could be identified. One of these was termed the L-type current because it was Long lasting, this was the previously recorded current activated by strong depolarisations. This current was the only current that displayed increased open probability in response to dihydropiridine agonists. Another type, termed T-type was found to have a small single channel conductance and was activated at weak depolarisations, and had previously been called LVA current. The term T-type refers to the Transient nature of this current as it inactivates rapidly and fully. The third type was termed N-type, as it had characteristics that were Neither L-type or T-type, and was present in Neurons. The N-type currents required a strong depolarisation to activate, unlike the T-type, and also required a strong repolarisation for recovery from inactivation, unlike the L-type (Nowycky et al., 1985).

Pharmacological examination of the N-type current proved it to be insensitive to DHPs, but consistently sensitive to ω-conotoxin GIVA, purified from the cone snail, *Conus geographus*. This peptide toxin also blocked L-type channels in a variety of neurons, including sensory, sympathetic and hippocampal, but did not block L-type channels in smooth muscle, skeletal muscle or cardiac muscle (McCleskey et al., 1987), and this action did not depend on second messengers, indicating even more diversity in the voltage-gated calcium channel superfamily.

N-type currents could also be recorded from presynaptic nerve terminals using a chick ciliary ganglion preparation (Stanley and Atrakchi, 1990). This current was not blocked by Nifedipine, a DHP antagonist, at a concentration that did block calcium currents in neurons. The current was blocked by ω-conotoxin GIVA, as was synaptic transmission. Nifedipine did not block synaptic transmission but ω-conotoxin GVIA did, providing evidence that N-type currents, but not L-type, were involved in synaptic transmission.

1.2.3 P/Q-Type Calcium Currents

Another toxin was used to distinguish another calcium current, that was similar to the N-type. The funnel web spider toxin, ω-agatoxin IVA, blocked calcium dependent spikes in mammalian cerebellar Purkinje neurons. ω-agatoxin IVA also blocked synaptic transmission at the squid giant synapse, but did not affect action potentials in the same cell, providing evidence that different calcium channels had different cellular roles. These channels responsible for these currents were purified from cerebellum and studies of these purified channels showed that they were not blocked by either DHP antagonists or by ω-conotoxin GIVA and so a new type of calcium channel that was involved in synaptic transmission but not in regenerative electrical activity had been identified and was called the P-type due to it being found in Purkinje cells (Llinas et al., 1989).

The P-type channels are not the only HVA channel present in Purkinje cells but do have a wide distribution in the central nervous system (Hillman et al., 1991).

Even though a large fraction of calcium channels in Purkinje cells are blocked by ω-agatoxin IVA and other channels are blocked by ω-conotoxin GVIA and DHP antagonists, there is still a fraction of the calcium current that is not blocked (Mintz et al., 1992).

Closer examination of the different calcium currents identified two more types in cerebellar granule cells. One that was identified had similar characteristics to the P-type and was sensitive to ω-agatoxin IVA, although with lower affinity, but had different inactivation kinetics to the P-type. These were termed Q-type currents. The P-type currents and the Q-type currents were later found to be mediated by products of different splice variants of the same gene (Bourinet et al., 1999).
Another calcium current was resistant to both organic L-type blockers and to the peptide toxin subtype-specific blockers, ω-conotoxin GVIA and ω-agatoxin IVA. These were termed R-type for Residual (Randall and Tsien, 1995). However, it was suggested that the R-type currents, found in cerebellar neurons, comprised several channel types, because the biophysical properties of the residual currents were not uniform (Tottene et al., 1996).

Table 1.1 summarises the different voltage-gated calcium conductances.

Current	Pharmacology	Activation	Inactivation	Conductance
L-type	Sensitive to DHPs	-30mV	Slow	High
N-type	Sensitive to ω conotoxin	-20mV	Intermediate, partial	High
P-type	Sensitive to ω agatoxin	-20mV	Slow, partial	High
Q-type	Sensitive to ω agatoxin	-20mV	Intermediate, partial	High
R-type	Insensitive to DHPs and peptide toxins	-20mV	Intermediate/fast, partial	High
T-type	Insensitive to DHPs and peptide toxins	-70mV	Fast, complete	Low

Table 1.1 Types of voltage-gated calcium currents

1.3 The Molecular Structure of Voltage-Dependent Calcium Channels

1.3.1 Protein Subunits

The proteins responsible for the L-type calcium currents were first purified from skeletal muscle transverse tubule membranes using labelled Nitrendipine (Curtis and Catterall, 1984). This identified distinct subunits: α (200kDa), β (50kDa) and γ (33kDa)

Then an additional subunit was discovered comprising 2 distinct proteins: the α_2 glycoprotein (143kDa) and δ (24-27kDa), α_2-δ (Takahashi and Catterall, 1987).

The primary structures of the L-type channel subunits were analysed by protein chemistry and subsequently the cDNAs were cloned (Tanabe et al., 1987). The α_1-subunit comprised 2000 amino acids, and had a similar secondary structure to the voltage-gated sodium channel pore forming subunit: 4 repeated domains, 6 transmembrane segments (S1-S6) in each, domains connected by intracellular linkers, loop between S5 and S6 in each domain is membrane associated and was so predicted to form the pore (termed the P-loop). The secondary structure of the β-subunit predicted it to have α-helices but to be hydrophilic and therefore not transmembrane (Ruth et al., 1989). The γ-subunit had 4 transmembrane regions predicted and was also glycosylated (Jay et al., 1990). The α_2-subunit was shown to be glycosylated and hydrophilic, but extracellular (Ellis et al., 1988). The α_2-δ was shown to have a disulphide bridge and the delta was shown to be transmembrane (Gurnett et al., 1996). Therefore the α_2-subunit was extracellular but was anchored in the membrane by the δ-subunit, to which it was bonded by a disulphide bridge. The α_2-δ was also shown to be two proteins resulting from one gene, which was post-translationally proteolysed and the disulphide bridge formed (De Jongh et al., 1990;Jay et al., 1991).

The accepted topography of the voltage-gated calcium channel complex is that the channel is made of a pore forming α_1-subunit, associated with an intracellular β-subunit, a transmembrane γ-subunit and a transmembrane and extracellular α_2-δ-subunit (Figure 1.1).

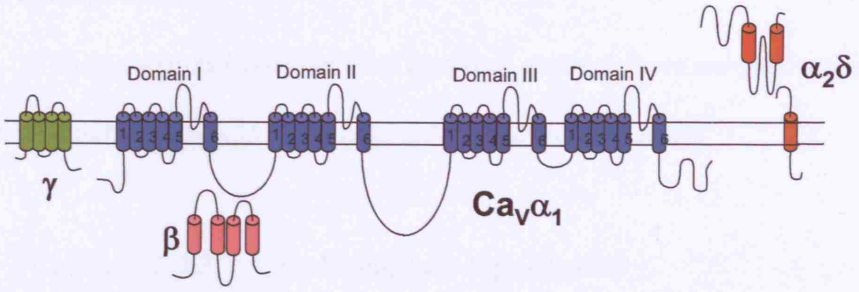

Figure 1.1. Subunits of voltage-gated calcium channels. A diagram representing the topology of the calcium channel subunits. Blue cylinders represent the transmembrane segments of the pore-forming α_1-subunit. The red cylinders represent the α-helices of the α_2-δ-subunit. The pink cylinders represent the α-helices of the intracellular β-subunit. The green cylinders represent the transmembrane segments of the γ-subunit.

Following this, the N-type channel was purified and immunoprecipitated from brain membrane preparations, using labelled ω-conotoxin GVIA. This revealed the channel responsible for the N-type current to comprise an α_1-subunit, a β-subunit and an α_2-δ-subunit (McEnery et al., 1991;Witcher et al., 1993). The N-type channel had a very similar structure to the L-type, but no γ-subunit had been found to associate with this complex.

1.3.2 The α_1-Subunits

Ten α_1-subunits have now been identified and have been assigned a similar systematic nomenclature to the voltage-gated potassium channels:

$Ca_V1.1$, 1.2, 1.3, 1.4, mediating the L-type currents.

$Ca_V2.1$, 2.2, 2.3, mediating the P/Q-, N- and R-type currents.

$Ca_V3.1$, 3.2, 3.3, mediating the T-type currents.

The relationships between the α_1-subunits are shown in figure 1.2.

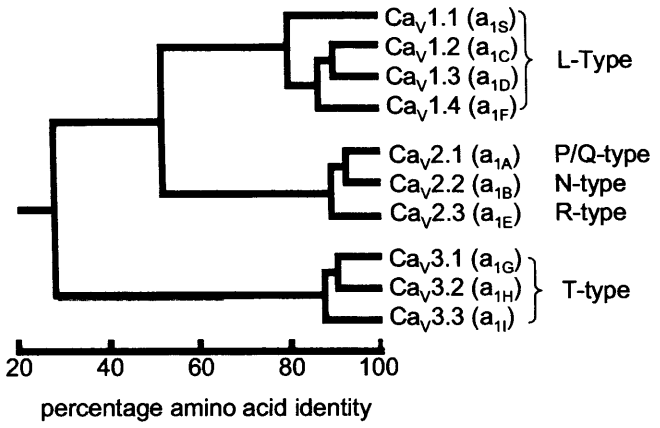

Figure 1.2. Voltage-dependent calcium channel α_1-subunits are classified into three families: Ca_V1, Ca_V2, and Ca_V3. Interfamily sequence identities are approximately 52% Ca_V1 versus Ca_V2) and 28% (Ca_V3 versus Ca_V1 or Ca_V2). Figure reproduced and modified from Ertel et al. (2000).

1.3.4 Activation and Gating

The channels are activated by depolarisation of the membrane. The 4th transmembrane segment of each of the four domains of the α_1-subunit (S4) contains conserved positively charged residues and this is thought to rotate and move out in response to an electric field. The movement of the S4 "voltage-sensor" causes a conformational change that opens the pore, similar to voltage-gated sodium channels (Catterall, 1988). The movement of the voltage-sensor causes a small current that can be recorded called the gating current (Aggarwal and MacKinnon, 1996). When the S4 moves in response to membrane depolarisation, the loop between S5 and S6, the P-loop, is exposed to the pore and this is the region of the calcium channel that confers selectivity for calcium ions (Tang et al., 1993). Mutations in two highly conserved glutamate residues in the P-loops impairs calcium permeation of the channel.
HVA channels are approximately twice as permeable to barium ions as to calcium ions (McDonald et al., 1994). This is unlike LVA channels, which are either more or equally permeable to calcium ions than to barium ions (Carbone and Lux, 1987).

1.3.5 Inactivation

Inactivation is the usual physiological mechanism for terminating the calcium current and prevents the breakdown of calcium concentration gradients and ensures precision of the calcium signal, spatially and temporally. Inactivation also ensures that channels remain impermeable, following a depolarisation, for the duration of time that the channel is in the inactivated state, even if the membrane is depolarised

again. In this way inactivation differs from deactivation, which is the response of the channels to repolarisation of the membrane. In the case of deactivation, channels are available to open again in response to subsequent depolarisation of the membrane. There are two kinds of inactivation of voltage-gated calcium channels: voltage-dependent inactivation and calcium-dependent inactivation. The α_1-subunit contains the inherent components of inactivation, although inactivation is modified by the auxiliary subunits (Zhang et al., 1994).

1.3.6 Voltage-Dependent Inactivation

There are two components of voltage-dependent inactivation, fast (hundreds of milliseconds) and slow (around 1 minute) (Sokolov et al., 2000;Shi and Soldatov, 2002). I will concentrate on the fast component of voltage-dependent inactivation here.

Experiments to investigate the molecular determinants have exploited differences in inactivation rates of different channel subtypes. Studies of chimeras between $Ca_V2.1$ and $Ca_V2.3$ implicated the sixth transmembrane segment (S6) of domain 1 on the α_1-subunit (Zhang et al., 1994).

Studies of chimeras between $Ca_V1.2$ and $Ca_V3.2$ added S6 of domain II and S6 of domain III to the molecular determinants of inactivation. If either of these segments in $Ca_V1.2$ are replaced by those of $Ca_V2.3$, the resulting channel has a fast inactivating phenotype like that of $Ca_V2.3$ rather than the slow inactivation phenotype

of $Ca_V1.2$ (Stotz et al., 2000). A point mutation in the S6 of domain IV, in which a single methionine is replaced with a glutamine, profoundly accelerates inactivation of $Ca_V2.1$ channels (Berjukow et al., 2001). In addition to these artificial mutations, a naturally occurring point mutation in S6 of domain III of $Ca_V2.1$ channels, which is associated with familial hemiplegic migraine, results in a channel with altered voltage-dependent inactivation kinetics (Kraus et al., 2000). Therefore S6 segments of each domain have been connected with voltage-dependent inactivation, leading to the conclusion that fast voltage-dependent inactivation is due to an overall conformational change in the entire channel (Stotz et al., 2004).

The cytoplasmic loop between domains I and II (I-II loop) has also been strongly implicated in voltage-dependent inactivation kinetics. Different splice variants of $Ca_V2.1$ channels have different inactivation properties and this may be the basis of the differences between P-type currents and Q-type currents. The insertion of a single valine residue in the I-II loop of $Ca_V2.1$ converts a Q-type current inactivation profile (pronounced inactivation) into a P-type current inactivation profile (non-inactivating) (Bourinet et al., 1999). The N-terminal tail also appears to be involved but its contribution to inactivation may be dependent on the β-subunit (Stephens et al., 2000)(see section 1.3.10).

A current theory that incorporates the involvement of both the S6 segments of the four domains and the I-II loop is the "hinged-lid" theory. This describes the I-II loop as gating particle that can dock in a site formed by the S6 segments, similar to

the mechanism of inactivation of the voltage-dependent sodium channels (West et al., 1992).

1.3.7 Calcium-Dependent Inactivation

This type of inactivation is usually associated with L-type channels and is the main mechanism of L-type channel inactivation. In low calcium concentrations, when barium ions are the charge carrier, there is only weak inactivation of L-type currents. Calcium-dependent inactivation of L-type currents has been extensively studied on $Ca_V1.2$ channels in cardiac tissue and is dependent on the calcium binding protein, calmodulin (Peterson et al., 1999).

1.3.8 Ca_V2 Family Channels and Ca^{2+}/Calmodulin

At one time there was evidence that only CaV2.1 channels, but not CaV2.2 or CaV2.3 channels were subject to calmodulin-dependent inactivation.

$Ca_V2.1$ channels were shown to display calcium-dependent facilitation and inactivation in a nerve terminal of the calyx synapse in the medial nucleus of the trapezoid body in the brain stem (Borst and Sakmann, 1998;Cuttle et al., 1998). CaV2.2 channels did not show such consistent calcium-dependent regulation, with some studies demonstrating CaV2.2 channels to be sensitive to this type of inactivation (Cox and Dunlap, 1994), but others showing no such regulation (Patil et al., 1998).

Ca^{2+}/Calmodulin directly binds to the C-terminus of some $Ca_V2.1$, where an EF motif is present (Chaudhuri et al., 2004), much like the IQ motif in L-type channels that is essential for calcium-dependent modulation. This increases the rate and extent of voltage-independent inactivation and enhances recovery from inactivation. Calmodulin can also cause facilitation of the calcium current via channel phosphorylation by a calmodulin-dependent kinase (Lee et al., 1999).

It has now been demonstrated that $Ca_V2.2$ channels are also regulated by Ca^{2+}/calmodulin in a similar manner to $Ca_V2.1$ channels (Liang et al., 2003). The mechanism for this regulation is different to that of L-type channels, and is dependent on pre-association of Ca^{2+}-free calmodulin with the channel and sensitive to intracellular calcium buffering, unlike calcium-dependent inactivation of L-type channels, which is not (Neely et al., 1994). It is probable that different experimental conditions with regards to intracellular calcium buffering is the reason for the variable results found for calcium-dependent inactivation of $Ca_V2.2$ channels.

1.3.9 Splice Variants of $Ca_V2.2$

Functional diversity can be achieved by alternative splicing of the RNA coding for the α_1-subunits (Lipscombe et al., 2002). The identified sites of splicing unsurprisingly occur in key functional domains (Bourinet et al., 1999; Lin et al., 1999; Lin et al., 2004; Thaler et al., 2004). There appears to be some specificity in distribution of expression of different splice variants, in particular splice variation in two regions of RNA, which code for part of the voltage sensing transmembrane

segments of domains III and IV, are differentially distributed, with one isoform expressed in the central nervous system and the other isoform in the peripheral nervous system. Absent exons in these regions feature in the dominant splice variant expressed in the central nervous system and increase the rate of channel activation (Lin et al., 2004). These variations in splicing of $Ca_V2.2$ are similar to the splice variants of $Ca_V2.1$ (see section 1.3.6 and Bourinet et al., 1999). Predictably, the region of the mature protein effected by this splicing has been identified as important in voltage-sensing (Stotz and Zamponi, 2001). The situation is not entirely clear cut with regards to distribution of different splice variants of $Ca_V2.2$ though, and multiple splice isoforms have been identified in individual DRGs (Bell et al., 2004). Closed state inactivation, which appears to be prevalent in trains of action potentials (Patil et al., 1998), only occurs in splice variants containing exon 18, which codes for a region located in the cytoplasmic loop connecting domain II and domain III of $Ca_V2.2$ (Thaler et al., 2002). These variations in splicing allow for functional specificity of the N-type voltage-gated calcium channels, along with the associated calcium channel auxiliary subunits.

1.3.10 Functional Effects of the Auxiliary Subunits

Although there is some evidence that the α_1-subunit can form functional channels without the presence of any auxiliary subunits (Perez-Reyes et al., 1989), the channels formed by the α_1-subunit alone display abnormal gating and conduction properties and there is no evidence that these exist in native systems. The two main

auxiliary subunits are the β-subunit and the α_2-δ-subunit. These subunits affect trafficking of the α_1-subunit and biophysical properties of the channel.

1.3.11 β-Subunits

Four β-subunits have been identified, β_{1-4}, and these appear to have a tissue-specific distribution. β_1a is found in skeletal muscle (Ruth et al., 1989), β_1b is found in other tissue such as brain and heart (Ludwig et al., 1997;Hullin et al., 1999), β_2 is found in cardiac muscle (Perez-Reyes et al., 1992), β_3 is mainly found in cardiac muscle, smooth muscle and neurons (Castellano et al., 1993b), and β_4 is mainly found in brain (Castellano et al., 1993a).

β-subunits consist of two conserved domains: An Src homology 3 (SH3) domain and a guanylate kinase (GK)-like domain (Hanlon et al., 1999) and are therefore members of the membrane-associated GK (MAGUK) family proteins. In addition to the two conserved regions, the β-subunits also have non-conserved regions centrally located and in the N-terminal and C-terminal tails, and these regions are variable in length. A groove in the GK domain is the site of interaction of the α **i**nteraction **d**omain (AID) region of the α_1-subunit and has been named the **A**ID **b**inding **p**ocket (ABP) (Van Petegem et al., 2004).

The AID is an 18 amino acid site located on the cytoplasmic loop connecting domain I and domain II of the α_1-subunit (the I-II loop) (Pragnell et al., 1994). The I-II loop contains at least one PKC phosphorylation site and phosphorylation of the I-II loop can influence the β-subunit effects on the α_1-subunit (Stea et al., 1995).

The interaction between the α_1-subunit and the β-subunit may be state dependent (De Waard et al., 1995;Canti et al., 2001). Recent analysis of the structural data of the β-subunit and its interaction with the α_1-subunit (Richards et al., 2004) suggests that the AID is embedded deeply in the folds of the α_1-subunit and empirical evidence from overlay assays show that the β-subunit does not dissociate from a peptide of the I-II loop (De Waard et al., 1995), suggesting there is a possibility that the interaction between the α_1-subunit and the β-subunit may not be dynamic.

In contrast though, dissociation rates have been recorded using surface plasmon resonance. This has shown that the β_3-subunit and the I-II loop of $Ca_V2.2$ have an affinity of 20nM with a K_{off} of 5.2 x 10-3s^{-1} (Canti et al., 2001). Similar affinities and K_{off} were found for the I-II loops of $Ca_V2.1$ and $Ca_V2.3$ for the β_1b-subunit (Bell et al., 2001).

1.3.12 β-Subunit Functional Effects

β-Subunits and Trafficking of the Channel

β-subunits are involved in trafficking of the α_1-subunit to the plasma membrane and therefore increase channel functional expression and hence current amplitude (Singer et al., 1991;De Waard et al., 1994). Antisense knockdown of β-subunits in neurons reduces current amplitude (Berrow et al., 1995;Campbell et al., 1995).

To study the β-subunit effects on the levels of channels at the membrane, gating currents have been measured in the absence and presence of co-expressed β-subunits in *Xenopus laevis* oocytes. These experiments have produced mixed results. Some have shown that β-subunit co-expression does not cause an increase of channel at the membrane (Neely et al., 1993). While others have shown that β-subunit co-expression does increase channel expression at the membrane (Josephson and Varadi, 1996). It has since been discovered that *Xenopus* oocytes contain an endogenous β_3-like-subunit, which is able to traffic channels, and that antisense knock-down of this endogenous β-subunit causes a reduction of functional channel at the membrane (Tareilus et al., 1997;Canti et al., 2001). This suggests that β-subunits are necessary for trafficking of channels to the membrane, and that previous experiments that suggested otherwise were not performed in the total absence of β-subunits. Similarly in COS7 cells, a mammalian derived cell line used as an expression system, currents were observed when $Ca_V2.1$, $Ca_V2.2$, or $Ca_V2.3$ were expressed without β-subunit co-expression but co-expression of β-subunits did increase current density (Berrow et al., 1997;Stephens et al., 1997;Meir and Dolphin, 1998;Stephens et al., 2000). When COS7 cells were checked for endogenous β-subunits, in order to interpret this result properly, although COS7 cells do contain mRNA for β-subunits, immunocytochemistry failed to detect any β-subunit protein present. This may indicate that there are low levels of endogenous β-subunit protein present in COS7 cells, so the results can not conclude that channels are able to be trafficked to the membrane in the complete absence of β-subunits (Meir et al., 2000).

The mechanism of the β-subunit involvement in trafficking is that there is thought to be an ER retention signal in the I-II loop of the α_1-subunit and β-subunits antagonise this (Bichet et al., 2000), allowing the α_1-subunit to be released from the ER and be trafficked to the plasma membrane. However, no ER retention signal has been identified.

1.3.13 The β-Subunits and Biophysical Properties of the Channel

β-subunits are not only involved in trafficking of the α_1-subunit, but they also affect the voltage-dependence and kinetics of activation and of inactivation of the channels. The evidence for these effects are outlined below.

All β-subunits hyperpolarise voltage dependence of activation and inactivation (Stephens et al., 2000;Birnbaumer et al., 1998). Single channel recordings have revealed that the voltage dependence of the mean open time is hyperpolarised in the presence of β-subunits (Meir et al., 2000;Wakamori et al., 1999). Although the α_1-subunit does contain the basic mechanical requirements of voltage-dependent inactivation (see section 1.3.6), the β-subunit dictates the kinetics of inactivation. The general order, with the fastest first, is $\beta_3>\beta_1b>\beta_4>\beta_2$ (Olcese et al., 1994;Meir and Dolphin, 2002).

When the β_2a-subunit is palmitoylated, it slows inactivation kinetics of Ca_V2 family channels. The slowing in inactivation kinetics is due to the palmitoylation of

the β_{2a}-subunit. If the two N-terminal cysteines that are palmitoylated in β_{2a}-subunits are mutated to serines, therefore preventing palmitoylation, the slowing of inactivation kinetics is opposed. This has been demonstrated for $Ca_V2.1$ (Chien and Hosey, 1998), $Ca_V2.2$ (Bogdanov et al., 2000), and $Ca_V2.3$ (Qin et al., 1998). The slowing of inactivation kinetics by β_{2a}-subunits is thought to be due to β_{2a}-subunit palmitoylation tethering the I-II loop of the α_1-subunit to the membrane (Restituito et al., 2000;Stotz et al., 2000). The effects of the β_{2a}-subunit on inactivation kinetics are dependent on identified amino acids on the N-terminal intracellular tail of the α_1-subunit (Stephens et al., 2000). The palmitoylation status of the N-terminal tail appears to be dynamic so may provide another mechanism of regulation of the channels (Hurley et al., 2000). Because the presence of the β_{2a}-subunit reduces the voltage-dependent inactivation, it unmasks the effect of Ca^{2+}/Calmodulin on inactivation and trains of action potential like stimulations cause facilitation and then inactivation of the $Ca_V2.1$ channel (Lee et al., 2000).

This supports the "hinged lid" theory of inactivation, with the I-II loop being the "lid" and if it is immobilised by being tethered to the membrane by a palmitoylated β_{2a}-subunit, then inactivation is resisted. Some splice variants of the β_2-subunit are not palmitoylated and in this case the channels are still trafficked to the plasma membrane as normal, but the current is reduced (Chien et al., 1996).

There seem to be two effects of β-subunits, and these have different affinities: (Canti et al., 2001). High affinity binding affects the maximum current in expression

systems, this is most probably via the mechanism of trafficking and this affinity is around 17nM, which incidentally is about the concentration of the endogenous β_3-subunit in *Xenopus* oocytes. The lower affinity binding, of around 120nM, appears to be responsible for the shift in the voltage-dependence of activation in the presence of β-subunits. There are two possible explanations of these effects: either there is one binding site for β-subunits and the affinity of this site for β-subunits is reduced once the channel is trafficked to the membrane, or there are two β-subunit binding sites on each α_1-subunit, each responsible for the different effects. This has not been demonstrated directly though, but the β-subunit does interact with other parts of the α_1-subunit in addition to the I-II loop (Canti et al., 2001).

Mutation of key residues in the I-II loop of $Ca_V2.2$ has some interesting effects on β-subunit modulation of the channel. Replacement of a trytophan residue with an alanine residue (W391A) in the I-II loop abolishes β_1b- and β_2a-subunit binding to the I-II loop (Leroy et al., 2005). This mutation abolishes β_1b-subunit effects on inactivation and activation but does not affect the β_2a-subunit effects on biophysics. The persistence of the β_2a-subunit effects on the mutated channel are thought to be due to the maintenance of a high concentration of the β_2a-subunit at the membrane by lipid modification of this protein (Leroy et al., 2005). The biophysical effects of the β_2a-subunit may also be maintained, despite a lack of association with the I-II loop, due to being via an additional interaction site such as on the N- of C-termini of the α_1-subunit.

Some β-subunits have been shown to bind to sites on both the N-terminus and the C-terminus of the α_1-subunit and this binding could be lower affinity than that for the I-II loop and could be selective between β-subtypes. The β_2a-subunit has been shown to bind to both the I-II loop and the C-terminal tail of $Ca_V2.3$ (Qin et al., 1997; Walker and De Waard, 1998; Stephens et al., 2000).

The N-terminal tail of $Ca_V2.1$ interacts with the β_2a-subunit and the β_4-subunit, but not the β_1-subunit or the β_3-subunit. The β-subunit cannot bind to both the C-terminal tail and the N-terminal tail of the α_1-subunit at the same time (they appear to compete for binding) but can bind to either the C-terminal tail or the N-terminal tail at the same time as binding to the I-II loop (Walker et al., 1999). The β_4-subunit causes a smaller hyperpolarising shift in the voltage dependence of activation of $Ca_V2.1$ than does the β_3-subunit, and this reduction in effect is due to the binding of β_4-subunit to the N-terminal tail of the α_1-subunit (Walker et al., 1999).

Mutation of a tyrosine residue in the I-II loop of $Ca_V2.2$ (Y388S) greatly reduces affinity of the I-II loop for β_1b-subunits (from 14nM to 329nM), but all the trafficking and biophysical effects are maintained (Butcher et al., 2006), showing that low affinity interactions between the β-subunit and the AID of the α_1-subunit are sufficient for these effects.

In summary, different subtypes of β-subunits not only have different effects on the properties of the channel, but also have different structural requirements, with

respect to interaction sites on the α_1-subunit, in order to exert these effects. This may lead to quite different expression and biophysical characteristics of channels associated with different β-subunits. Furthermore, alternative splice variants of α_1-subunits can differ in their ability to interact with some β-subunits (Pan and Lipscombe, 2000), giving rise to even more diversity in voltage-gated calcium channel function.

1.3.14 Functional Effects of the α_2-δ-Subunit

This subunit consists of two proteins, an extracellular α_2-subunit and a transmembrane δ-subunit. They are the product of one gene that is post translationally cleaved and joined by disulphide bridges (Tanabe et al., 1987; Chang and Hosey, 1988; Witcher et al., 1993;Liu et al., 1996). There have been four α_2-δ-subunits cloned, α_2-δ_{1-4} (Ellis et al., 1988;Klugbauer et al., 1999;Barclay et al., 2001; Qin et al., 2002). The α_2-δ-subunit increases current density of HVA channels (Mikami et al., 1989; Mori et al., 1991) and accelerates activation and inactivation kinetics of $Ca_V1.2$ (Bangalore et al., 1996).

1.3.15 Functional Effects of the γ-Subunits

The effect of the γ-subunits on channel function is unclear. $\gamma_{1,2,3,4}$ may affect the inactivation kinetics of Ca_V2 family channels (Rousset et al., 2001). The γ_7-

subunit may be involved in expression of the channel in expression systems (Moss et al., 2002). A novel γ-subunit has been found in neurons and a mutation in this γ-subunit results in the stargazer phenotype in mice, thus the subunit is termed "stargazin" (Letts et al., 1998). The presence of this subunit causes a hyperpolarising shift in the voltage-dependence of inactivation of $Ca_V2.1$ channels that may significantly reduce the availability of the channels at the resting membrane potential of neurons.

1.4 Physiological Function of Voltage-Gated Calcium Channels

Although there are a variety of functions of voltage-gated calcium channels, three in particular have received most of the attention: regenerative electrical excitability (action potentials), excitation-contraction coupling and excitation-secretion coupling. The latter two roles are due to the importance of calcium ions as an intracellular second messenger and the part that voltage-gated calcium channels play in regulating the intracellular concentration of Ca^{2+}.

1.4.1 Regenerative Electrical Excitability

As previously mentioned, calcium-dependent action potentials have been recorded form crustacean muscle fibres and these voltage-gated calcium channels

entirely account for the regenerative electrical excitability in the muscles of many invertebrates such as arthropods, molluscs and nematodes, in a similar way to voltage-gated sodium channels in most neurons (Fatt and Ginsborg, 1958). They are also responsible for the regenerative electrical excitability in smooth muscle and cardiac pacemaker sinoatrial node neurons in vertebrates, where activation of T-type channels is the basis for the initial depolarisation of the membrane, in order that the membrane reaches the threshold required to activate the sodium channels (Nilius, 1986). Voltage-gated calcium channels also contribute, along with voltage-gated sodium channels, to the action potentials of cardiac ventricular myocytes (Nuss and Marban, 1994). The sodium channels are responsible for the initial fast depolarisation of the membrane but the sodium current inactivates rapidly and it is the more slowly inactivating calcium channels that are responsible for keeping the membrane depolarised for several milliseconds.

1.4.2 Intracellular Calcium Ion Concentration.

Calcium ions are an important intracellular second messenger and so voltage-gated calcium channels provide a mechanism of signal transduction. In simple terms, they turn an electrical signal, in the form of membrane depolarisation, such as an action potential, into a chemical signal, in the form of an increase in intracellular calcium ion concentration.

Resting intracellular calcium concentration is low, 30-200nM, in living cells and this is maintained by the ATP-dependent Ca^{2+} pump (Carafoli, 1992) and Na^{+}/Ca^{2+} exchanger in cell surface membranes (Hilgemann et al., 1991) and by the ATP-dependent Ca^{2+} pump in internal membranes such as the sarcoplasmic reticulum

(SR) and the endoplasmic reticulum (ER) (Laporte et al., 2004). This maintenance of a low intracellular concentration on Ca^{2+} ions allows for a dramatic increase in Ca^{2+} concentration in the local vicinity of calcium channels from small calcium ion flux in response to membrane depolarisation.

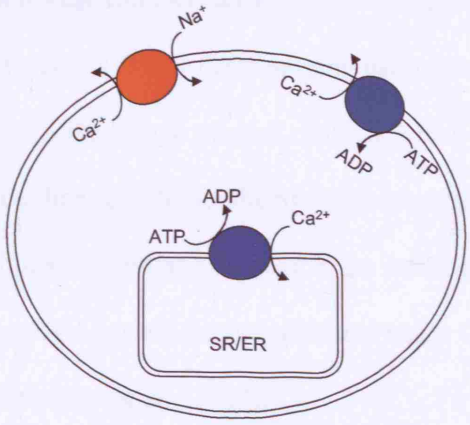

Figure 1.3. Low intracellular calcium ion concentration is maintained by the Na^{+}/Ca^{2+} exchanger and the ATP-dependent Ca^{2+} pump in the plasma membrane of the cell and the ATP-dependent Ca^{2+} pump in the membranes of the sarcoplasmic reticulum (SR) and the endoplasmic reticulum (ER).

1.4.3 Excitation-Contraction Coupling

Calcium ions enter the cytoplasm of muscle cells either though L-type calcium channels in the cell surface plasma membrane or through calcium release channels in intracellular membranes of the sarcoplasmic reticulum or endoplasmic reticulum (Laporte et al., 2004).

Tropomyosin and the troponin complex act to inhibit the productive contact between actin and myosin when the intracellular calcium ion concentration is low. When the calcium ion concentration is increased, the low affinity site on the troponin complex becomes occupied, and the resulting cascade of conformational changes allows the myosin to move along the actin and the muscle to contract (Yasui et al., 1968).

The calcium release channels are ryanodine receptors and inositol trisphosphate (IP_3) receptors. The voltage-sensing part of the ryanodine receptor on the plasma membrane is the L-type calcium channel, which directly couples action potentials to the ryanodine receptor on the SR in skeletal muscle, without the need for extracellular Ca^{2+} influx. In cardiac muscle, it is the influx of extracellular Ca^{2+} that triggers the activation of the ryanodine receptor and hence Ca^{2+} release from intracellular stores (Imagawa et al., 1987).

1.4.4 Excitation-Secretion coupling

Ca^{2+} influx was first identified as being important for transmitter release when it was demonstrated that reducing extracellular Ca^{2+} concentration reduced transmitter release (Katz and Miledi, 1969). The reverse is also true, increasing extracellular calcium concentration increases transmitter release. Building on this work, recording from the pre-synaptic terminal of the squid giant synapse in voltage-clamp, showed that when sodium channels and potassium channels were blocked, graded depolarisation of the membrane caused a graded calcium current and this co-incided with graded transmitter release (Llinas et al., 1980).

$Ca_V2.1$ and $Ca_V2.2$ channels localize at high density in presynaptic membranes (Westenbroek et al., 1992; Westenbroek et al., 1995) and calcium entry through $Ca_V2.1$ and $Ca_V2.2$ calcium channels is recognised as the trigger for neurotransmitter release from pre-synaptic nerve terminals (Wheeler et al., 1994). The intracellular Ca^{2+} concentration required for transmitter release is at least 20-50μM. Given the low resting intracellular calcium ion concentration, the high concentration required is probably only achieved in microdomains around the calcium channels (Llinas et al., 1992; Stanley, 1993). Therefore, for efficient transmitter release, close proximity is required between the synaptic vesicle docking and release machinery and the calcium channels.

1.4.5 Synaptic Proteins

The synaptic proteins Syntaxin 1A, SNAP-25 and VAMP have all been shown immunochemically to associate with $Ca_V2.1$ and $Ca_V2.2$ calcium channels (Bennett et al., 1992; O'Connor et al., 1993). The intracellular loop between domains II and III (the II-III loop) of the $Ca_V2.1$ and $Ca_V2.2$ α_1-subunits is the region responsible for the physical interaction between the vesicle docking machinery and the calcium channels. Syntaxin 1A, SNAP-25 and VAMP have all been shown to interact specifically with the II-III loop. A specific site on the II-III loop, amino acids 718-963, has been identified as the point of interaction and termed the synprint (**syn**aptic **p**rotein **int**eraction) site (Rettig et al., 1996). This feature provides a mechanism by which presynaptic Ca^{2+} channels are able to target synaptic vesicles to dock at a source of Ca^{2+} for fast and efficient exocytosis (Figure 1.6). Not only are

vesicles targeted to calcium channels, but they are specifically targeted to calcium channels that are active, due to the calcium-dependent nature of the interaction between the channels and the release machinery (Sheng et al., 1996).

Interestingly, the modulation also flows in the opposite direction and syntaxin affects the biophysical properties of the channel. Binding of syntaxin to both $Ca_V2.1$ and $Ca_V2.2$ channels stabilizes the inactivated state resulting in less calcium current (Bezprozvanny et al., 1995) and shifts the steady-state inactivation curve (Jarvis et al., 2000). The interaction of synataxin and the synprint site of $Ca_V2.2$ is antagonised by PKC or Ca^{2+}/Calmodulin-dependent kinase type II (CaM KII) phosphorylation of the synprint site (Yokoyama et al., 1997) and cleavage of syntaxin by botulinum toxin C1 prevents the effects of syntaxin on inactivation (Bergsman and Tsien, 2000).

Cysteine string protein, a chaperone protein associated with synaptic vesicles, also localizes to vesicle clusters in pre-synaptic nerve terminals and increases calcium current by increasing the number of available calcium channels (Chen et al., 2002).

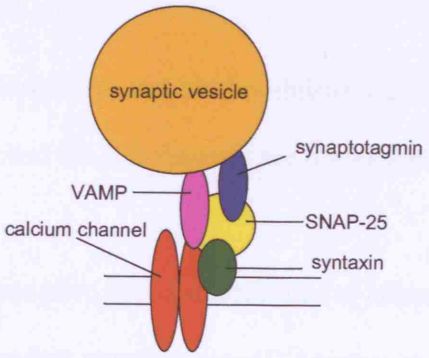

Figure 1.4. Voltage-gated calcium channel and the vesicle release machinery. Syntaxin, SNAP-25 and VAMP directly associate with the channel.

1.4.6 Phosphorylation of Calcium Channels

α_1-subunits of L-type calcium channels are substrates for both protein kinase A and protein kinase C. Protein kinase A (PKA) dependent phosphorylation stimulates L-type calcium current in cardiac myocytes when activated by cAMP via stimulation of β-adrenergic receptors (Bean et al., 1984). This increase in calcium current is not due to an increase in single channel conductance or an increase in functional channel expression, but is an increase in open probability. The phosphorylation, mediated by PKA, shifts gating to more hyperpolarised potentials, increasing the open probability of the channels. Both the α_1-subunit and the β-subunit of the channels are substrates for phosphorylation by PKA (Catterall, 2000).

The effects of phosphorylation of L-type calcium channels by protein kinase C (PKC) seems to be more complex in that currents can be stimulated or inhibited depending on the receptor that stimulates the PKC and on the preparations in which this has been studied. The different effects may be mediated by phosphorylation of different sites on the α_1-subunit of the channel (McHugh et al., 2000).

PKC-dependent phosphorylation also modulates Ca_V2 family channels (Stea et al., 1995). Both $Ca_V2.2$ and $Ca_V2.3$ channels are up-regulated in neurons by a PKC-dependent pathway.

Other protein kinases have been demonstrated to affect $Ca_V2.2$ channels. These include cGMP-dependent protein kinase (D'Ascenzo et al., 2002) and mitogen-activated protein kinase (MAPK) (Fitzgerald, 2002).

1.4.7 PI(4,5)P_2 Modulates Voltage-Dependent Calcium Channels

Activity of voltage-dependent calcium channels decreases with time in whole-cell and inside-out patch-clamp recordings. This run-down suggests that in intact cells, active channels are maintained persistently by an intracellular factor. One mechanism has been identified as being phosphorylation, in the case of L-type channels (Strauss et al., 1997), but N-type and P/Q type channels are regulated by phospatidyinositol-4,5-bisphospate (PI(4,5)P_2) (Wu et al., 2002). PI(4,5)P_2 not only maintains activity of $Ca_V2.1$ and $Ca_V2.2$ channels at the membrane but also depolarises the activation curve of $Ca_V2.1$ channels. The shift in activation of the channels is opposed by PKA phosphorylation of the channel (Wu et al., 2002).

1.4.8 G-Proteins Modulate Voltage-Dependent Calcium Channels

Gβγ subunits of heterotrimeric G-proteins modulate Ca_V2 family calcium channels directly, independently of any intracellular second messenger pathways (Dolphin, 2003). The main effects of Gβγ modulation are to reduce maximum current and cause a depolarizing shift in the voltage-dependence of activation. This kind of modulation of calcium channels is dealt with more thoroughly in section 1.6.

1.5 Heterotrimetric G-Proteins

Heterotrimeric guanine nucleotide binding proteins (G-proteins) are important intracellular signalling molecules. They are so named because their effects are

exerted via GDP-GTP exchange. Heterotrimeric G-proteins comprise an α-subunit a β-subunit and a γ-subunit. They can be activated by stimulation of a G-protein coupled receptor (GPCR) by an agonist, which releases the bound G-proteins to interact with effectors.

1.5.1 GPCRs are Cell Surface Receptors

Most drugs, hormones and neurotransmitters act via cell surface receptors, of which GPCRs are a major class. They comprise the 4th largest superfamily of genes in the human genome. They mediate the effects of many neurotransmitters, chemoattractants, hormones, cytokines and sensory stimulants such as photons and odorants. GPCRs are so named because they exert their effects via their association with heterotrimeric G-proteins. GPCRs are single proteins that have 7 transmembrane domains, with an extracellular amino terminus and an intracellular carboxyl terminus (Pardo et al., 1992). The amino terminus can be involved in ligand binding, either directly or to influence ligand specificity. The intracellular carboxyl tail of the GPCR, along with the cytoplasmic loops that connect the transmembrane domains, is involved in binding to the heterotrimeric G-proteins.

1.5.2 GPCRs Provide an Activation Pathway for Heterotrimeric G-Proteins

The binding of an agonist to a GPCR causes a conformational change, which allows interaction with heterotrimeric G-proteins, forming a high affinity agonist-receptor-G-protein complex. This catalyses guanine nucleotide exchange on the α-subunit of the G-protein, leading to dissociation of Gα-GTP and Gβγ (Figure 1.7) (Natochin et al., 2001). GTP bound Gα dissociates from the receptor and interacts with intracellular signalling molecules such as adenylate cyclase and phospolipase C. Gβγ also dissociates from the receptor and interacts with effectors. Gα hydrolyses GTP to GDP and Gα-GDP reassociates with Gβγ and Gαβγ reassociates with the receptor.

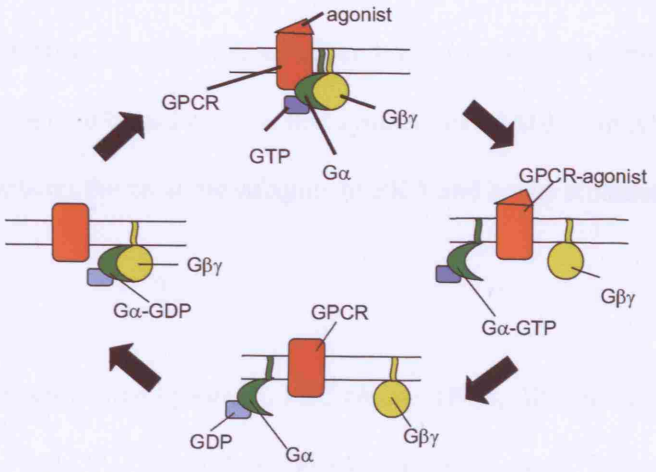

Figure 1.5. G-protein coupled receptors act via heterotrimeric G-proteins. When an agonist binds to a G-protein coupled receptor (GPCR), Gα-GTP and Gβγ dissociate from the receptor and each other. Gα hydrolyses GTP. Gα-GDP reassociates with Gβγ. Gα-GDP-Gβγ reassociates with the receptor.

1.5.3 Gα Effectors

There are over 20 subtypes of Gα identified, and these can be classified into 4 groups according to the signalling pathways in which they are involved (Milligan and Kostenis, 2006).

There are two major pathways controlled by Gα. These are the adenylate cyclase (AC)/cyclic AMP (cAMP) pathway (Adams et al., 1991) and the phospholipase C (PLC)/inositol trisphosphate/diacylglycerol (DAG) pathway (Figure 1.7) (Nishizuka, 1992).

The $G\alpha_s$ family stimulate some types of AC, to increase cAMP levels. The $G\alpha_{i/o}$ family inhibit some types of AC, to reduce levels of cAMP (Adams et al., 1991). AC is a membrane bound enzyme that synthesises cAMP from AMP. cAMP binds to PKA, releasing the catalytic subunits of PKA and hence stimulating kinase activity.

PLC is also stimulated by $G\alpha_{q/11}$. PLC cleaves ($PI(4,5)P_2$) into inositol -1,4,5-trisphosphate (IP_3) and DAG (Sternweis and Smrcka, 1992). Both IP_3 and DAG are intracellular second messengers. IP_3 acts on intracellular receptors to release Ca^{2+} ions from intracellular stores. DAG activates the membrane bound protein kinase, PKC.

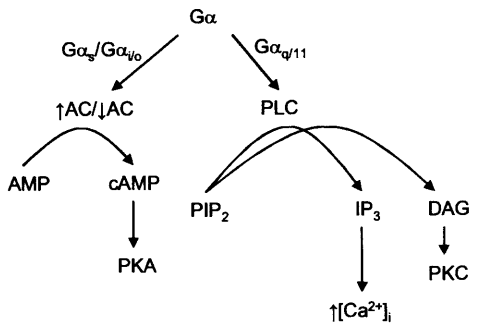

Figure 1.6. Gα activates intracellular signalling cascades. $G\alpha_s$ and $G\alpha_{i/o}$ stimulate and inhibit the adenylate cyclase (AC) pathway, respectively, and $G\alpha_{q/11}$ stimulates the phospholipase C (PLC) pathway. AC converts adenosine monophosphate (AMP) to cyclic AMP (cAMP). cAMP stimulates protein kinase A. PLC cleaves phosphoinositol-4,5-bisphosphate (PIP2) into inositol-1,4,5-triphosphate (IP_3) and diacylglycerol (DAG). IP_3 releases Ca^{2+} from intracellular stores, raising intracellular Ca^{2+} concentration. DAG stimulates protein kinase C (PKC).

1.5.4 Gβγ Effectors

For a long time Gβγ subunits of heterotrimeric G-proteins were thought of as only an "off-switch" for terminating the Gα signal (Neer, 1995) and the reassociation of Gα and Gβγ has been demonstrated as an essential step in the cessation of $G\alpha_s$ stimulation of adenylate cyclase (Sunahara et al., 1997).

A novel role for Gβγ subunits was found when it was demonstrated that Gβγ could activate voltage-gated potassium channels in cardiac myocytes by directly interacting with the channel, rather than through a second messenger (Logothetis et al., 1987). Gβγ has now been shown to activate a number of second messengers such as PLC (Katz et al., 1994), adenylate cyclase (Tang et al., 1991) and PI3 Kinase

(Stephens et al., 1994). Gβγ subunits can also inhibit the Ca_V2 family of voltage-gated calcium channel, and this is the topic of the next section.

1.6 G-Protein Modulation of Voltage-Gated Calcium Channels

1.6.1 G-Protein Activation Reduces Calcium Currents

GPCR stimulation was shown to reduce action potential duration in cultured DRGs without altering resting membrane potential or resting conductance (Dunlap and Fischbach, 1978). The same group then showed that the reduction in action potential duration was due to inhibition of voltage-dependent calcium channels and that the application of GABA, noradrenaline and 5-HT reduced the TTX-resistant tail current seen in response to depolarising steps (Dunlap and Fischbach, 1981). They suggested that this inhibition was most likely due to a change in the number of available channels or a change in conductance of the channels rather than a shift in channel kinetics.

It was noticed in another similar study that there was no reduction in current size in response to very large membrane depolarisations. This indicated that transmitters changed the voltage dependence of calcium channel activation but did not change the level of functional expression of the channels (Bean, 1989). Similar results were seen with other transmitters, implying a common mechanism. The adenosine analogue, 2-chloroadenosine, reduced calcium currents in primary

cultured dorsal root ganglion neurons (DRGs) (Dolphin et al., 1986). Action potentials were reduced in duration but there was no effect on the reversal potential of the calcium current. Baclofen, acting via $GABA_B$ receptors, also shortened action potential duration and reduced calcium currents. There was an unmodulated component of the calcium current, suggesting that within the mixed population of calcium channels present in the cell, there were both channels that were modulated and channels that were not modulated. Baclofen also reduced the peak calcium current in DRGs. GTP-γ-S, a non-hydrolysable analogue of GTP, which prevents Gα and Gβγ reassociating and so the G-protein signal is not switched off, reduced calcium currents and also reduced the effects of baclofen (Scott and Dolphin, 1986). This provided evidence that G-proteins were responsible for the effect of neurotransmitters on calcium currents, which could be the basis of the common mechanism. The same effect was demonstrated by applying somatostatin and somatostatin analogues to rat superior cervical ganglion neurons (SCGs) (Ikeda and Schofield, 1989). Confirmation of G-protein involvement in this system was demonstrated by applying GTP-γ-S, which had the same effect on currents as somatostatin and reduced the effects of somatostatin, confirming the same G-protein pathway was responsible. Baclofen inhibition is increased by application of GTP-γ-S and reduced by GDP-β-S (a GDP analogue that prevents dissociation of Gα and Gβγ, and thus reduces activation of heterotrimeric G-proteins). If pertussis toxin (PTX) was added to the medium, modulation was also reduced. PTX causes $G\alpha_{i/o}$-GDP to be stabilised and thus confirms participation of $G\alpha_{i/o}$ subtypes of G-protein (Scott and Dolphin, 1986; Dolphin and Scott, 1987). Forskolin and cAMP had no

effect on baclofen inhibition of calcium currents, effectively ruling out an adenylate cyclase mediated pathway of modulation. Adenosine A_1 agonist, 2-chloroadenosine, had similar effects to baclofen and was affected by the GTP and GDP analogues in a similar way. Modulation of $Ca_V2.1$ and $Ca_V2.2$ channels by GABA, and prevention of this modulation by GDP-β-S, was confirmed by using the specific peptide toxins for these channel subtypes (Holz et al., 1986). Using primary cultured cerebellar neurons, it was demonstrated that adenosine, acting via A_1 receptors, reduced glutamate release and therefore neurotransmission (Dolphin and Prestwich, 1985). This pathway was also PTX-sensitive and therefore mediated by $G\alpha_{i/o}$.

The same kind of modulation could be shown at nerve terminals using a calyx of Held preparation (Takahashi et al., 1998). This giant pre-synaptic terminal allows currents to be recorded directly from the pre-synaptic membrane. Baclofen reduced EPSCs in a similar way to that of reducing extracellular calcium concentration. Baclofen did not affect potassium currents and GDP-β-S abolished baclofen effects on pre-synaptic calcium currents and EPSCs.

1.6.2 G-Protein Modulation is Voltage-Dependent and Membrane-Delimited

Closer examination of the mechanism of this modulation revealed that the GPCR agonist must be present in the patch pipette to inhibit currents, and a localised soluble second messenger is not involved (Forscher et al., 1986). In cell-attached patches of chick DRGs, noradrenaline applied to the extra-patch membrane did not cause calcium current inhibition within the patch, but did cause a reduction in whole-

cell calcium current. The conclusion of this study was that noradrenaline must either be acting directly on the calcium channel or on a molecule that was tightly coupled to the calcium channel.

It was noticed that the depression of the voltage-gated calcium currents induced by transmitter application was a change in the voltage-dependence of activation but no change in the currents evoked by large membrane depolarisations (Bean, 1989). This led to the "willing" and "reluctant" model, in which unmodulated channels were in a "willing" state, that is open easily, and modulated channels were in a "reluctant" state and required larger depolarisations to open. The model predicted a depolarised current-voltage relationship and biphasic activation of modulated channels (Bean, 1989).

Double-pulse facilitation was also demonstrated in G-protein modulated currents in DRGs (Grassi and Lux, 1989) and SCGs (Ikeda, 1991). Application of DHPs had no effect on facilitation of residual (DHP-insensitive) currents but application of GDP-β-S in the patch pipette reduced the degree of facilitation. This supported the "willing" and "reluctant" model by the pre-pulse relieving the channel of inhibition by G-proteins, thus converting "reluctant" channels into "willing" channels and confirming the voltage-dependent nature of G-protein modulation.

There is also a voltage-independent component that manifests as a reduction in current size that cannot be removed by a depolarising pre-pulse (Diverse-Pierluissi and Dunlap, 1993). This study found two distinct forms of G-protein modulation of

calcium channels by GABA and noradrenaline. GABA modulation could be removed by pre-pulse and was not affected by PKC inhibitors or stimulators. Noradrenaline modulation was not removed by pre-pulse and was eliminated by the application of PKC inhibitors, and was therefore via a different mechanism.

A train of action potential-like high frequency waveforms also relieves the channel from inhibition and therefore this could be a mechanism of modulation of output by input frequency (frequency modulation) in neurons (Williams et al., 1997). This facilitation was confirmed to be due to modulation of $Ca_V2.2$ channels and was dependent on the frequency and number of depolarisations. This research concluded that firing rates and patterns of discharge of neurons could influence responses to transmitters acting via $Ca_V2.2$ channels.

Action potential-like trains in the presence of the $GABA_B$ agonist, baclofen, cause short term facilitation in cultured hippocampal neurons by releasing channels from inhibition and this mechanism may be responsible for the autoreceptor inhibition seen with glutamate and GABA (Brody and Yue, 2000).

1.6.3 Modulation is via a $G\alpha_{i/o}$ Pathway

To further explore the G-proteins involved, antibodies for $G\alpha_i$ and $G\alpha_o$ were injected into NG108 cells. $G\alpha_o$ antibodies attenuated the calcium current reduction in response to noradrenaline application, cells injected with $G\alpha_i$ antibodies had a normal response to noradrenaline application (McFadzean et al., 1989). These results were

supported by application of antisense oligonucleotides directed against $G\alpha_o$ abolishing or diminishing dopamine inhibition of calcium currents and this reduction in transmitter effect correlated with the inhibition of *in vitro* translation of the $G\alpha_o$-subunit (Baertschi et al., 1992). Another study showed that injection of antisense oligonucleotides to $G\alpha_i$ and $G\alpha_o$ to cultured DRG neurons depleted $G\alpha_i$ and $G\alpha_o$ proteins. Injection of $G\alpha_o$ antisence oligonucleotides reduced the baclofen mediated inhibition of calcium currents via $GABA_B$ receptors. $G\alpha_i$ antisense oligonucleotide injection did not have this effect (Campbell et al., 1993). The channels involved were confirmed to be $Ca_V2.2$ by the use of ω-conotoxin GVIA (Menon-Johansson et al., 1993).

However, some studies showed that both $G\alpha_o$ and $G\alpha_i$ were involved by application of neuropeptide Y (NPY) and bradykinin to cultured DRGs (Ewald et al., 1989). NPY acts through $G\alpha_o$ alone and caused reduction in calcium currents, bradykinin acted through both $G\alpha_o$ and $G\alpha_i$, and caused a reduction in calcium currents through both these G-protein subtypes.

1.6.4 Gβγ Mediates the Modulation, Not Gα

There was already some feeling that Gβγ might directly activate voltage-gated potassium channels. Gβγ perfusion was shown to be able to directly gate cardiac potassium channels (Kurachi et al., 1989). Purified Gβγ perfused onto the

intracellular face of exercised patches showed Gβγ, not Gα, activated single channel potassium currents (Logothetis et al., 1987).

Two groups demonstrated that $Ca_V2.1$ and $Ca_V2.2$ channel modulation was mediated by Gβγ, not Gα, and this was the mechanism of transmitter modulation of N- and P/Q-type currents (Herlitze et al., 1996; Ikeda, 1996). Over-expressing Gβγ or injecting purified Gβγ protein into cells that were expressing $Ca_V2.1$ or $Ca_V2.2$ channels resulted in a modulation of currents with characteristics that were consistent with that of neurotransmitter modulation. The voltage-dependence of activation was depolarised and the kinetics of activation were slowed. These effects were not seen with over-expression or injection of $G\alpha_o$. Gβγ over-expression also occluded noradrenaline mediated modulation of currents. Gα prevented noradrenaline modulation too, but this was consistent with Gβγ buffering. This is similar to the buffering seen with over-expression of a minigene coding for the Gβγ binding domain of β-adrenergic kinase 1 (βARK), which reduces GPCR agonist mediated modulation and tonic facilitation in COS7 cells (Stephens et al., 1998b).

1.6.5 Which Gβγ-Subtypes?

Examination of the subtypes of Gβγ that could produce this effect by over-expressing combinations of Gβ and Gγ in cultured SCGs revealed that all combinations of Gβγ could produce marked facilitation. Dimers containing $G\beta_5$,

however, did produce less facilitation than dimers containing any other Gβ-subtype (Ruiz-Velasco and Ikeda, 2000). In this study, only $G\beta_4$ alone without Gγ produced significantly more facilitation than control, all other Gβ-subtypes alone had no effect. This may have been due to coupling with endogenous Gγ, rather than Gβ acting as the modulator alone, as Gβ and Gγ normally act as a functional monomer and Gγ is required for correct folding of Gβ (Clapham and Neer, 1997). Over-expression of Gγ alone cannot produce modulation of currents (Garcia et al., 1998). The reason for $G\beta_5$ containing dimers being less effective than dimers containing all other Gβ-subtypes may be because $G\beta_5$ has 53% homology to the other Gβ-subtypes (Clapham and Neer, 1997) and $G\beta_5$ preferentially interacts with regulators of G-protein signalling (RGS) rather than Gγ (Snow et al., 1998) or that $G\beta_5$ couples to $G\alpha_q$ rather than $G\alpha_{i/o}$ (Fletcher et al., 1998).

Gα subtypes appear to confer specificity of different Gαβγ combinations for signalling between specific receptors and channels. It has been suggested that $G\alpha_{o1}$ is responsible for muscarinic receptor modulation and $G\alpha_{o2}$ responsible for somatostatin receptor mediated modulation (Kleuss et al., 1991). Injecting $G\alpha_{o2}$ antisense oligonucleotides showed that $G\alpha_{o2}$ was responsible for the effect that stimulating the somatostatin receptor has on calcium currents (Degtiar et al., 1996). Therefore any specificity of Gβγ subtype in native systems may be due to specificity of GPCR and Gα interaction rather than Gβγ and calcium channel specificity.

There are some studies to support an effector role for Gα in the modulation of calcium current in this way. $G\alpha i_3$ transfection increases modulation of $Ca_V2.1$ and $Ca_V2.2$ by activation of μ-opioid receptors in oocytes, but this may be due to increased coupling of the receptor to endogenous Gβγ dependent on $G\alpha_{i3}$ (Jeong and Ikeda, 1999).

Inhibition has been shown to involve Gβγ coupled to $G\alpha_o$ but not $G\alpha_i$. Voltage-dependent inhibition mediated by the α_2-adrenoceptor is reduced by $G\alpha_o$ antibodies but not by $G\alpha_i$ antibodies (Delmas et al., 1999). This specificity may be due to sub-cellular compartmentalisation and location of different Gα subtypes. In recordings from dendrites and cell bodies of cultured sympathetic neurons the N-type currents in the dendrites were more sensitive to inhibition by transmitters via G-proteins than the N-type currents in the cell bodies, and this was mediated by Gβγ coupled to $G\alpha_o$. This my be due to the sub-cellular location of G-protein subtypes, with only $G\alpha_o$ subtypes being present in the dendrites in close proximity to the N-type channels that are most sensitive to Gβγ modulation (Delmas et al., 2000). This hypothesis has been supported by a study showing that activation of $G\alpha_o$ and $G\alpha_i$ pathways have the same effects on channel modulation in an expression system in terms of extent of inhibition and the voltage-dependence of that inhibition (Bertaso et al., 2003). In the same study, activation of a $G\alpha_q$ pathway did inhibit calcium currents, but this was in a voltage-independent manner and was via PKC-dependent phosphorylation. This mechanism of modulation has also been seen in chick sensory neurons by activation of α_2-adrenoceptors. It was suggested that Gβγ mediated the voltage-independent effects by activation of PKC and the voltage-dependent effects

were due to Gα activation of an unknown second messenger. However, the situation is complicated by the PKC phosphorylation-dependent down-regulation of the receptor at the membrane (Diverse-Pierluissi and Dunlap, 1995). Both these mechanisms, and the $G\alpha_{i/o}$ mediated mechanism, seemed to be present in these cells as the noradrenaline effect was blocked by PKC inhibitors but GABA mediated reduction of calcium currents was not (Diverse-Pierluissi and Dunlap, 1993).

GPCR and voltage-gated calcium channels have been shown to interact with each other (Beedle et al., 2004) and another possible mechanism of signalling specificity may be selective coupling between types of GPCR and calcium channel subtypes.

1.7 Molecular Mechanisms of G-Protein Modulation

The previous section outlined the evidence leading to the now accepted view that Gβγ dimers mediate GPCR modulation of channel behaviour. But the molecular nature of this interaction is still unknown and this is the focus of the investigations in this thesis.

1.7.1 Gβγ Interacts Directly with the Channel

The kinetics of this modulatory pathway are so fast that it seemed likely to researchers that it did not involve any other factors and that Gβγ dimers bound directly to the calcium channel (Hille, 1994). There is now plenty of evidence that

Gβγ dimers can interact directly with various sites on the Ca_V2 family α_1-subunits, and this is discussed in 1.7.3.

Single channel recordings have revealed that in the presence of Gβγ, there is a longer latency to first opening and stronger depolarisations reduce the latency to first opening (Patil et al., 1996; Jones and Elmslie, 1997). Once the channel in a recording has opened, however, subsequent openings have the same kinetics as unmodulated channels and in addition to this, single channel conductance is unchanged by the presence of Gβγ (Meir et al., 2000). These results led to the hypothesis that Gβγ bound channels did not open, and Gβγ must first dissociate in order for the channel to be activated. However there is some evidence that Gβγ bound channels can open, but with low probability (Lee and Elmslie, 2000). The accepted mechanism of pre-pulse facilitation and recovery, thus the dynamic nature of Gβγ modulation of Ca_V2 family channels is the temporary dissociation of Gβγ from the channel during the pre-pulse and the subsequent reassociation following membrane repolarisation. The stoichiometry of this relationship between channel and G-protein is unknown. Models have been proposed in which up to four Gβγ dimers might bind to the channel complex in order to stabilise the closed state of the channel (Boland and Bean, 1993).

The low probability openings, which fit with the reluctant part of the willing-reluctant model, have been observed in single channel recordings of N-type currents from bullfrog sympathetic ganglion neurons by perfusing noradrenaline and depolarising the membrane to +40mV. At voltages less than +40mV, channels display the long latency to first opening and high open probability following the first

opening, as the willing model predicts. G-proteins have been said to cause a modal shift in gating of $Ca_V2.2$ channels. Gating currents have slower kinetics in the presence of Gβγ (Jones et al., 1997). If the test pulse is more depolarised, the latency to first opening decreases and the gating current kinetics increase, Gβγ modulation causes a depolarising shift in the voltage-dependence of gating charge movement. Therefore Gβγ appears to impede the outward gating movement of the voltage-sensor, S4, by stabilising the channel in the closed state. Gβγ modulation by GTP-γ-S dialysis, whilst blocking ionic currents with La^{3+}, shows not only a depolarising shift in the voltage-dependence of the gating currents but also that the gating currents are reduced in magnitude by GTP-γ-S. G-proteins not only stabilise the voltage-sensor but also oppose the conformational change (signal transduction step) of voltage-sensor activation and channel opening.

1.7.2 Facilitation and Re-inhibition

The rate of re-inhibition of the channel following pre-pulse facilitation is dependent on the concentration of Gβγ and greater concentrations of GTP-γ-S increase the reinhibition rate (Lopez and Brown, 1991; Elmslie and Jones, 1994). Over-expression of Gβγ in heterologous expression systems increases the rate of recovery from pre-pulse facilitation and over-expression of a βARK minigene instead, reduces the rate of recovery (Stephens et al., 1998a). The rate of pre-pulse facilitation is not affected by the concentration of Gβγ (Stephens et al., 1998a) and models have been proposed in which Gβγ must completely dissociate from the

channel before the channel can open (Lopez and Brown, 1991). The longer latency to the first opening in single channel recordings in the presence of Gβγ would support this hypothesis.

The decay of facilitation can be fit with a single exponential and the rate constant is directly proportional to the concentration of Gβγ (Zamponi and Snutch, 1998). This suggests that pre-pulse facilitation is due to the dissociation of a single Gβγ dimer from the channel and recovery from facilitation is due to the reassociation of a single Gβγ dimer (Zamponi and Snutch, 1998). However, models based on the binding of a single Gβγ dimer do not fit the experimental data (Golard and Siegelbaum, 1993) and the theory of dissociation and reassociation of a single Gβγ dimer does not disprove the Boland and Bean model of four Gβγ dimers binding to the channel to effect the inhibition. Although the exact stoichiometry of calcium channel and Gβγ is unclear, it seems acceptable to consider only one Gβγ binding to the channel as the experimental evidence suggests that it is the dynamic situation between one channel and one Gβγ dimer that effects the modulation.

1.7.3 The Site of Interaction

The most commonly proposed binding site of Gβγ is the cytoplasmic loop between domain I and II of the α_1-subunit (the I-II loop). But other parts of the channel may also play a role: the C-terminal tail, the N-terminal tail and Domain I have all been implicated.

1.7.4 The I-II Loop

Gβγ has a variety of other effectors (see 1.5.4) and many of these have a common Gβγ binding motif. A QXXER motif on type 2 adenylate cyclase and PLCβ2 appears to be the molecular determinant for Gβγ interaction (Chen et al., 1995). The Ca_V2 family of channels contain a QXXER motif in the I-II loop. The relevant motifs are QQIER in $Ca_V2.1$ and QQIER in $Ca_V2.2$. The I-II loop of L-type channels, which are not modulated by Gβγ, do not contain this motif (it is QQLEE) (Pragnell et al., 1994). It is quite possible that the Gβγ interaction site on the Ca_V2 family channels is also dependent on a QXXER motif, and there is some evidence that this is the case.

Several groups have shown that Gβγ dimers bind directly to the I-II loop α_1-subunit of $Ca_V2.1$ and $Ca_V2.2$. The point mutation R387E, which is the last amino acid of the motif QQIER of the I-II loop of $Ca_V2.1$, giving QQIEE, completely abolished GTP-γ-S stimulation of modulation of the channel. This implies that the binding of Gβγ to the I-II loop QXXER motif is essential for Gβγ modulation (De Waard et al., 1997; Herlitze et al., 1997). In addition to this, peptides derived from the I-II loop of $Ca_V2.1$ or $Ca_V2.2$ in the patch pipette of whole-cell recording prevents modulation (Herlitze et al., 1997; Zamponi et al., 1997). A peptide containing the sequence QXXER blocks modulation, presumably by competing for Gβγ binding . A peptide containing the sequence AXXAA instead, does not affect Gβγ modulation.

A chimeric channel of $Ca_V2.1$ with the I-II loop replaced with that of $Ca_V2.2$ displays increased modulation compared to wild type $Ca_V2.1$, but not to the same level as wild type $Ca_V2.2$, suggesting that there are other determinants in Gβγ

modulation aside from the I-II loop (Zamponi et al., 1997). Yeast-2-hybrid studies have shown point mutations in the I-II loop peptide, made by site directed mutagenesis, interfere with Gβγ binding and these mutations also interfere with modulation of the channel (Garcia et al., 1998). Employment of a surface plasmon resonance based system gave Gβγ an affinity of 62nM for the I-II loop of $Ca_V2.2$. The I-II loop of $Ca_V1.3$ did not bind Gβγ (Bell et al., 2001).

But there is some evidence that the I-II loop is not as important as has been suggested: Chimeric channels with the I-II loops of $Ca_V2.1$ or $Ca_V2.3$ inserted into $Ca_V2.2$ had the same Gβγ modulation as wild type $Ca_V2.2$ (Page et al., 1997). But the I-II loop of $Ca_V2.2$ inserted into an otherwise unmodulated variant of $Ca_V2.3$ did confer some aspects of modulation in that in the presence of GTP-γ-S, currents displayed kinetic slowing and pre-pulse facilitation, as associated with classic Gβγ modulation of $Ca_V2.2$. However the I-II loop of $Ca_V2.2$ inserted into $Ca_V1.2$ did not confer Gβγ modulation (Canti et al., 1999). These results taken together seem to suggest that although the QXXER motif in the I-II loops of Ca_V2 family channels are essential for the binding of Gβγ to the I-II loop, the same residues, and in fact the whole of the I-II loop of Ca_V2 family channels, are neither sufficient nor essential for the channels to be modulated by Gβγ. This could indicate that the observed interaction of Gβγ with the I-II loop of Ca_V2 family channels may not be responsible for Gβγ modulation of the channel.

1.7.5 Calcium Channel β-Subunits and Gβγ Modulation

Despite the questionability of the involvement of the I-II loop, the wealth of evidence that the QXXER motif, which is within the AID region of the I-II loop, is involved has led to research into whether the β-subunit was also involved in Gβγ modulation.

Campbell (Campbell et al., 1995) suggested that G-proteins compete with the calcium channel β-subunit due to observations implying that the β-subunit reduced G-protein interaction with the calcium channel. This theory was tested by site-directed mutagenesis of an amino acid in the β-subunit binding site to prevent β-subunit binding, but this had no effect on G-protein modulation (Zhang et al., 1996). They also made a series of chimeric channels in which domains of the $Ca_V2.2$ channel were replaced with the corresponding domains of $Ca_V2.1$ or $Ca_V1.2$. The I-II loops from $Ca_V2.1$ and $Ca_V1.2$ inserted into $Ca_V2.2$ and co-expressed with β_1b did not reduce modulation. But replacement of domain I, including the N-terminus, along with the C-terminal tail of $Ca_V2.2$ with that from $Ca_V2.1$, significantly reduced modulation. The opposite chimera in which domain I, the N-terminus and the C-terminus of $Ca_V2.1$ were replaced with those of $Ca_V2.2$, resulted in a channel that was modulated in the same way as wild type $Ca_V2.2$. When antisense technology was used to knockdown β-subunits by 90%, modulation of residual calcium currents in DRGs, by application of baclofen, was increased (Campbell et al., 1995). Similar results were obtained in expression systems: when β-subunits were expressed in *Xenopus* oocytes, channel modulation was reduced (Bourinet et al., 1996; Qin et al., 1997). These experiments only looked at modulation at a single potential though, and

since β-subunits affect the voltage-dependence of activation and Gβγ modulation is voltage-dependent, with peak modulation occurring at around the half-maximal activation point, the V_{50}, of the current-voltage relationship (Canti et al., 2000), the interpretation is difficult. An additional complication in the interpretation of these results is that *Xenopus* oocytes express an endogenous β_3-like-subunit, so these experiments were not performed in the complete absence of β-subunits (Tareilus et al., 1997).

A more thorough analysis of Gβγ modulation in the presence and absence of over-expressed β-subunits showed that the maximum inhibition in the absence of over-expressed β-subunits, around 70% inhibition, was comparable to that with over-expressed β_1b-subunits (70% inhibition), β_3-subunits (62% inhibition), and β_4-subunits (59% inhibition). Due to the hyperpolarising shift of the current-voltage relationship in the presence of over-expressed β-subunits, the maximum inhibition occurred at -20mV rather than -10mV when β-subunits were over-expressed (Canti et al., 2000).

It has been suggested in the past that Gβγ may compete with and displace β-subunit (Sandoz et al., 2004), but recent structural studies of the interaction between the β-subunit and the α_1-subunit show that it is unlikely that the β-subunit ever dissociates from the AID of the α_1-subunit (Van Petegem et al., 2004;Richards et al., 2004). However, if the β-subunit and Gβγ were in competition then it is feasible that the rate of dissociation of Gβγ from the channel, and therefore the rate of facilitation,

would be dependent on the concentration of β-subunit present. Over-expression of β-subunits does seem to increase the facilitation rate during the pre-pulse (Roche and Treistman, 1998; Canti et al., 2000), but this result could be interpreted to mean that β-subunits simply reduce the affinity of the channel for Gβγ, but not necessarily by competing for binding.

An intracellular dose-response curve for β-subunits on facilitation rate in the presence of Gβγ shows two concentration-dependent effects of β-subunits (Canti et al., 2000). At high concentrations of over-expressed β_3-subunits, facilitation rate can be fit with a single fast exponential. At intermediate concentrations of over-expressed β_3-subunits, the facilitation rate can be fit with two exponentials. The proportion of channels that could be fit with the fast exponential component was the same proportion of channels as had hyperpolarised steady-state inactivation, an effect of the β_3-subunit, and both these proportions had the same dependence on β_3-subunit concentration, supporting the hypothesis that when β-subunits are bound the facilitation rate is higher. The fast time constant did not vary with β_3-subunit concentration but the slow time constant did. An explanation for this could be that the β_3-subunit binds to free channels during the pre-pulse, thus creating more channels with a fast facilitation rate and so affecting the time constant.

1.7.6 The C-Terminus

Another Gβγ interaction site has been identified on the C-terminal tail of $Ca_V2.3$ by binding studies with GST fusion proteins. This has provided evidence the

site on the C-terminus is the functional interaction site, rather than the site previously identified in the I-II loop. Replacing the I-II loop of $Ca_V2.3$ with the I-II loop of $Ca_V1.3$, which does not bind $G\beta\gamma$, gave a chimera that was fully modulated by stimulation of the muscarinic receptor, M_2R (Qin et al., 1997). In addition, when the C-terminal tail of $Ca_V2.3$ was replaced with that of $Ca_V1.3$, the channel was not modulated, indicating that although two binding sites for $G\beta\gamma$ on the $Ca_V\alpha_1$-subunit have been identified, only one of these, the one on the C-terminal tail, is responsible for functional effects of $G\beta\gamma$. The reverse chimeras would show whether replacement of the C-terminus of $Ca_V1.3$ with that of $Ca_V2.3$ could confer modulation, this has not been published.

If the C-terminus of $Ca_V2.2$ is truncated so that the region that is homologous to the part of the C-terminus of $Ca_V2.3$ that is essential for modulation is removed, there is no change in the modulation of the channel by GTP-γ-S perfusion (Meza and Adams, 1998). Deletion of the proximal part of the C-terminus of $Ca_V2.2$ (amino acids 1877-2338), gave a channel that did display modulation by GTP-γ-S perfusion. The region of $Ca_V2.3$ homologous to this region of $Ca_V2.2$ had been shown previously to bind $G\beta\gamma$, and is the region shown to be the functional interaction site of $Ca_V2.3$ (Qin et al., 1997). This indicates that the molecular determinants for the modulation of the different members of the Ca_V2 family may be different. However in one study, if the C-terminus of $Ca_V2.2$ was truncated, the modulation of currents by activation of a somastatin receptor was reduced (Hamid et al., 1999). Deletion of proximal third of $Ca_V2.2$ C-terminus (amino acids 1955-2336), did reduce inhibition

mediated by stimulation of the somatostatin receptor, but the channel was still modulated and displayed full kinetic slowing.

1.7.7 The N-Terminus

Gβγ modulation of $Ca_V2.1$ and $Ca_V2.2$ has always been consistently observed, but this is not the case for $Ca_V2.3$. In some cases $Ca_V2.3$ was modulated by Gβγ (Yassin et al., 1996; Meza and Adams, 1998), but in others it was not modulated (Page et al., 1997).

The basis of this discrepancy was identified as being due to the original rat clone being N-terminally truncated and starting at the second methionine. This truncation resulted in a channel which was unmodulated (Page et al., 1998). On examination of the modulation of the two splice variants, it was clear that the N-terminus of $Ca_V2.3$ was essential for Gβγ modulation (Page et al., 1998). Modulation of $Ca_V2.2$ was shown to have the same dependence on the N-terminus and when the distal portion of the N-terminus of $Ca_V2.2$ was truncated, Gβγ modulation was abolished (Page et al., 1998).

This discovery gave a new insight into the molecular basis of Gβγ modulation that was in need of further investigation. When the N-terminus of $Ca_V2.1$ was replaced with the N-terminus of $Ca_V2.2$, modulation of the chimeric channel was comparable to that of wild type $Ca_V2.2$. The region of the N-terminus that was responsible was narrowed down further by deleting an 11 amino acid sequence in the N-terminus of $Ca_V2.2$ and thus abolishing modulation (Page et al., 1998). These 11

amino acids are highly conserved across the Ca_V2 family of channels. Interestingly, deletion of these 11 amino acids or mutation of some of the single residues reduced the β_2a-subunit mediated retardation of inactivation (Stephens et al., 2000). Mutation of two arginine residues, at amino acid positions 52 and 54, within this 11 amino acid region, abolishes G$\beta\gamma$ modulation of $Ca_V2.2$ (Canti et al., 1999). It has been suggested that this RAR motif in the N-terminus of $Ca_V2.2$, that is essential for G$\beta\gamma$ modulation, may form a PIP_2 binding site (Dolphin, 2003). It is similar to the positively charged motifs in GIRKS that have been shown to bind PIP_2 and result in membrane association (Zhang et al., 1999). These interactions between the N-terminus and the C-terminus of GIRKs and PIP_2 produces a channel conformation that favours G$\beta\gamma$ modulation and PIP_2 presence in the membrane is essential for G$\beta\gamma$ activation of GIRKs (Huang et al., 1998).

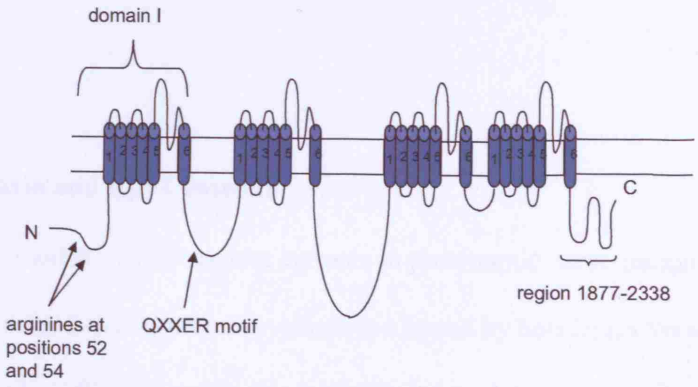

Figure 1.7. Several sites on the Ca_V2 family a1-subunits are implicated in G$\beta\gamma$ interaction with the channel. The I-II loop binds G$\beta\gamma$ directly. Deletion of parts of the N-terminal or C-terminal tail can affect modulation. Replacement of domain I with that of an unmodulated channel affect modulation.

1.7.8 Crosstalk

Gβγ modulation of Ca_V2 family channels has been demonstrated to be affected by the interaction of other proteins with the calcium channel, namely by PKC, causing phosporylation, and by syntaxin (Figure 1.10).

1.7.9 PKC and Gβγ Crosstalk

PKC phosphorylation, stimulated by mGluR activation or application of phorbol esters, increases $Ca_V2.2$ channel activity in native cells (Swartz et al., 1993). The phosphorylation of $Ca_V2.2$ by PKC opposes Gβγ modulation (Swartz, 1993). The PKC phosphorylation site that is responsible for this effect has been identified as a threonine residue at amino acid position 422 on the I-II loop (Zamponi et al., 1997), (Hamid et al., 1999). This crosstalk appears to be dependent on Gβ isoform as only modulation by Gβγ dimers containing $G\beta_1$ is affected, and modulation by dimers containing $G\beta_2$, $G\beta_3$ or $G\beta_4$ are not (Cooper et al., 2000).

1.7.9 Syntaxin and Gβγ Crosstalk

Gβγ modulation of calcium currents in presynaptic nerve terminals is eliminated if the SNARE protein syntaxin is cleaved by botulinum toxin C1 (Stanley and Mirotznik, 1997). However, this inhibition of modulation by syntaxin cleavage can be overcome by over-expressing Gβγ (Jarvis et al., 2000). The interactions between $Ca_V2.2$ and the SNARE proteins are regulated by phosphorylation by PKC and Ca^{2+}/Calmodulin dependent protein kinase II. These kinases phosphorylate 2 or 3

sites in the synprint region and this phosphorylation prevents interaction with the SNAREs (Yokoyama et al., 1997). Therefore, transmitters that regulate these kinases can indirectly regulate the channel-SNARE interactions via second messenger pathways and there is also evidence that Gβγ dimers can directly regulate the vesicle release machinery (Blackmer et al., 2005).

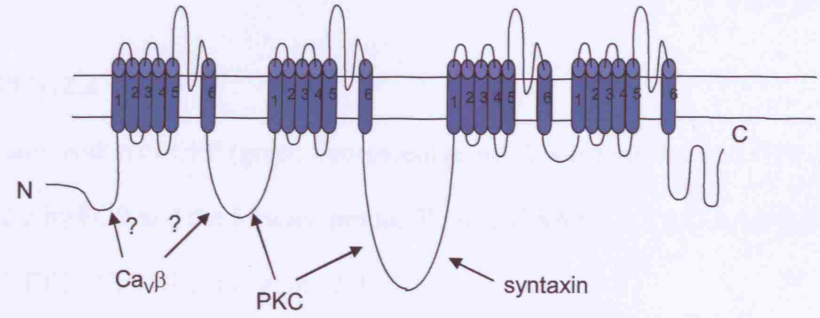

Figure 1.8. Crosstalk affects Gβγ modulation if the channel. Interactions of PKC, syntaxin and calcium channel b-subunits have all been shown to affect Gβγ modulation of the channel.

In this study I have attempted to further investigate the role of the N-terminal tail of the $Ca_V2.2\alpha_1$-subunit in the modulation of the channel by G-protein βγ-subunits.

Chapter 2 Methods

2.1 Molecular biology methods

The following cDNAs were used: Rabbit $Ca_V2.2$ (GenBank D141757), rat β_1b (X 11394), mouse $\alpha_2\delta$-2 (AF247139), bovine $G\beta_1$ (M13236), bovine $G\gamma_2$(M37183).

GFP$Ca_V2.2$

The stop codon of GFP (green fluorescent protein) was removed and GFP fused to $Ca_V2.2$ by PCR and the forward primer 5' GAT GAA CTA TAC AAA ATG GTC CGC TTC GG 3' (Raghib et al., 2001)

$Ca_V2.2$(R52,54A)

Two point mutations were added using PCR and the following primers: Forward primer 5' TCG ATC GCG CAG GCC GCG GCG ACC ATG GCG CT 3', Reverse primer 5' GTC GCT TCT GCT CTT CTT GG 3' (Canti et al., 1999).

Palmitoylation Motif $Ca_V2.2$ and **Palmitoylation Motif $Ca_V2.2$(R52,54R)**

Palmitoylation motif constructs were made by Wendy Pratt by PCR using primers based on the sequence of the first 11 amino acids of $G\alpha_q$, which contains two palmitoylated cysteine residues (Thiyagarajan et al., 2002). The following primers were used: Forward Primer: 5' ATG ACT CTG GAG TCC ATC ATG GCA TGC TGC CTC GTC CGC TTC GGG GAC GAG 3', Reverse primer: 5' GAG GCA GCA

TGC CAT GAT GGA CTC CAG AGT CAT GAT CAA GCT TCG ACC TCG 3' and either $Ca_V2.2$ or $Ca_V2.2$(R52,54A) in the pMT2 vector were used as templates. The additional bases added to the gene coded for the following amino acids on the N-terminus of the protein:

M T L E S I M A C C L

Mutated Palmitoylation Motif $Ca_V2.2$

The mutated palmitoylation motif construct was made by Wendy Pratt using the following primers: Forward primer: 5' CAT GGC AAG CAG CCT CGT C 3', Reverse primer: 5' GAC GAG GCT GCT TGC CAT G 3' and palmitoylation motif $Ca_V2.2$ in the vector pMT2 as a template. The additional bases added to the gene coded for the following amino acids on the N-terminus of the protein:

M T L E S I M A S S L

Heamaglutinin tagged $Ca_V2.2$

HA tagged $Ca_V2.2$ was made by Manuela Nieto-Rostro by PCR using the following primers: Forward primer: 5' CAC GGT ACC GAA TTC ACC ATG TAC CCA TAC GAC GTC CCA GAC TAC GCT GTC CGC TTC GGG 3' Reverse primer: 5' AAC TCT GCA AAG TAC AAT GC 3'. The additional bases added to the gene coded for the following amino acids on the N-terminus of the protein: **Y P Y D V P D Y A**

The Isolated N-Terminus

The isolated N-terminus was made by introduction of a stop codon at amino acid position 95 (Raghib et al., 2001) using the following primers: Forward primer 5' GCG ACT AGT ATG GTC CGC TTC GGG GAC 3', Reverse primer 5' GTA CTC GAG CTA AGG CCA CTC GGT GAT GCG 3'.

The α_2A-Gαo Fusion Construct

The efficiency of GPCR and G-protein coupling is dependent on the ratio of GPCR and G-proteins and the absolute concentrations of each (Kenakin, 1997). This can clearly be an issue when studying GPCR stimulated pathways in heterologous expression systems as it is difficult to achieve precise concentrations and ratios. In addition, although the specificity of these relationships is highly selective in native cells, in expression systems, it is not so specific. It is for these reasons that, for many of the experiments in this thesis, I have used a GPCR-Gα fusion protein to provide a pathway for stimulation of endogenous G$\beta\gamma$ subunits.

The fusion protein provides a 1:1 stoichiometry of GPCR and Gα, removing one of the amplification steps in this pathway, and it also ensures close physical proximity of the two proteins thus creating the best chance for efficient signal transduction.

The fusion protein that I have used was created by fusing the C-terminus of the α_2A adrenoceptor to the N-terminus of Gαo. The construction of this tandem construct has been described previously (Cavalli et al., 2000).

2.2 The *Xenopus* Oocyte Expression System

The *Xenopus* oocyte expression system was first introduced in 1971 (Gurdon et al., 1971). It provides a way of studying recombinant proteins by the introduction of mRNA into the cytoplasm (Gurdon et al. 1971) or cDNA plasmids into the nucleus (Swick et al., 1992). The pMT2 cDNA expression vector was used because it has an adenovirus major late promoter, which has high activity levels in *Xenopus* oocytes so high levels of functional heterologous protein are expressed (Swick et al., 1992). *Xenopus* oocytes are large and robust hence microinjection and electrophysiological recording with multiple electrodes is relatively easy.

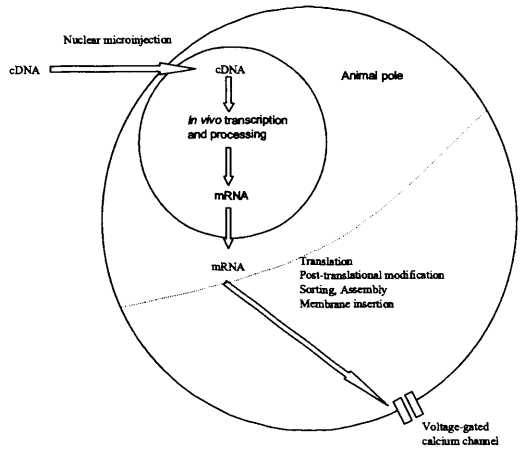

Figure 2.1 The *Xenopus* Oocyte Expression System
Many foreign proteins are modified and targeted appropriately in *Xenopus* oocytes. The genetic material enabling their synthesis is introduced by microinjection of cDNA into the nucleus.

2.2.1 Oocyte Collection

Adult, female *Xenopus laevis* were anaesthetised by immersion in ethyl-m-aminobenzoate solution (0.25%, Sigma, UK) for 40 minutes, and then decapitated. The ovaries were removed via two 1cm incisions in the skin and subcutaneous muscle of the abdominal wall.

Ovarian tissue was then divided into small pieces using fine forceps and oocytes were defolliculated in collagenase (type 1A, 1.5mg/ml, Sigma, UK) in a Ca^{2+}-free ND96 solution (96mM NaCl, 2mM KCl, 1mM $MgCl_2$, 5mM HEPES, pH7.5 with 10mM NaOH) for 1.5 hours at 18°C. The collagenase solution was then drained off and replaced with Ca^{2+}-free ND96 and incubated at 18°C for a further 1 hour. The oocytes were then washed with Ca^{2+}-free ND96 three times, then with ND96 containing 1mM Ca^{2+} a further three times. Healthy looking oocytes at stages V and VI were selected and incubated overnight at 18°C in ND96 medium containing penicillin (100mg/ml) and streptomycin (100IU/ml).

2.2.2 cDNA Injection

Solutions of individual cDNA constructs in TE buffer (10mM Tris-HCl, pH8.0, 1mM EDTA) were stored at -20°C.

Solutions of the recombinant subunits of interest were made and 4.9nl was injected directly into the nucleus of each oocyte using a Drummond microinjector (Laser laboratory systems, UK) and a glass injection pipette. Injection pipettes were pulled from thin walled borosilicate capillary glass (Laser Laboratory Systems, UK), using a microelectrode puller (Flaming/Brown model P-97, Sutter Instruments Co.,

USA) and cut to give a tip diameter of 1μm. The injection pipette was back-filled with mineral oil and placed on the micro-injector. The air and some oil was expelled from the tip of the pipette before filling by suction from a drop of cDNA solution placed on a piece of parafilm to provide a clean surface.

Each oocyte was individually injected into the animal pole whilst being held steady using a pair of fine forceps. The membrane of the oocyte is opaque so the exact location of the nucleus must be guessed; this is known as "blind injection" and results in some (around 20% on average) oocytes not expressing channels due to missing the nucleus during the injection process.

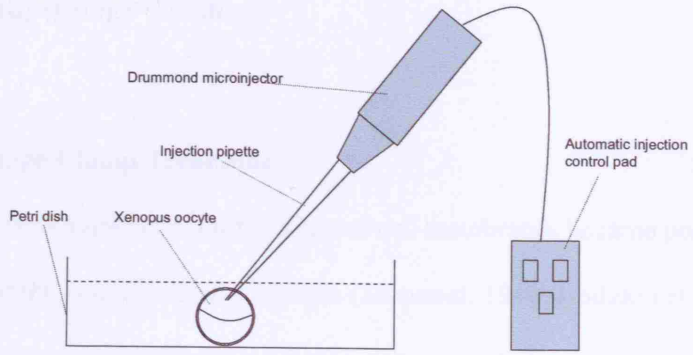

Figure 2.2 Injection Apparatus
The injection pipette was filled with cDNA solution by suction. Each oocyte was individually injected into the animal pole with 4.9nl of cDNA solution. The volume injected could be set using the automatic injection control pad.

Following injection, the oocytes were incubated for a further 48-72 hours at 18°C in ND96 solution, to allow the recombinant proteins to be expressed.

2.2.3 BAPTA Injection

1-6 hours prior to recording, each oocyte was injected, into the cytoplasm, with 9nl K_3-1,2-bis(aminophenoxy)ethane-*N,N,N',N'*-tetra-acetic acid (BAPTA) (100mM). This was required to chelate intracellular Ca^{2+} to prevent activation of endogenous Ca^{2+} activated chloride currents.

2.3 Electrophysiology Methods

2.3.1 The Voltage-Clamp Technique

Direct measurements of currents across cell membranes became possible with the invention of the voltage-clamp technique (Marmont, 1949; Hodgkin et al., 1949; Cole, 1949). Voltage-clamp allows ion flow across a membrane to be measured as electrical current, whilst holding the membrane voltage stable using a feedback amplifier, to eliminate capacity current. The theory can be explained by thinking of the cell membrane as a simple circuit (Figure 2.1).

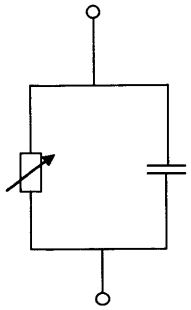

Figure 2.3. The membrane can be viewed as a simple electrical circuit in which a variable resistor, representing ion channels, and a capacitor, representing the membrane, are connected in parallel.

The current flowing across the membrane can be described by Equation 2.1

$I_m = I_i + C*dV/dt$ Equation 2.1

Where I_m is the current flowing across the membrane, I_i is the ionic current, C is the capacity current, and dV/dt is the rate of change of potential difference. In the case of voltage-clamp, dV/dt = 0, therefore $I_m = I_i$.

The two electrode-voltage clamp circuit is shown (Figure 2.2). The membrane potential is set by the experimenter. This is compared to the actual membrane potential as measured by the voltage electrode. The difference between the set potential and the measured potential is injected as electrical current back into the cell

to maintain the set potential. This injected current is recorded and is equivalent to the ionic current across the membrane.

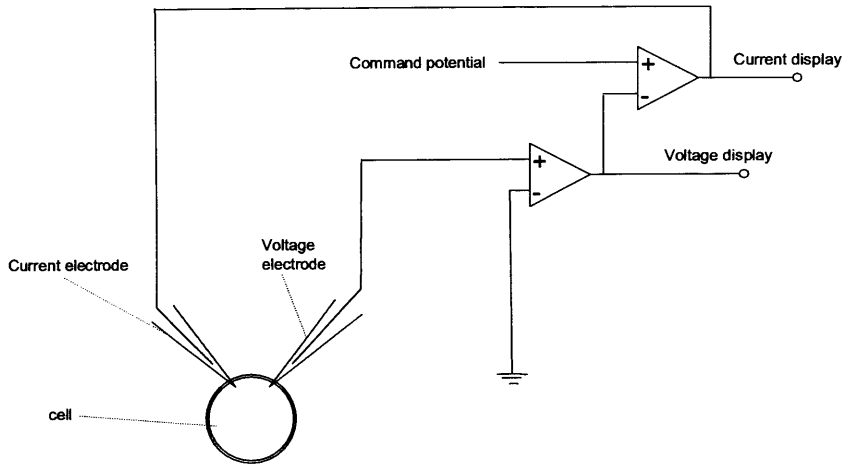

Figure 2.4. The Two-Electrode Voltage-Clamp circuit. The potential difference across the membrane is measured by the voltage electrode and the earth (which is in the bath solution). This voltage is compared to the command potential, set by the experimenter. The difference between the two is fed-back to the cell via the current electrode to maintain a constant membrane potential. The injected current is displayed as it is equivalent to the ionic current across the membrane.

There are two major advantages to the voltage-clamp: Firstly, it allows the ionic current to be separated from the capacitive current. This means that the current measured in voltage-clamp is directly representative of the ions passing across the membrane. Secondly, channel behaviour can be observed whilst the membrane potential is uniform rather than changing freely, both spatially and temporally, as might be the case in more physiological situations.

Voltage-clamp has an additional advantage when studying voltage-gated channels, which is that voltage steps can be applied to the membrane and the

conductance of the membrane at these potentials can be measured in order to obtain a current-voltage relationship. A brief spike of capacity current flows at the beginning and end of each voltage step.

2.3.2 Electrophysiological Recording Equipment

Microelectrodes were pulled, using a micropipette puller (details as above), from borosilicate glass capillary tubing (0.94mm diameter) containing an internal filament. The pipettes were pulled to give a resistance of 0.3-1MΩ when filled with 3M KCl, which was used for making recordings, and placed in recording solution.

Two electrode tips were placed in Perspex electrode holders (electrode holders contain an electrode wire made of silver that has been coated in chloride ions by immersion in bleach for 20 minutes) and fixed to two headstages (Axon Instruments, USA), which were mounted on two manipulators situated either side of the recording chamber.

The reference electrode was a Ag/AgCl pellet (Clark Electromedical Intruments, UK) in a separate chamber linked by an agar bridge to the recording chamber to avoid leakage of the Ag^+ ions into the recording chamber.

The HS-2A headstages were connected to a GeneClamp 500 amplifier (all Axon instruments, USA). The amplifier was then connected to a PC via a DigiData 1200 series interface (Axon Instruments, USA)

Data was acquired using clampex software (Pclamp version 6, axon instruments, USA).

2.3.3 Perfusion System

The 400µl recording chamber allowed a perfusion rate of 4ml min^{-1} to permit fairly rapid application and wash-out of solutions. The perfusion-in was gravity-driven through a length of flexible tubing and perfusion-out was driven by an electric peristaltic pump. The external recording solution contained 2mM CsOH, 5mM HEPES, 10mM $Ba(OH)_2$ and 70mM NaOH.

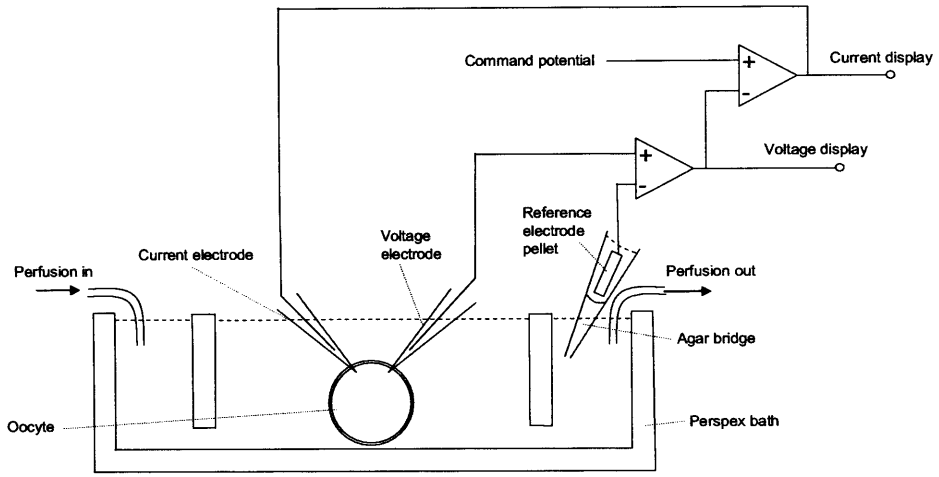

Figure 2.5 The recording chamber and simplified voltage-clamp circuit
The oocyte rests in a bath that is continually perfused with fresh saline. The voltage electrode, together with the bath or 'reference' electrode, monitors changes in the oocyte membrane potential resulting from ion channel activity. The clamp-amplifier constantly compares the actual membrane potential (Vm) with the command potential (Vc) set by the researcher. The clamp-amplifier must increase Vm by a specific amount, the output voltage, to maintain Vc at all times. This is achieved by the injection of current into the cell. The amount of current injected is always exactly equal, but of opposite polarity, to the net current flow through the channels. The current injected (in amps) is recorded and displayed by the clamp-amplifier.

2.3.4 Recording of Currents through Voltage-Dependent Calcium Channels in *Xenopus* Oocytes

The tips of the electrodes were immersed in the recording solution and placed near to, but not touching, the oocyte membrane. The electrodes' potential differences with respect to the bath solution were then zeroed using the amplifier to remove DC offset and lack of drift was ensured. The resistance of each electrode was checked to ensure resistances of between 0.3 and 1 MΩ. The electrodes could then be inserted into the oocyte at the "ten-to-two" positions and a seal allowed to form around the glass. To do this the electrodes are advanced towards the membrane and pressed against the membrane until a dimple in the membrane surface is visible. Then a gentle tap on the manipulator affects penetration. If the gain and stability of the amplifier are turned down to zero, the command voltage can be set to a value that is close to the resting membrane potential of the cell before switching the voltage-clamp on. This minimises the stress caused to the cell membrane when switching the amplifier to voltage-clamp. The clamp was then "tuned" by increasing the stability (phase-lag) to 600μs and gain to 10,000 to give the fastest possible clamp without compromising stability and causing the membrane potential to oscillate. The command voltage was then slowly increased to clamp the membrane at -100mV. This usually resulted in a leak current of between 30 and 150nA.

2.3.5 Leak Subtraction P/4 protocol

Four pulses, each the same duration and one quarter of the magnitude of the test pulse, but opposite polarity were applied before the test pulses. During these steps the probability of $Ca_V2.2$ channel activation is very low; any current elicited during these pulses was assumed to be leak and therefore subtracted from the current evoked by the test pulse.

2.3.6 Filtering and Sampling

Signals were low pass Bessel filtered at 1kHz (-3dB) and sampled at a rate of either 5 or 10kHz.

2.4 Analysis of currents

Initial analysis was carried out in clampfit (pclamp6, axon instruments). The current amplitudes were measured isochronally; the mean current between 10 and 15ms from start of each test pulse was found (Figure 2.4).

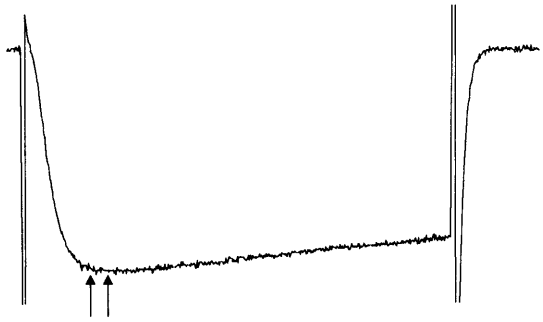

Figure 2.6 Mean currents were measured between 10 and 15 ms into test pulse (indicated by red arrows).

These were then imported into Origin 7, graphing and data analysis software, (OriginLab, USA).

Data are expressed mean ± SEM. All data were normally distributed, this was confirmed using the Shapiro-Wilk method. Statistical analysis was performed using Student's t-test. Differences with P values of 0.05 and under are referred to as significant throughout.

Chapter 3 Results 1

3.1 The current-voltage relationship

The current-voltage relationships (IV) were recorded using a pulse protocol of sequential voltage steps from holding potential of -100mV to between -60mV and +70mV at 5mV intervals (Figure 3.1A). The mean currents between 10-15ms from the start of the test pulse were measured and plotted against test potential (Figure 3.1B).

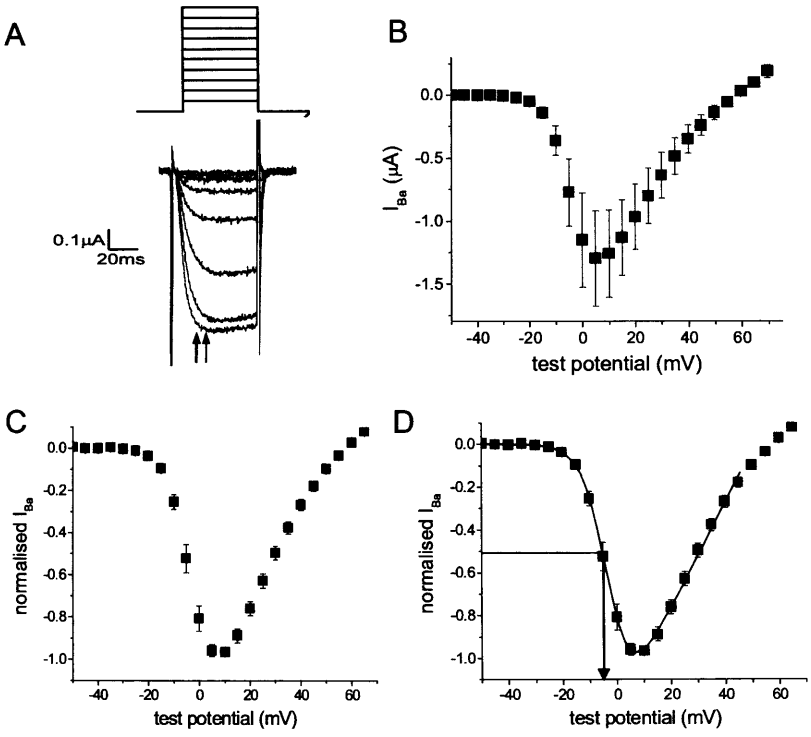

Figure 3.1. Current-voltage relationship for $Ca_V2.2/\beta_1b/\alpha_2\delta$-2. ***A*** Command voltage steps and corresponding current trace. Mean current measured between 10-15ms into test pulse (indicated by red arrows). ***B*** Current plotted against test potential. ***C*** Mean normalised current plotted against test potential. ***D*** Fit is a combination of a Boltzmann and a straight line. V_{50} = -2.76±0.17 mV (indicated by green arrow).

When oocytes express proteins from injected cDNA, they do so at variable degrees (as do all heterologous expression systems). Therefore, the whole-cell currents can vary enormously between oocytes, even within the same ovary. One of the factors influencing this could be the volume of cDNA solution injected, as with such small volumes as 4.9nl, it is very difficult to ensure accuracy. The developmental stage of the oocytes may also influence the amount of protein that is synthesised and trafficked to the plasma membrane. To allow the whole-cell currents from different oocytes to be compared, it was necessary to normalise the currents. This was done by dividing the current at each potential by the maximum current for that cell, which usually occurred at a test potential of +5 - +20mV. Figure 3.1C shows the normalised currents plotted against test potential. These points were fit with a combination of a Boltzmann and a straight line using equation 3.1 (Figure 3.1D). Fitting this curve allows the half activation, V_{50}, to be found (indicated by green arrow Figure 3.1D)

$$I = G_{max}(V-V_{rev})/(1+\exp(-(V-V_{50})/k)) \qquad \text{Equation 3.1}$$

Where G_{max} is maximum slope conductance, V_{50} is mid-point of activation, V_{rev} is the apparent reversal potential, and k is the slope factor for activation.

3.2 Over-expressing $G\beta_1\gamma_2$

$G\beta_1$ and $G\gamma_2$ were co-expressed with the calcium channel subunits in a ratio of α_1:$G\beta_1$:$G\gamma_2$, 3:1:1, to provide a high concentration of free $G\beta_1\gamma_2$ dimers.

The high concentration of free $G\beta_1\gamma_2$ causes the channels to be tonically modulated by $G\beta\gamma$. This modulation is removed by strong depolarization, this is known as facilitation and is a defining characteristic of $G\beta\gamma$ modulation of the Ca_V2 family channels. The three-pulse protocol is routinely used to study $G\beta\gamma$ modulation of Ca_V2 family channels. This consists of two identical test pulses separated by pre-pulse to 100mV (Figure 3.2A). To demonstrate pre-pulse facilitation, the three-pulse protocol was applied to cells expressing $Ca_V2.2\alpha_1$, β_1b, $\alpha_2\delta$-2, $G\beta_1$ and $G\gamma_2$. The current-voltage relationship shows that the test pulse after the pre-pulse, P2, evoked a larger current than the test pulse before the pre-pulse, P1, at all test potentials at which the currents were activated (Figure 3.2B).

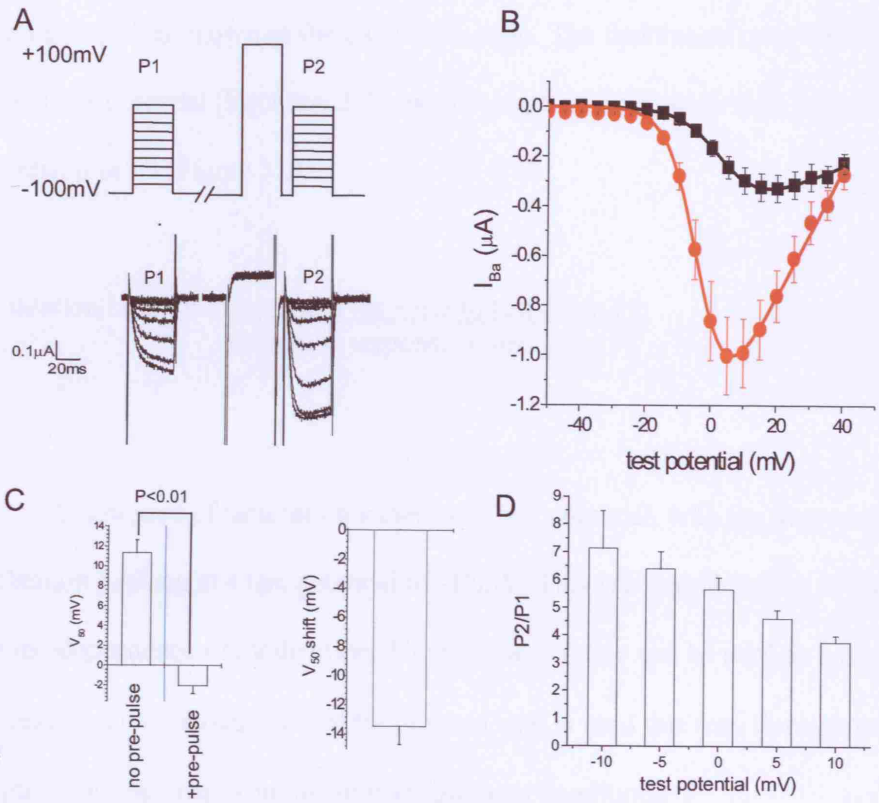

Figure 3.2. When $G\beta_1\gamma_2$ is over-expressed a depolarising pre-pulse affects facilitation. ***A*** Three pulse protocol voltage commands and corresponding current trace. ***B*** Current plotted against test potential (n=15). No pre-pulse black squares, + pre-pulse red circles. ***C*** V_{50} with and without pre-pulse (left). Shift in V_{50} due to pre-pulse (right). ***D*** Facilitation ratio plotted against test potential (n=15).

The pre-pulse also causes a hyperpolarising shift in the half activation potential, V_{50} (Figure 3.2C). This is a manifestation of the voltage-dependence of modulation. A combination of a Boltzmann and a straight line was fit, and the V_{50} found before and after the pre-pulse. The shift in V_{50} of -13.4 ± 1.3 mV (n=15) due to pre-pulse was significant, $P<0.01$.

The ratio of the current in response to test pulse P1 and the current in response to test pulse P2 is known as the facilitation ratio. The facilitation ratio was calculated at each test potential (Equation 3.2) and the graph of facilitation ratio against test potential plotted (Figure 3.2D).

$$\text{Facilitation ratio} = \frac{\text{current in response to test pulse P2}}{\text{current in response to test pulse P1}} \qquad \text{Equation 3.2}$$

The degree of facilitation varied with test potential, with the degree of facilitation peaking at a test potential of -10mV. This is a manifestation of the voltage-dependence of modulation. The facilitation ratio can be used as a measure of the degree of Gβγ modulation of the channel, and is used this way throughout this chapter as a reference point to compare different conditions.

3.2.1 $Ca_V2.2$(R52,54A) does not display pre-pulse facilitation when $G\beta_1\gamma_2$ is over-expressed

Previously, two arginines in the N-terminus of $Ca_V2.2$ have been shown to be essential for Gβγ modulation. If the arginines at positions 52 and 54 on the N-terminus of $Ca_V2.2$ are mutated to alanines, Gβγ modulation is completely abolished (Canti et al. 1999). I have reproduced these results here by expressing the

$Ca_V2.2$(R52,54A) along with the auxiliary subunits β_1b and $\alpha_2\delta$-2 and $G\beta_1\gamma_2$. The current-voltage relationships of $Ca_V2.2$(R52,54A) are almost identical before and after the pre-pulse when $G\beta_1\gamma_2$ is over-expressed (Figure 3.3A). There is a slight reduction in current in response to test pulse P2, after the pre-pulse, compared to the current in response to test pulse P1, before the pre-pulse. This is probably due to inactivation of the channel during the pre-pulse. The properties of inactivation are addressed in section 1.3. The half activation potential, V_{50}, after the pre-pulse is the same as that before the pre-pulse (Figure 3.3B) The facilitation ratio of $Ca_V2.2$(R52,54A) is close to 1 (Figure 3.3C), indicating an absence of pre-pulse facilitation and therefore Gβγ modulation. The absence of Gβγ modulation of $Ca_V2.2$(R52,54A) is further supported by the monophasic shape of the activation of the current (Figure 3.3D).

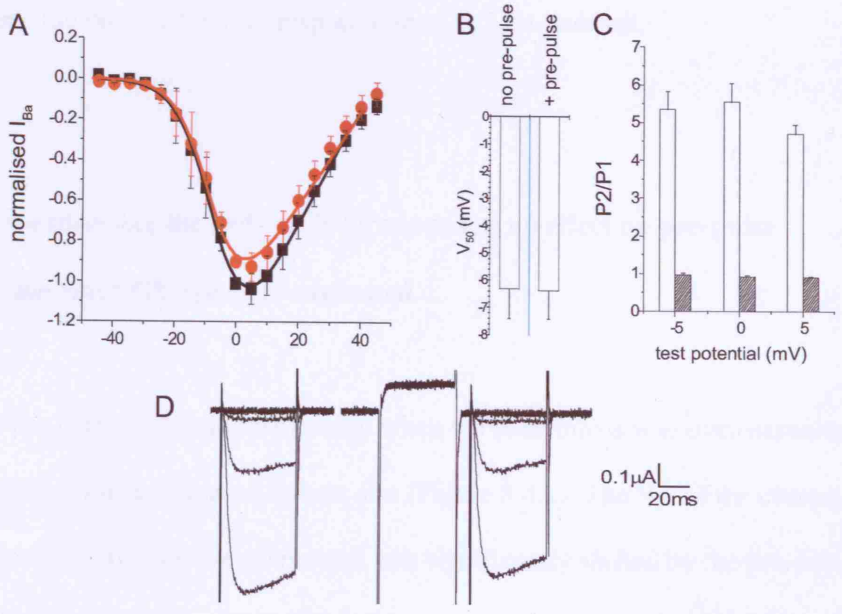

Figure 3.3. $Ca_V2.2$(R52,54A) does not display pre-pulse facilitation when Gβγ over-expressed. ***A*** Normalised current plotted against test potential (n=5). No pre-pulse black squares, + pre-pulse red circles. ***B*** V_{50} with and without pre-pulse (n=5). ***C*** Facilitation ratio plotted against test potential, $Ca_V2.2$ open bars (n=6), $Ca_V2.2$(R52,54A) hatched bars (n=5). ***D*** Current trace of $Ca_V2.2$(R52,54A) when Gβγ over-expressed.

3.2.2 Isolated N-terminus

Previously, cDNA coding for the first 95 amino acids of $Ca_V2.2$ had been made (Raghib et al., 2001). This construct allowed the isolated N-terminus of $Ca_V2.2$ to be expressed as a discrete protein fragment along with $Ca_V2.2$, β_1b, $\alpha_2\delta$-2. It was hypothesised that if a binding site for $G\beta\gamma$ was contained within the N-terminus of $Ca_V2.2$, then the over-expression of the isolated N-terminus could cause sequestering of free $G\beta_1\gamma_2$, therefore reducing the availability of $G\beta_1\gamma_2$ for modulation of the channel and causing a reduction in modulation. The ratio of the injected cDNA of the isolated N-terminus was 1:1 concentration ratio with respect to the cDNA of the $Ca_V2.2\alpha_1$ subunit. As a control, cDNA coding for the isolated N-terminus was replaced with empty vector plasmid in the injection solution at the same concentration ratio of 1:1 with respect to the $Ca_V2.2\alpha_1$ subunit.

3.2.3 Co-expressing the isolated N-terminus has no effect on pre-pulse facilitation when $G\beta_1\gamma_2$ is over-expressed.

The current-voltage relationship when the N-terminus was over-expressed shows the pre-pulse increased current size (Figure 3.4A). The V_{50} of the current with the isolated N-terminus over-expressed was significantly shifted by the pre-pulse ($P<0.01$) (Figure 3.4B) and this shift in V_{50} was comparable to the shift in V_{50} seen when the cDNA coding for the isolated N-terminus in the injection solution was

replaced with empty vector plasmid (Figure 3.4C). There was a small reduction in the facilitation ratio when the isolated N-terminus was expressed compared to when cDNA coding for the isolated N-terminus was replaced in the injection solution with the empty vector plasmid, but my results did not show this reduction to be significant (Figure 3.4D).

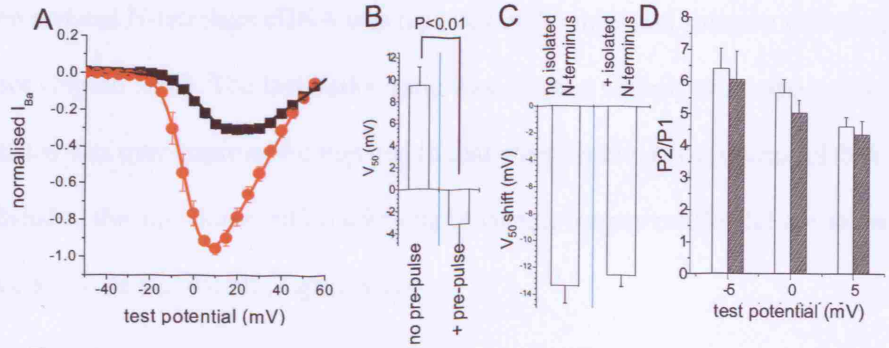

Figure 3.4. Co-expressing the isolated N-terminus has no effect on pre-pulse facilitation when Gβγ over-expressed. ***A*** Normalised current plotted against test potential. No pre-pulse black squares, + pre-pulse red circles (n=6). ***B*** V_{50} with and without pre-pulse (n=6). ***C*** Shift in V50 due to pre-pulse, with isolated N-terminus (n=6) compared to without (n=15). ***D*** Pre-pulse facilitation ratio plotted against test potential. $Ca_V2.2$ (n=15) open bars, $Ca_V2.2$ + isolated N-terminus hatched bars (n=6).

The isolated N-terminus is a small fragment so may be degraded quickly so in an attempt to increase the concentration of the isolated N-terminus at the membrane, the cDNA ratio of the isolated N-terminus in the injection solution was increased to 3:1 isolated N-terminus:$Ca_V2.2\alpha_1$. All other cDNAs were kept at a ratio of 1:1 with respect to the $Ca_V2.2\alpha_1$.

3.2.4 Co-expressing the isolated N-terminus in a higher ratio had no effect on pre-pulse facilitation when $G\beta_1\gamma_2$ was over-expressed.

The current-voltage relationship when the isolated N-terminus was over-expressed in a higher ratio of cDNA concentration, showed that the pre-pulse increased current size (Figure 3.5A). The V_{50} was significantly shifted by pre-pulse (Figure 3.5B) and this shift was shown to not be significantly different from that when isolated N-terminus cDNA was replaced in the injection solution with empty vector (Figure 3.5C). The facilitation ratio was reduced slightly when the isolated N-terminus was over-expressed compared to that when isolated N-terminus cDNA was replaced in the injection solution with empty vector, but my results did not show this reduction to be significant (Figure 3.5D).

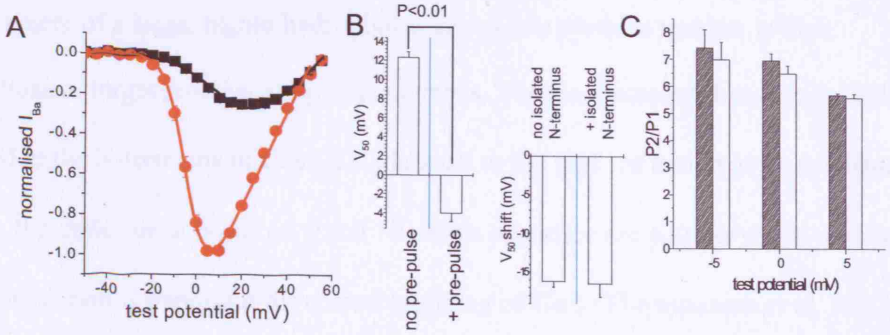

Figure 3.5. Co-expressing a higher ratio of the isolated N-terminus had no effect on pre-pulse facilitation when Gβγ over-expressed. ***A*** Normalised current plotted against test potential. No pre-pulse black squares, + pre-pulse red circles (n=3). ***B*** V_{50} with and without pre-pulse (n=3). ***C*** Pre-pulse facilitation ratio plotted against test potential. $Ca_V2.2$ (n=3) open bars, $Ca_V2.2$ + isolated N-terminus hatched bars (n=3).

3.2.5 Palmitoylation motif $Ca_V2.2$(R52,54A) did not display pre-pulse facilitation when $G\beta_1\gamma_2$ over-expressed.

The possibility that the RAR sequence at positions 52 and 54 on the N-terminus of $Ca_V2.2$ might form a PIP_2 binding site, thus anchoring the N-terminal tail to the membrane, has been suggested previously (Dolphin 2003). This would mean that when the arginines were mutated, and the N-terminal tail no longer anchored, the mobile N-terminus might prevent $G\beta\gamma$ interaction and so prevent modulation of the channel. To investigate this, a sequence of ten amino acids, containing two palmitoylation sites, was added to the N-terminus of $Ca_V2.2$(R52,54A). This construct was termed palmitoylation motif $Ca_V2.2$(R52,54A).

Palmitoylation is a common lipid modification resulting in the covalent attachment of a large, highly hydrophobic group to a cysteine residue, which functions to target proteins in lipid membranes. The ten amino acid sequence that was added to the N-terminus of $Ca_V2.2$ is identical to the first ten amino acids of $G\alpha q$. In $G\alpha q$, the cysteines at positions 9 and 10 of this sequence are palmitoylated and this palmitoylation is important for correct targeting of $G\alpha q$ (Thiyagarajan et al. 2002).

3.2.6 Palmitoylation motif $Ca_V2.2$(R52,54A) did not display pre-pulse facilitation when $G\beta_1\gamma_2$ was over-expressed.

The current-voltage relationship was almost identical before and after pre-pulse (Figure 3.6A). The V_{50} was similar before and after pre-pulse, and my results showed these to not be significantly different from each other (Figure 3.6B). The very slight shift in V_{50} before and after pre-pulse for the palmitoylation motif $Ca_V2.2$(R52,54A) was significantly different to the shift in V_{50} seen for wild-type $Ca_V2.2$ ($P<0.01$) (Figure 3.6C). The facilitation ratio for the palmitoylation motif $Ca_V2.2$(R52,54A) was close to 1, and this was significantly smaller than the facilitation ratio of wild type $Ca_V2.2$ ($P<0.01$) (Figure 3.6D).

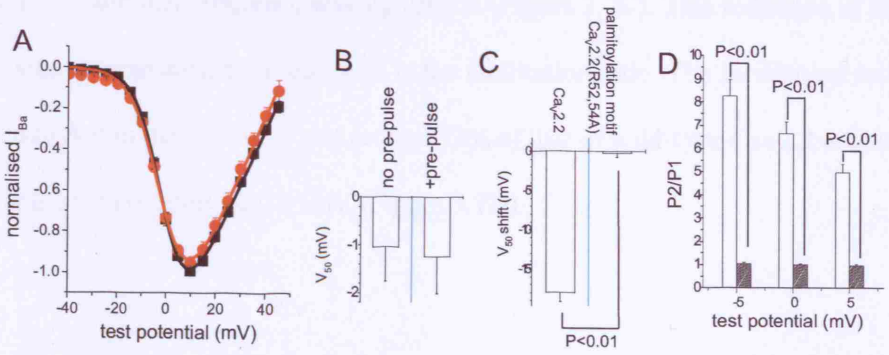

Figure 3.6. Palmitoylation motif $Ca_V2.2$(R52,54A) did not display pre-pulse facilitation when $G\beta\gamma$ over-expressed. ***A*** Normalised current plotted against test potential. No pre-pulse black squares, + pre-pulse red circles (n=10). ***B*** V_{50} with and without pre-pulse (n=10). ***C*** Shift in V_{50} due to pre-pulse. $Ca_V2.2$ (n=10) compared to palmitoylation motif $Ca_V2.2$(R52,54A) (n=10). ***D*** Pre-pulse facilitation ratio plotted against test potential. Control (n=10) open bars, palmitoylation motif $Ca_V2.2$(R52,54A) hatched bars (n=10).

The palmitoylation motif was added to the wild type $Ca_V2.2$ (termed palmitoylation motif $Ca_V2.2$), i.e. with the arginines at positions 52 and 54. This construct was originally made as a control for the palmitoylation motif $Ca_V2.2$(R52,54A).

3.2.7 Palmitoylation motif $Ca_V2.2$ showed reduced pre-pulse facilitation ratio when $G\beta_1\gamma_2$ over-expressed.

The current-voltage relationship of the palmitoylation motif $Ca_V2.2$ showed that the pre-pulse did increase current size (Figure 3.7A). The V_{50} of the current was significantly shifted by the pre-pulse ($P<0.01$)(Figure 3.7B). However, the shift in V_{50} of the palmitoylation motif $Ca_V2.2$ was around 5.3mV smaller than that of wild-type $Ca_V2.2$, and this difference was significant (Figure 3.7C). This reduction in shift in V_{50} was accompanied by a reduction in the facilitation ratio. The facilitation ratio of palmitoylation motif $Ca_V2.2$ was around 72% of that of wild-type $Ca_V2.2$ at test potentials of -5mV, 0mV and +5mV (Figure 3.7D).

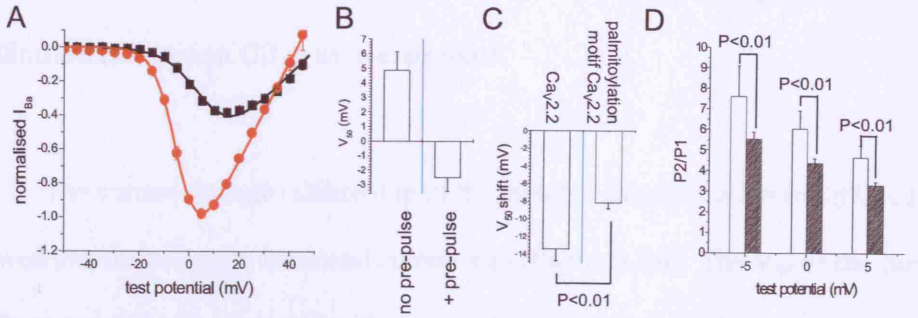

Figure 3.7. Palmitoylation motif $Ca_V2.2$ displays reduced pre-pulse facilitation when Gβγ over-expressed. ***A*** Normalised current plotted against test potential. Control black squares, + pre-pulse red circles (n=19). ***B*** V_{50} with and without pre-pulse (n=19). ***C*** Shift in V_{50} due to pre-pulse. Wild type $Ca_V2.2$ (n=15) compared to palmitoylation motif $Ca_V2.2$ (n=19). ***D*** Pre-pulse facilitation ratio plotted against test potential. $Ca_V2.2$ (n=15) open bars, palmitoylation motif $Ca_V2.2$ hatched bars (n=19).

This may indicate that the mobility of the N-terminus is required for Gβγ modulation, and that reducing this mobility has a negative effect on Gβγ modulation.

As a control, a mutated palmitoylation motif $Ca_V2.2$ was made. This construct consisted of the same ten amino acid sequence added onto the N-terminus of $Ca_V2.2$, but with two cysteines mutated to serines to prevent palmitoylation and thus any membrane anchoring effects of palmitoylation would be lost.

3.2.8 The mutated palmitoylation motif $Ca_V2.2$ showed reduced pre-pulse facilitation ratio when $G\beta_1\gamma_2$ over-expressed.

The current-voltage relationship of the mutated palmitoylation motif $Ca_V2.2$ showed that the pre-pulse increased current size (Figure 3.8A). The V_{50} of the current of the mutated palmitoylation motif was significantly shifted by the pre-pulse ($P<0.01$) (Figure 3.8B). The shift in V_{50} was around 6.0mV smaller than the shift in V_{50} of the wild-type $Ca_V2.2$ current, and this difference was significant ($P<0.01$) (Figure 3.8C). The facilitation ratio was around 68% of the facilitation ratio of wild-type $Ca_V2.2$ at test potentials of -5mV, 0mV and +5mV (Figure 3.8D). This reduction in pre-pulse facilitation was significant at test potentials of 0mV and +5mV.

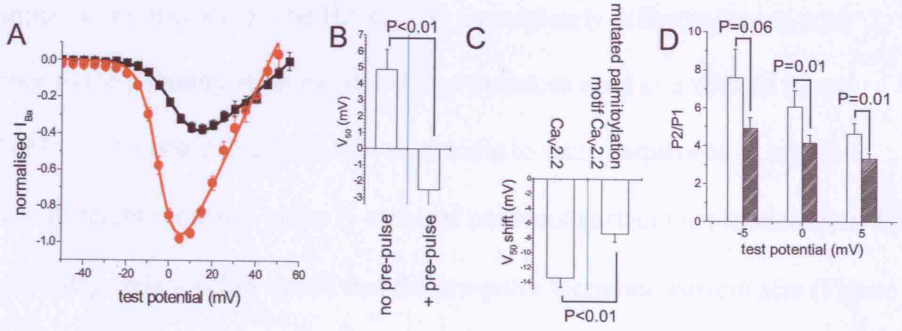

Figure 3.8. Mutated palmitoylation motif $Ca_V2.2$ displays reduced pre-pulse facilitation when $G\beta\gamma$ over-expressed. ***A*** Normalised current plotted against test potential. No pre-pulse black squares, + pre-pulse red circles (n=12). ***B*** V_{50} with and without pre-pulse (n=12). ***C*** Shift in V_{50} due to pre-pulse. Wild type $Ca_V2.2$ (n=15) compared to mutated palmitoylation motif $Ca_V2.2$ (n=12). ***D*** Pre-pulse facilitation ratio against test potential. $Ca_V2.2$ (n=15) open bars, mutated palmitoylation motif hatched bars (n=12).

Based on these results, it seemed unlikely that any mobility reducing effect of the N-terminal palmitoylation motif was responsible for the reduction in facilitation. It was then necessary to determine whether the reduction in pre-pulse facilitation, which was caused by the palmitoylation motif and the mutated palmitoylation motif added onto the N-terminus, was specific to those sequences or whether anything added onto the N-terminal tail would affect Gβγ modulation.

3.2.9 Haemagglutinin tagged $Ca_V2.2$ had reduced pre-pulse facilitation when $G\beta_1\gamma_2$ was over-expressed.

A construct consisting of a nine amino acid haemagglutinin (HA) tag sequence on the N-terminus of $Ca_V2.2$ was expressed in place of the wild type $Ca_V2.2$ (see appendix for methods). The HA tag has a completely different amino acid sequence to the palmitoylation motif and was therefore used as a control to see whether the reduction in modulation was specific to some sequences or whether adding a different sequence to the N-terminal tail would affect Gβγ modulation. The current-voltage relationship shows that the pre-pulse increased current size (Figure 3.9A). The V_{50} of the current was significantly shifted by the pre-pulse ($P<0.01$) (Figure 3.9B). The shift of the V_{50} was around 6.4mV smaller than the shift in V_{50} due to pre-pulse of the wild-type $Ca_V2.2$ current (Figure 3.9C). The facilitation ratio of the HA tagged $Ca_V2.2$ was about 64% of that for wild-type $Ca_V2.2$ at test

potentials of -5mV, 0mV and +5mV (Figure 3.9D), and this difference was significant at these potentials.

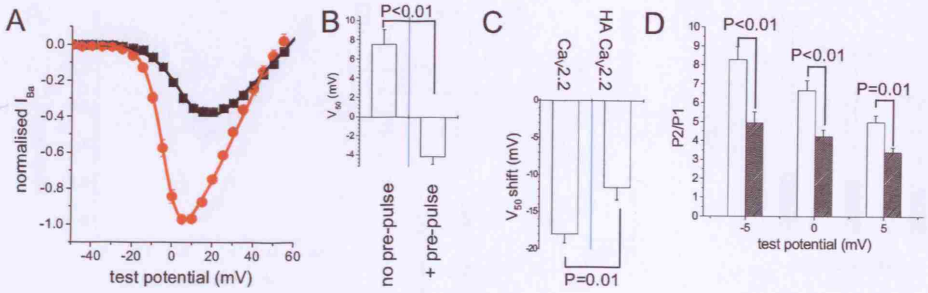

Figure 3.9. HA $Ca_V2.2$ displays reduced pre-pulse facilitation when Gβγ over-expressed. ***A*** Normalised current plotted against test potential. No pre-pulse black squares, + pre-pulse red circles (n=8). ***B*** V_{50} with and without pre-pulse (n=8). ***C*** Shift in V_{50} due to pre-pulse. HA $Ca_V2.2$ (n=8) compared to wild type $Ca_V2.2$ (n=10). ***D*** Pre-pulse facilitation ratio plotted against test potential. Control (n=10) open bars, HA $Ca_V2.2$ hatched bars (n=8).

3.2.10 GFP tagged $Ca_V2.2$ had reduced pre-pulse facilitation when $G\beta_1\gamma_2$ was over-expressed.

A construct consisting of a green fluorescent protein (GFP) fused to the N-terminus of $Ca_V2.2$ (Raghib et al. 2001) was expressed as another control. The current-voltage relationship of GFP tagged $Ca_V2.2$ shows that the pre-pulse increased current size (Figure 3.10A). The V_{50} of the current was significantly shifted by the pre-pulse (P=0.01) (Figure 3.10B). The shift of the V_{50} was around 13.7mV smaller than that of the wild-type $Ca_V2.2$ current (Figure 3.10C). The facilitation ratio was

about 41% of that for wild-type $Ca_V2.2$ at test potentials of -5mV, 0mV and +5mV (Figure 3.10D).

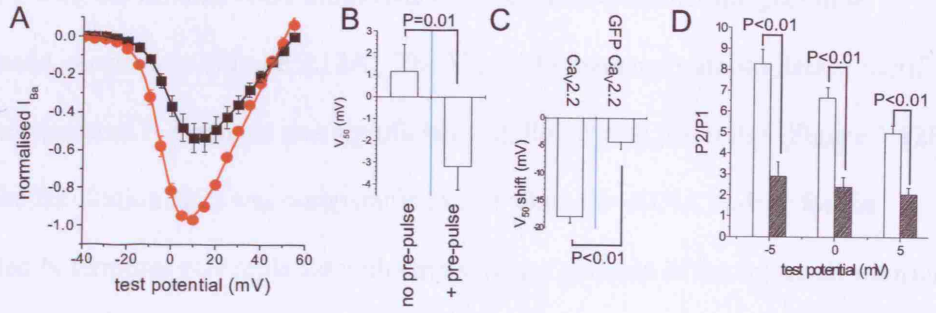

Figure 3.10. GFP $Ca_V2.2$ displays reduced pre-pulse facilitation when $G\beta\gamma$ over-expressed. ***A*** Normalised current plotted against test potential. No pre-pulse black squares, + pre-pulse red circles (n=12). ***B*** V_{50} with and without pre-pulse (n=12). ***C*** Shift in V_{50} due to pre-pulse. GFP $Ca_V2.2$ (n=12) compared to wild type $Ca_V2.2$ (n=10). ***D*** Pre-pulse facilitation ratio plotted against test potential. $Ca_V2.2$ (n=10) open bars, GFP $Ca_V2.2$ hatched bars (n=12).

3.2.11 Co-expressing the isolated N-terminus with palmitoylation motif $Ca_V2.2$ or mutated palmitoylation motif $Ca_V2.2$ had no effect on pre-pulse facilitation when $G\beta_1\gamma_2$ was over-expressed.

Expressing the isolated N-terminus with either the palmitoylation motif $Ca_V2.2$ or the mutated palmitoylation motif $Ca_V2.2$ had no further effect on pre-pulse facilitation of the two constructs when co-expressed at a 1:1 ratio with respect to the $Ca_V2.2a1$ subunit. The current-voltage relationship of the palmitoylation motif $Ca_V2.2$ with the isolated N-terminus over-expressed, showed that the pre-pulse increased current size (Figure 3.11A). The V_{50} of the palmitoylation motif $Ca_V2.2$

plus the isolated N-terminus was significantly shifted by the pre-pulse (Figure 3.11B) and the facilitation ratio was comparable to that when the cDNA coding for the isolated N-terminus was replaced with empty vector plasmid in the injection solution (Figure 3.11C). The current-voltage relationship of the mutated palmitoylation motif $Ca_V2.2$ with the isolated N-terminus over-expressed showed that the pre-pulse increased current size (Figure 3.12A). The V_{50} of the mutated palmitoylation motif plus the isolated N-terminus was significantly shifted by the pre-pulse (Figure 3.12B) and the facilitation ratio was comparable to that when the cDNA coding for the isolated N-terminus was replaced with empty vector plasmid in the injection solution (Figure 3.12C).

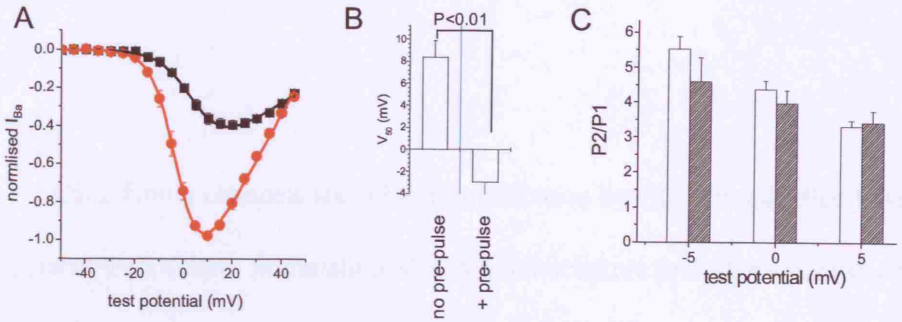

Figure 3.11. Co-expressing the isolated N-terminus and palmitoylation motif $Ca_V2.2$ had no effect on pre-pulse facilitation when Gβγ was over-expressed. ***A*** Normalised current plotted against test potential. No pre-pulse black squares, + pre-pulse red circles (n=9). ***B*** V_{50} with and without pre-pulse (n=9). ***C*** Pre-pulse facilitation ratio plotted against test potential. Palmitoylation motif $Ca_V2.2$ (n=19) open bars, palmitoylation motif $Ca_V2.2$ + isolated N-terminus hatched bars (n=9).

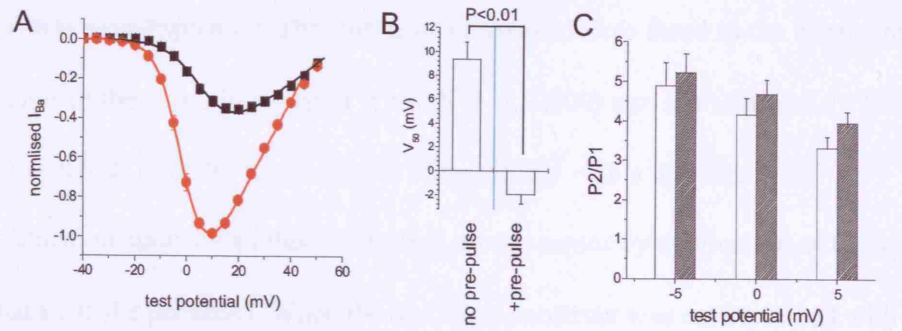

Figure 3.12. Co-expressing the isolated N-terminus with mutated palmitoylation motif $Ca_V2.2$ had no effect on pre-pulse facilitation when Gβγ was over-expressed. ***A*** Normalised current plotted against test potential. No pre-pulse black squares, + pre-pulse red circles (n=9). ***B*** V_{50} with and without pre-pulse (n=9). ***C*** Pre-pulse facilitation ratio plotted against test potential. Mutated palmitoylation motif $Ca_V2.2$ (n=12) open bars, mutated palmitoylation motif $Ca_V2.2$ + isolated N-terminus hatched bars (n=9).

3.3 Clonidine mediated inhibition

Ca_V2 family channels are subject to inhibition by Gβγ subunits that have dissociated from Gαi/o. Stimulation of α_2A adrenoceptors provides a pathway for activation of Gi/o G-proteins and so α_2A adrenoceptor stimulation can inhibit Ca_V2 family channels via Gβγ. In order to investigate Gβγ modulation in an acutely activated system, rather than the tonic situation attained when $G\beta_1\gamma_2$ is over-expressed, cDNA coding for the α_2A adrenoceptor – Gαo tandem construct (α_2A-Gαo) was over-expressed. This construct consists of Gαo fused to the intracellular C-terminus of the α_2A adrenoceptor (Cavalli et al., 2000) also see section 2.1. This fusion product provides a high degree of specificity with a low degree of amplification upon stimulation of the α_2A adrenoceptor by application of the agonist clonidine in the perfusate. When the α_2A-Gαo construct was co-expressed with the calcium channel subunits, $G\beta_1\gamma_2$ was not over-expressed and the Gβγ that were activated and involved in channel modulation were endogenous to the oocytes. The advantage of using the receptor and endogenous Gβγ over over-expressing $G\beta_1\gamma_2$ is that the currents can be recorded in the absence of Gβγ modulation and endogenous Gβγ can be acutely activated so that unmodulated and modulated currents can be compared directly.

Clonidine inhibited currents when applied in the perfusate at a concentration of 100nM. Current-voltage relationships were recorded in the absence and presence

of clonidine (Figure 3.13A). The mean currents between 10-15ms into the test pulses were plotted against test potential (Figure 3.13B). Currents were inhibited at all potentials at which the current was activated.

The inhibition was calculated as a percentage of control current at each test potential (Equation 3.3) and plotted against test potential (Figure 3.13C).

% inhibition = 100-((+clonidine/control)*100) Equation 3.3

The degree of inhibition varied with test potential. This is a feature of the voltage-dependence of modulation.

The application of clonidine caused a depolarising shift in the V_{50} of the current of 3.92±0.4mV, compared to the current recorded in the absence of clonidine (Figure 3.13D).

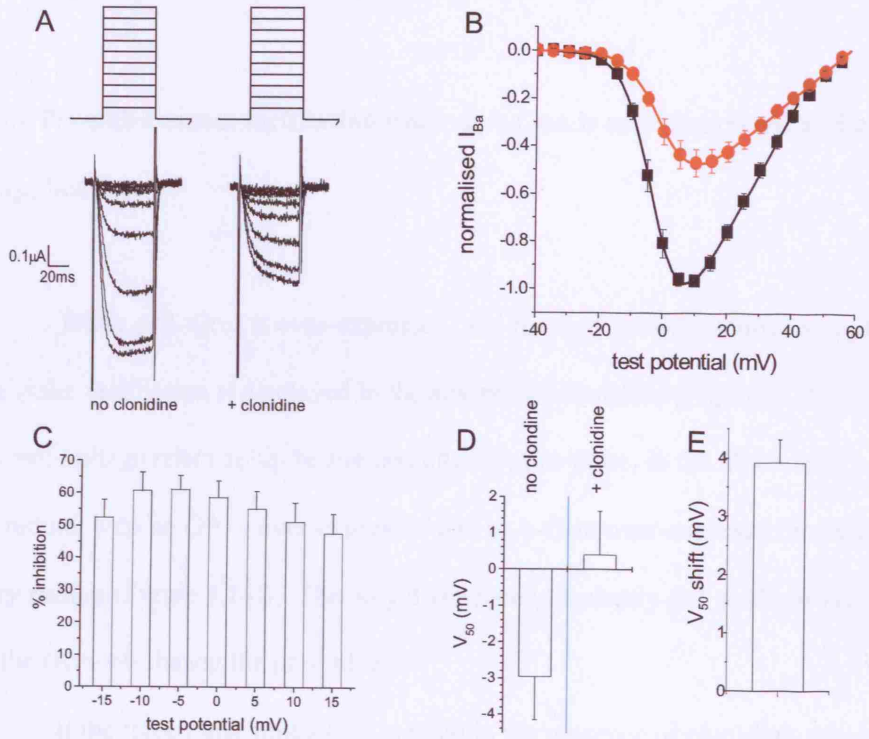

Figure 3.13. Application of clonidine in the perfusate mediates channel inhibition when α_2A-Gα_o is over-expressed. ***A*** Pulse protocol and corresponding current traces of IVs in absence (left) and presence (right) of clonidine. ***B*** Normalised current plotted against test potential (n=6). No clonidine black squares, + clonidine red circles. ***C*** % inhibition plotted against test potential (n=6). ***D*** V_{50} in absence and presence of clonidine (n=6). ***E*** Shift in V_{50} due to clonidine (n=6).

3.4 Pre-pulse facilitation in the presence of clonidine

3.4.1 Pre-pulse causes facilitation when α_2A-Gαo is over-expressed and clonidine is applied

When α_2A-Gαo is over-expressed, and the three pulse protocol is applied, no pre-pulse facilitation is displayed in the absence of clonidine (Figure 3.14A). The current-voltage relationship before and after the pre-pulse, in the absence of clonidine, with no G$\beta_1\gamma_2$ over-expressed and α_2A-Gαo over-expressed instead, looks very similar (Figure 3.14B). The only difference is probably due to slight inactivation of the channels during the pre-pulse.

If the three pulse protocol is applied in the presence of clonidine, when α_2A-Gαo is over-expressed, the current in response to P2 is larger than that in response to P1 (Figure 3.14C). The current-voltage relationship, before and after the pre-pulse, in the presence of clonidine, shows that pre-pulse facilitation is present at all test potentials at which current is activated (Figure 3.14D). The facilitation ratio can be calculated and plotted against test potential (Figure 3.14E). The degree of facilitation varies with test potential, and this is a feature of the voltage-dependence of modulation. In the presence of clonidine the V_{50} is hyperpolarised by 4.5mV by the pre-pulse (Figure 3.14F).

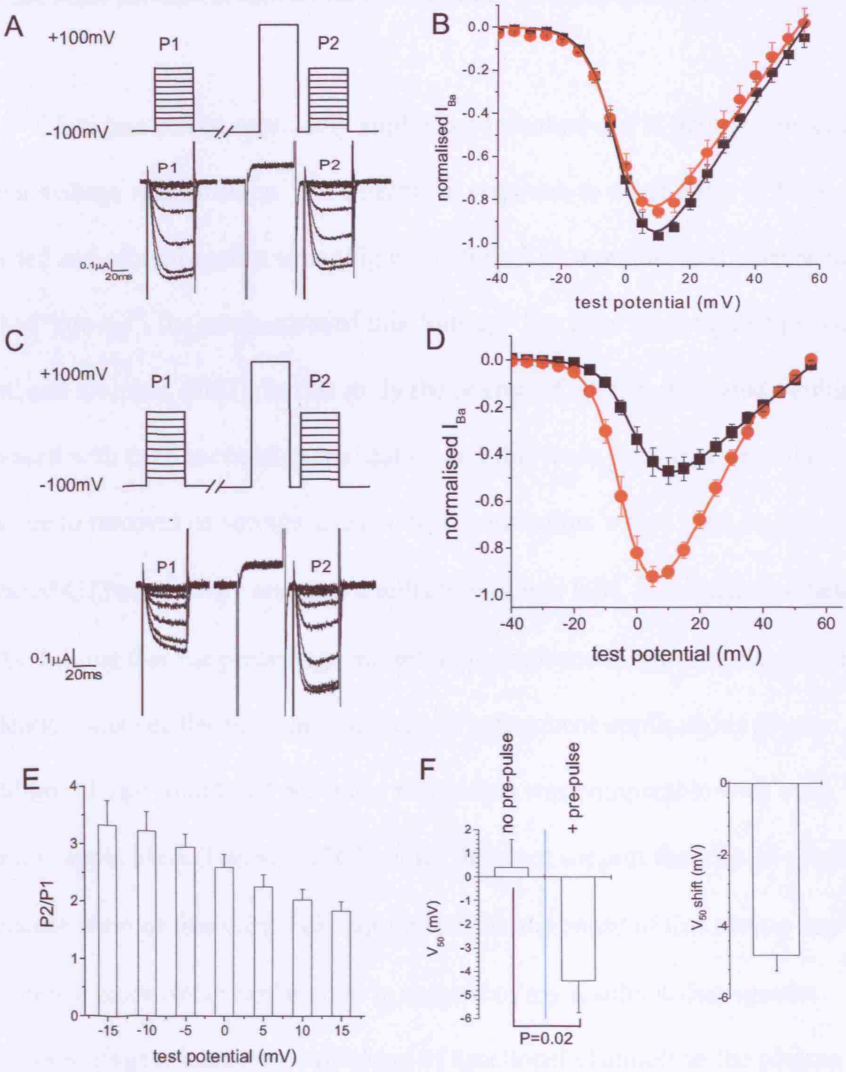

Figure 3.14. When α_2A-Gα_o is over-expressed and in the presence of clonidine, pre-pulse facilitation is displayed by $Ca_V2.2$ channel. ***A*** Three-pulse protocol and corresponding current traces of IVs before and after pre-pulse in absence of clonidine. ***B*** Normalised current plotted against test potential (n=6). No pre-pulse black squares, + pre-pulse red circles. ***C*** Three-pulse protocol and corresponding current traces of IVs before and after pre-pulse in presence of clonidine. ***D*** Normalised current plotted against test potential (n=6). No pre-pulse black squares, + pre-pulse red circles. ***E*** Facilitation ratio in presence of clonidine plotted against test potential (n=6). ***F*** V_{50} with and without pre-pulse (left) (n=6). Shift in V_{50} due to pre-pulse (right) (n=6).

3.5 Clonidine mediated inhibition is reversible and repeatable.

Clonidine can be repeatedly applied and washed-out in between recording current-voltage relationships. The currents in response to a test pulse of 0mV were recorded and plotted against time (Figure 3.15A). The unmodulated current displays a level of "run-up", the mechanism of this "run-up" has been investigated previously (Canti and Dolphin, 2003). In this study the degree of agonist mediated inhibition decreased with each successive application and this leads the suggestion that the run-up is due to removal of voltage-independent modulation, which may be due to increased GTPase activity and thus a reduction in free Gβγ. In contrast to these results, I found that the percentage inhibition in response to the first clonidine application was smaller than the responses to subsequent applications (Figure 3.15B). In addition, I also found that pre-pulse facilitation was comparable with each clonidine application (Figure 3.15C), which does not support the idea of a reduction in concentration of free Gβγ. I did not investigate the cause of this run-up any further but I think a more likely explanation in support of my results is that agonist stimulation triggers increased trafficking of functional channels to the plasma membrane. My proposal is supported by the dependence of run-up on the expression of β-subunits (Canti and Dolphin, 2003), which play a role in trafficking of voltage - dependent calcium channels (see section 1.3.11).

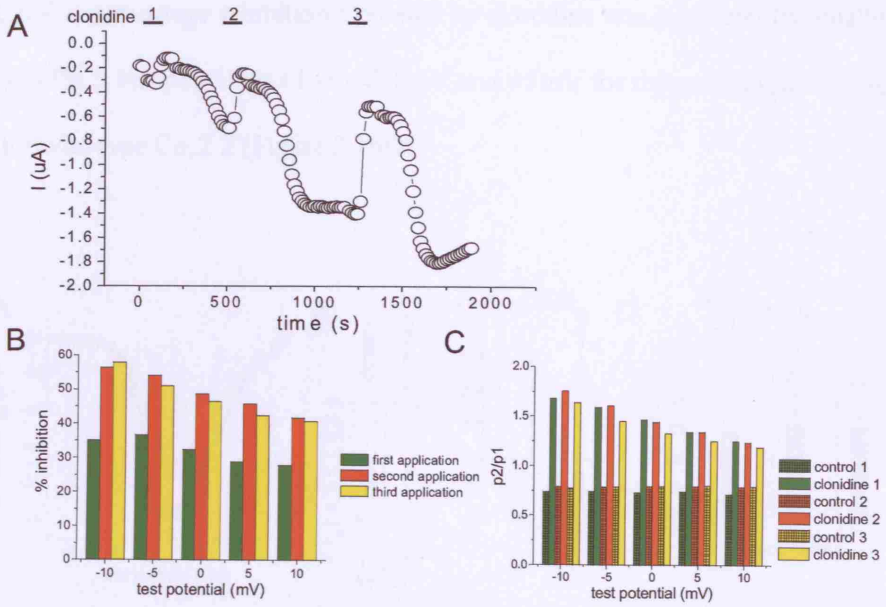

Figure 3.15. Repeated applications of clonidine when α_2A-Gα_o is over-expressed show that the effect is reversible and repeatable. ***A*** Current at 0mV test potential plotted against time for repeated application and wash out of clonidine. ***B*** Clonidine mediated inhibition for first (green bars), second (red bars) and third (yellow bars) application of clonidine. ***C*** Pre-pulse facilitation ratio before, during and after three clonidine applications. Without clonidine (hatched bars) with clonidine (non-hatched bars).

3.6 Clonidine Mediated Modulation

3.6.1 Palmitoylation motif $Ca_V2.2$ has reduced clonidine mediated inhibition when α_2A-Gαo is over-expressed

The current-voltage relationship of when α_2A-Gαo is over-expressed and clonidine is applied, shows that clonidine does inhibit the palmitoylation motif $Ca_V2.2$ current (Figure 3.16A). The application of clonidine also caused a depolarising shift in V_{50} of 1.67±0.6mV compared to that in the absence of clonidine (Figure 3.16B). The shift in V_{50} due to clonidine was significantly smaller by around 2.2mV for the palmitoylation motif $Ca_V2.2$ than for the wild type $Ca_V2.2$ (Figure

3.16C). The percentage inhibition mediated by clonidine was significantly smaller by around 47% at test potentials of -5mV, 0mV and +5mV for the palmitoylated $Ca_V2.2$ than for wild type $Ca_V2.2$ (Figure 3.16D).

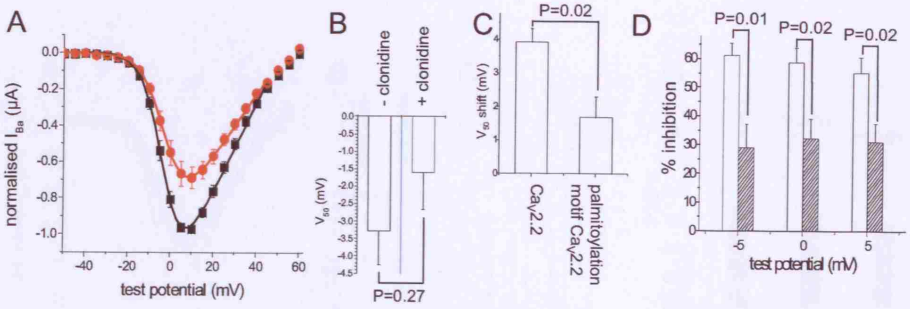

Figure 3.16. Clonidine mediates inhibition of palmitoylation motif $Ca_V2.2$ (n=9) when α_2A-$G\alpha_o$ is over-expressed. ***A*** Normalised current plotted against test potential. - clonidine black squares, + clonidine red circles (n=9). ***B*** V_{50} in absence and presence of clonidine (n=9). ***C*** Shift in V_{50} due to clonidine, palmitoylation motif $Ca_V2.2$ (n=9) compared to wild type $Ca_V2.2$ (n=6). ***D*** % inhibition plotted against test potential. Wild type $Ca_V2.2$ open bars (n=6), mutated palmitoylation motif $Ca_V2.2$ shaded bars (n=9).

3.6.2 Palmitoylation motif $Ca_V2.2$ has reduced pre-pulse facilitation when α_2A-Gαo is over-expressed and clonidine is applied.

The current-voltage relationship of palmitoylation motif $Ca_V2.2$ when α_2A-Gαo is over-expressed and clonidine is applied shows pre-pulse facilitation (Figure 3.17A). The V_{50} of the palmitoylation motif current was significantly hyperpolarised by 3.27±1.0mV by the pre-pulse (Figure 3.17B). The shift in V_{50} due to pre-pulse of the palmitoylation motif $Ca_V2.2$ was significantly smaller by around 1.7mV than that for the wild type $Ca_V2.2$ current (Figure 3.17C). The facilitation ratio of the palmitoylation motif $Ca_V2.2$ was around 40% smaller than the facilitation ratio of

wild type $Ca_V2.2$ at test potentials of -5mV, 0mV and +5mV (Figure 3.17D). This reduction in facilitation ratio was significant.

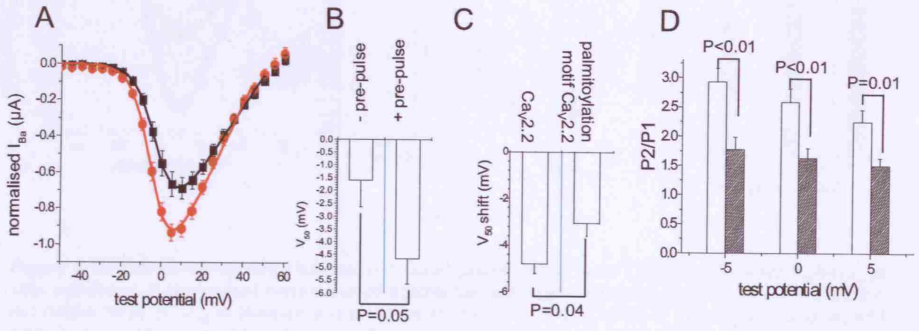

Figure 3.17. Pre-pulse facilitation of palmitoylation motif $Ca_V2.2$ (n=9) is displayed when α_2A-Gα_o is over-expressed and clonidine applied. ***A*** Normalised current plotted against test potential. - pre-pulse black squares, + pre-pulse red circles (n=9). ***B*** V_{50} before and after pre-pulse (n=9). ***C*** Shift in V_{50} due to pre-pulse, palmitoylation motif $Ca_V2.2$ (n=9) compared to wild type $Ca_V2.2$ (n=6). ***D*** Pre-pulse facilitation ratio plotted against test potential. Wild type $Ca_V2.2$ open bars (n=6), palmitoylation motif $Ca_V2.2$ shaded bars (n=9).

3.6.3 Mutated palmitoylation motif $Ca_V2.2$ has reduced clonidine mediated inhibition when α_2A-Gαo is over-expressed.

The current-voltage relationship of the mutated palmitoylation motif $Ca_V2.2$ shows that currents are inhibited when clonidine is applied (Figure 3.18A). Clonidine application caused a depolarising shift in V_{50} of 1.60±1.1mV (Figure 3.18B). My results did not show this shift to be significant. The shift in V_{50} due to clonidine of the mutated palmitoylation motif $Ca_V2.2$ was 2mV smaller than the shift in V_{50} due to clonidine of the wild type $Ca_V2.2$, and this difference was significant (Figure 3.18C). The percentage inhibition mediated by clonidine of the mutated palmitoylation motif

$Ca_V2.2$ was around 20% smaller than that of wild type $Ca_V2.2$ at potentials -5mV, 0mV and +5mV(Figure 3.18D), and this difference was significant at these potentials.

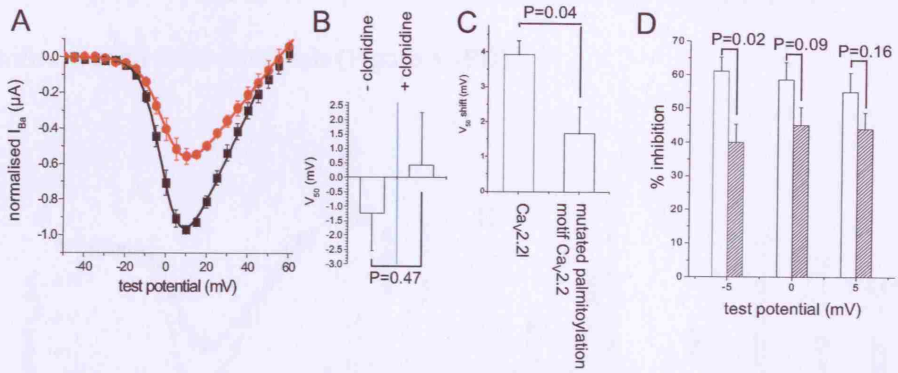

Figure 3.18. Clonidine mediates inhibition of mutated palmitoylation motif $Ca_V2.2$ (n=8) when α_2A-$G\alpha_o$ is over expressed. ***A*** Normalised current plotted against test potential. - clonidine black squares, + clonidine red circles (n=8). ***B*** V_{50} in absence and presence of clonidine (n=8). ***C*** Shift in V_{50} due to clonidine, wild type $Ca_V2.2$ (n=6) compared to mutated palmitoylation motif $Ca_V2.2$ (n=8). ***D*** % inhibition plotted against test potential. Wild type $Ca_V2.2$ (n=6) open bars, mutated palmitoylation motif $Ca_V2.2$ (n=8)shaded bars.

3.6.4 Mutated palmitoylation motif $Ca_V2.2$ has reduced pre-pulse facilitation when α_2A-Gαo is over-expressed and clonidine is applied.

The current-voltage relationship in the presence of clonidine before and after pre-pulse of the mutated palmitoylation motif $Ca_V2.2$ when α_2A-Gαo is over-expressed shows pre-pulse facilitation (Figure 3.19A). The V_{50} of the mutated palmitoylation motif $Ca_V2.2$ current was significantly hyperpolarised by 3mV by the pre-pulse (Figure 3.19B). The shift in V_{50} due to pre-pulse of the mutated palmitoylation motif $Ca_V2.2$ was 1.2mV smaller than the shift in V_{50} due to pre-pulse of the wild type $Ca_V2.2$ in the presence of clonidine when α_2A-Gαo was over-

expressed (Figure 3.19C). This difference between the mutated palmitoylation motif $Ca_V2.2$ and wild type $Ca_V2.2$ was significant. The pre-pulse facilitation ratio of the mutated palmitoylation motif $Ca_V2.2$ was around 15% smaller than that of wild type $Ca_V2.2$ at test potentials of -5mV, 0mV and +5mV, and this difference was significant at all these potentials (Figure 3.19D).

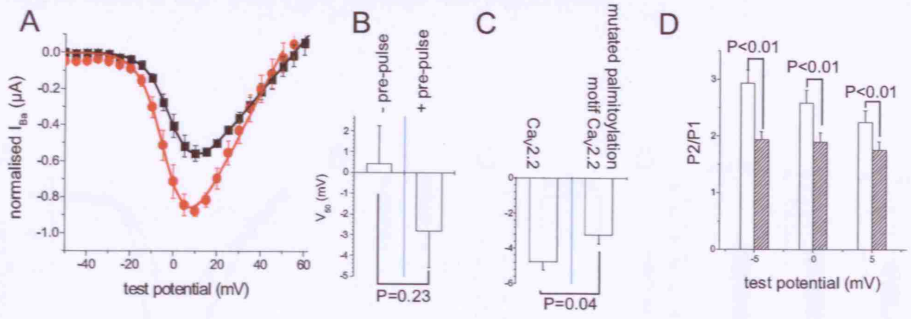

Figure 3.19. Pre-pulse facilitation of mutated palmitoylation motif $Ca_V2.2$ (n=8) is displayed when α_2A-Gα_o is over-expressed and clonidine applied. ***A*** Normalised current plotted against test potential. - pre-pulse black squares, + pre-pulse red circles (n=8). ***B*** V_{50} in before and after pre-pulse (n=8). ***C*** Shift in V_{50} due to pre-pulse, wild type $Ca_V2.2$ (n=6) compared to mutated palmitoylation motif $Ca_V2.2$ (n=8). ***D*** Pre-pulse facilitation ratio plotted against test potential. Wild type $Ca_V2.2$ open bars (n=6), mutated palmitoylation motif $Ca_V2.2$ shaded bars (n=8).

3.6.5 HA tagged $Ca_V2.2$ has reduced clonidine mediated inhibition when α_2A-Gαo is over-expressed.

The current-voltage relationship of the HA tagged $Ca_V2.2$ in the absence and presence of clonidine with α_2A-Gαo over-expressed, shows that clonidine did mediate inhibition (Figure 3.20A). Clonidine application caused a depolarising shift

of 3mV in the V_{50} of the HA tagged $Ca_V2.2$ current, and this was significant (Figure 3.20B). The shift in the V_{50} of the HA tagged $Ca_V2.2$ current due to clonidine application was significantly smaller than that of wild type $Ca_V2.2$ by around 4mV (Figure 3.20C). The clonidine mediated inhibition of the HA tagged $Ca_V2.2$ was around 15% smaller at test potentials of -5mV, 0mV and +5mV than the clonidine mediated inhibition of wild type $Ca_V2.2$ (Figure 3.20D). This difference between the HA tagged $Ca_V2.2$ and wild type $Ca_V2.2$ was significant.

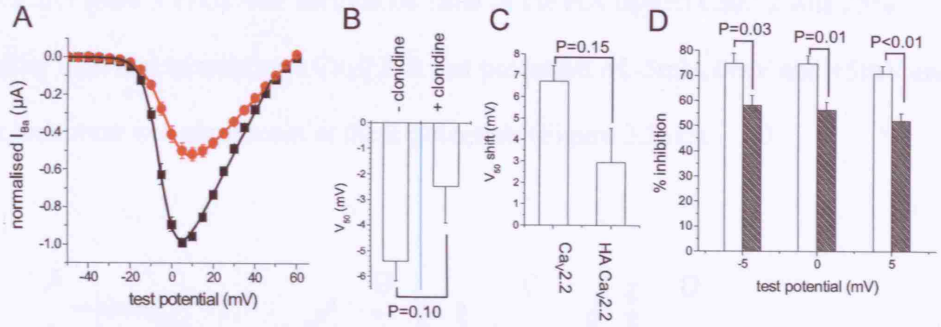

Figure 3.20. Clonidine mediates inhibition of HA $Ca_V2.2$ (n=8) when α_2A-$G\alpha_o$ is over-expressed. ***A*** Normalised current plotted against test potential. - clonidine black squares, + clonidine red circles (n=8). ***B*** V_{50} in presence and absence of clonidine (n=8). ***C*** Shift in V_{50} due to clonidine, wild type $Ca_V2.2$ (n=4) compared to HA $Ca_V2.2$ (n=8). ***D*** % inhibition plotted against test potential. Wild type $Ca_V2.2$ open bars (n=4), HA $Ca_V2.2$ shaded bars (n=8).

3.6.6 HA tagged $Ca_V2.2$ has reduced pre-pulse facilitation when α_2A-Gαo is over-expressed and clonidine is applied.

The current-voltage relationship of the HA tagged $Ca_V2.2$ before and after pre-pulse when α_2A-Gαo is over-expressed and clonidine is applied shows pre-pulse facilitation (Figure 3.21A). The V_{50} of the HA tagged $Ca_V2.2$ was shifted by -5mV by pre-pulse and this shift was significant (Figure 3.21B). The -5.26±1.5mV shift in V_{50} due to pre-pulse of the HA tagged $Ca_V2.2$ current was similar to that of wild type $Ca_V2.2$ (Figure 3.21C). The facilitation ratio of the HA tagged $Ca_V2.2$ was 25% smaller than that of wild type $Ca_V2.2$ at test potentials of -5mV, 0mV and +5mV and this reduction was significant at these potentials (Figure 3.21D).

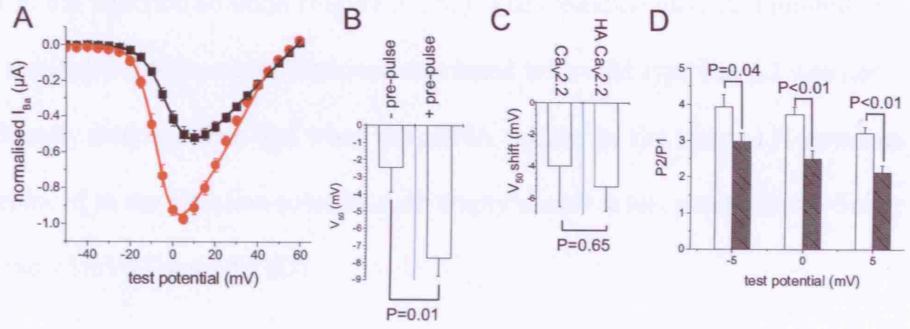

Figure 3.21. Pre-pulse facilitation of HA $Ca_V2.2$ (n=8) is displayed when α_2A-Gα_o is over expressed and clonidine applied. ***A*** Normalised current plotted against test potential. - pre-pulse black squares, + pre-pulse red circles (n=8). ***B*** V_{50} before and after pre-pulse (n=8). ***C*** Shift in V_{50} due to pre-pulse, wild type $Ca_V2.2$ (n=4) compared to HA $Ca_V2.2$ (n=8). ***D*** Pre-pulse facilitation ratio plotted against test potential. Wild type $Ca_V2.2$ open bars (n=4), HA $Ca_V2.2$ shaded bars (n=8).

3.6.7 Over-expressing an isolated N-terminus had no effect on clonidine mediated inhibition of wild type $Ca_V2.2$ when α_2A-Gαo is over-expressed.

The first 95 amino acids of $Ca_V2.2$ were expressed as a discrete fragment at a cDNA ratio of 1:1 $Ca_V2.2\alpha_1$:isolated N-terminus.

The current-voltage relationships in the absence and presence of $Ca_V2.2$ when the isolated N-terminus was over-expressed showed clonidine mediates inhibition (Figure 3.22A). Clonidine application significantly hyperpolarised the V_{50} of the wild type $Ca_V2.2$ when the isolated N-terminus was over-expressed (Figure 3.22B). The shift in V50 due to clonidine application of the wild type $Ca_V2.2$ when the isolated N-terminus was over-expressed was not significantly different to that of wild type $Ca_V2.2$ when the cDNA coding for the isolated N-terminus was replaced with empty vector in the injection solution (Figure 3.22C). The clonidine mediated inhibition when the isolated N-terminus was over-expressed with wild type $Ca_V2.2$ was not significantly different than that when the cDNA coding for the isolated N-terminus was replaced in the injection solution with empty vector at test potentials of -5mV, 0mV and +5mV (Figure 3.22D).

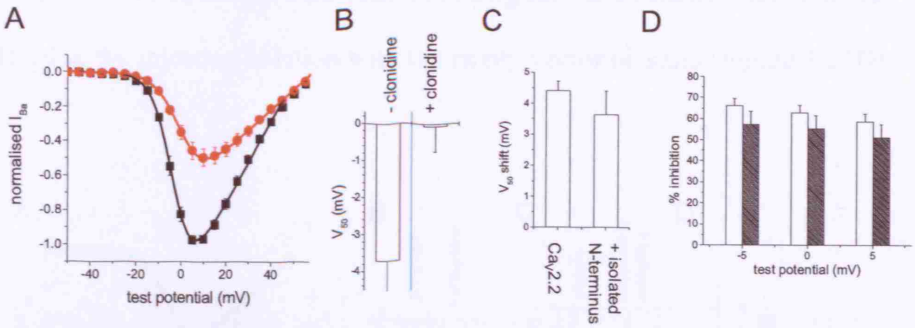

Figure 3.22. Clonidine mediates inhibition of $Ca_V2.2$ + isolated N-terminus (n=7) when α_2A-Gα_o is over-expressed. ***A*** Normalised current plotted against test potential. - clonidine black squares, + clonidine red circles (n=7). ***B*** V_{50} in absence and presence of clonidine (n=7). ***C*** Shift in V_{50} due to clonidine, without isolated N-terminus over-expressed (n=5) compared to with isolated N-terminus over-expressed (n=7). ***D*** % inhibition plotted against test potential. - isolated N-terminus open bars (n=5), + isolated N-terminus shaded bars (n=7).

3.6.8 Over-expressing an isolated N-terminus had no effect on pre-pulse facilitation of wild type $Ca_V2.2$ when α_2A-Gαo is over-expressed and clonidine is applied.

The current-voltage relationship, before and after pre-pulse, of wild type $Ca_V2.2$ when the isolated N-terminus was over-expressed, and when α_2A-Gαo was over-expressed and clonidine was applied shows pre-pulse facilitation (Figure 3.23A). The V_{50} of the current with the isolated N-terminus over-expressed was significantly shifted by the pre-pulse ($P<0.01$) (Figure 3.23B) and this shift in V_{50} was comparable to the shift in V_{50} seen when the cDNA coding for the isolated N-terminus in the injection solution was replaced with empty vector plasmid (Figure 3.23C). There was no difference in the facilitation ratio when the isolated N-terminus

was expressed compared to when cDNA coding for the isolated N-terminus was replaced in the injection solution with the empty vector plasmid (Figure 3.23D).

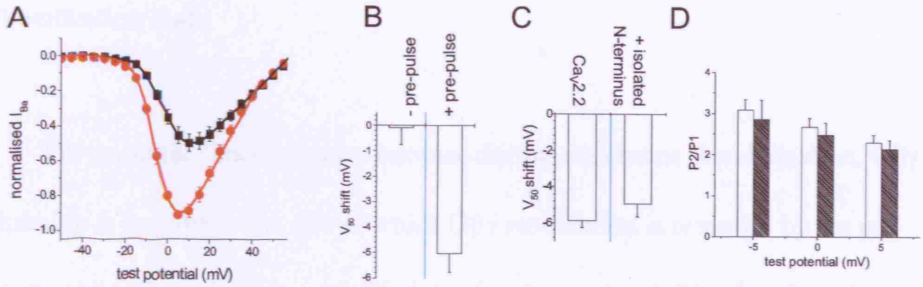

Figure 3.23. Pre-pulse facilitation of $Ca_V2.2$ + isolated N-terminus (n=7) is displayed when α_2A-Gα_o is over-expressed and clonidine applied. ***A*** Normalised current plotted against test potential. - pre-pulse black squares, + pre-pulse red circles (n=7). ***B*** V_{50} before and after pre-pulse (n=7). ***C*** Shift in V_{50} due to pre-pulse, without isolated N-terminus over-expressed (n=5) compared to with isolated N-terminus over-expressed (n=7). ***D*** Pre-pulse facilitation ratio plotted against test potential. - isolated N-terminus open bars (n=5), + isolated N-terminus shaded bars (n=7).

Chapter 4. Results 2

4.1 Facilitation Rate

Pre-pulse facilitation occurs because during membrane depolarisation, Gβγ modulation is removed. The rate at which Gβγ modulation is removed by the pre-pulse was investigated using a modified three-pulse protocol. The duration of the pre-pulse was varied between 0.2ms – 50ms to determine the kinetics of facilitation (in discussion talk about dissociation and add the affinity calculations). As pre-pulse duration was increased, the current in response to test pulse, P2, increased. This was due to the greater degree of facilitation that occurs during longer pre-pulses (Figure 4.1).

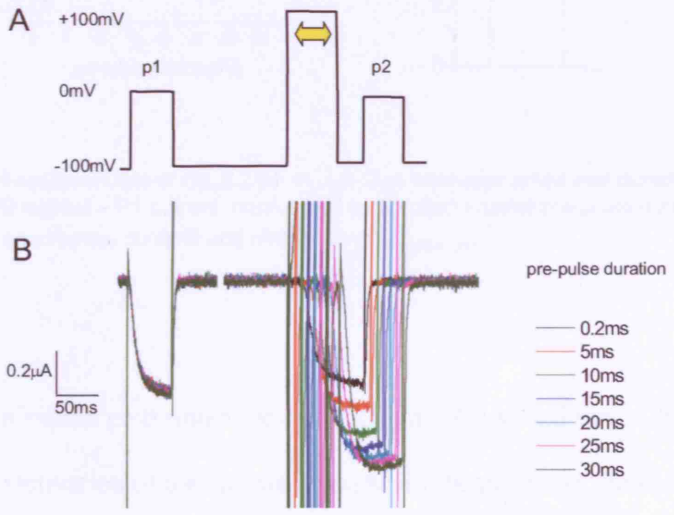

Figure 4.1. Facilitation rate of $Ca_V2.2$ when α_2A-Gαo over-expressed and clonidine applied. ***A*** Modified three pulse protocol, duration of the pre-pulse is varied. ***B*** Corresponding current trace for $Ca_V2.2$ shows P2 current increases as pre-pulse duration increases.

The difference between P1 current and P2 current was calculated, normalised and plotted against pre-pulse duration (Figure 4.2A). A single exponential (Equation 4.1) could be fit, to give a time constant of facilitation (Figure 4.2B).

$$y = y_0 + Ae^{-x/\tau_{facilitation}} \qquad \text{Equation 4.1}$$

Where y_0 is the offset, A is the amplitude and $\tau_{facilitation}$ is the time constant of facilitation.

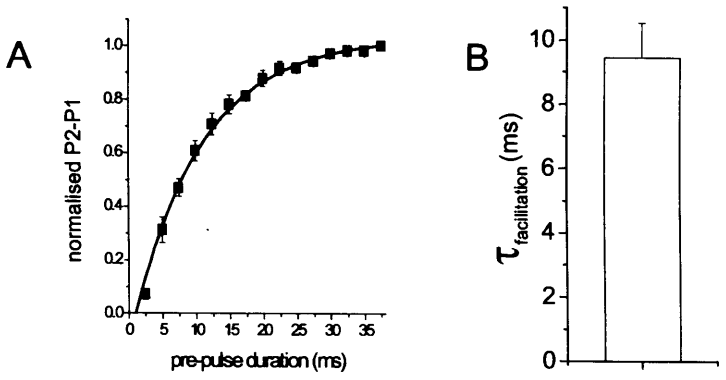

Figure 4.2. Facilitation rate of $Ca_V2.2$ when α_2A-Gαo over-expressed and clonidine applied. ***A*** P2 current – P1 current, normalised and plotted against pre-pulse duration (n=5). ***B*** An exponential curve fit and histogram of $\tau_{facilitation}$.

The fit doesn't quite go through the origin (Figure 4.2A) and this is due to a small amount of inactivation of the current, even when the pre-pulse duration is very small. At longer pre-pulse durations inactivation probably still occurs but this is more trivial

when the facilitation ratio is high; when the facilitation ratio is low, the degree of inactivation becomes of greater consequence.

4.1.1 Palmitoylation motif $Ca_V2.2$ had a higher rate of facilitation than wild type $Ca_V2.2$ when α_2A-Gαo over-expressed and clonidine applied.

The modified three-pulse protocol was applied to oocytes expressing the palmitoylation motif $Ca_V2.2$, β_1b, $\alpha_2\delta$-2 and the α_2A-G_αo tandem, in the presence of clonidine. Figure 4.3 shows the voltage steps (Figure 4.3A) and the corresponding current trace (Figure 4.3B).

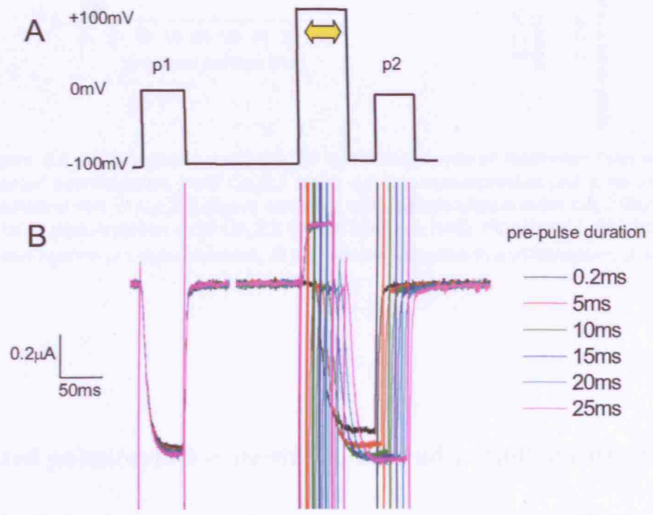

Figure 4.3. Facilitation rate of palmitoylation motif $Ca_V2.2$ when α_2A-Gαo over-expressed and clonidine applied. ***A*** Modified three pulse protocol ***B*** Corresponding current trace for palmitoylation motif $Ca_V2.2$.

This allowed the facilitation rate of the palmitoylation motif $Ca_V2.2$ to be compared to that of wild type $Ca_V2.2$. The normalised difference between the P1 current and the P2 current was plotted for both the wild type $Ca_V2.2$ and the palmitoylated $Ca_V2.2$. It is clear from the graph that the facilitation rate of the palmitoylation motif $Ca_V2.2$ was faster (Figure 4.4A). The time constant of the exponential fit of the palmitoylation motif was significantly smaller than that of wild type $Ca_V2.2$ (Figure 4.4B).

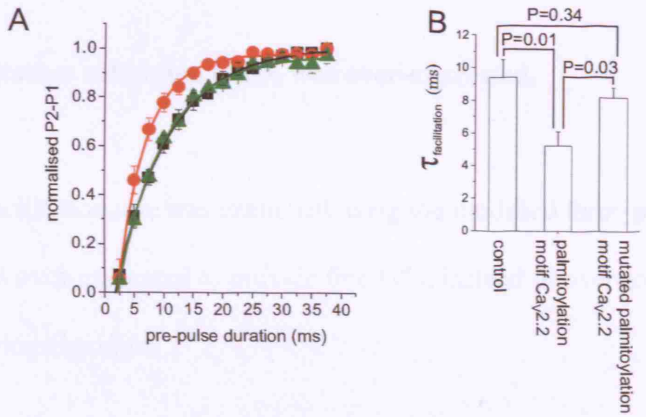

Figure 4.4. Palmitoylation motif $Ca_V2.2$ had a faster rate of facilitation than wild type $Ca_V2.2$ and mutated palmitoylation motif $Ca_V2.2$ when α_2A-Gαo over-expressed and in the presence of clonidine ***A*** Facilitation rate of $Ca_V2.2$ (black squares, n=5), palmitoylation motif $Ca_V2.2$ (red circles, n=7) and mutated palmitoylation motif $Ca_V2.2$ (green triangles, n=5). P2 current – P1 current, normalised and plotted against pre-pulse duration. ***B*** An exponential curve fit and histogram of $\tau_{facilitation}$.

4.1.2 Mutated palmitoylation motif $Ca_V2.2$ had a similar rate of facilitation to wild type $Ca_V2.2$ when α_2A-Gαo was over-expressed and clonidine applied.

The modified three-pulse protocol was also applied to oocytes expressing the mutated palmitoylation motif $Ca_V2.2$, β_1b, $\alpha_2\delta$-2 and the α_2A-G$_\alpha$o tandem. The

normalised difference between the P1 current and the P2 current was plotted (Figure 4.4A). The graph shows that the mutated palmitoylation motif $Ca_V2.2$ had a similar facilitation rate to wild type $Ca_V2.2$. My results did not show the time constants for the facilitation rate of the mutated palmitoylation motif $Ca_V2.2$ and wild type $Ca_V2.2$ to be significantly different from each other (Figure 4.4B). However, the time constants of the facilitation rates of the palmitoylation motif $Ca_V2.2$ and the mutated palmitoylation motif $Ca_V2.2$ were significantly different.

4.2 Facilitation rate when $G\beta_1\gamma_2$ was over-expressed.

Facilitation rate was examined using the modified three-pulse protocol when $G\beta_1\gamma_2$ was over-expressed to provide free $G\beta\gamma$, instead of over-expressing α_2A-Gαo and applying clonidine.

4.2.1 Palmitoylation motif $Ca_V2.2$ had a faster rate of facilitation than wild type $Ca_V2.2$ when $G\beta_1\gamma_2$ was over-expressed.

The three-pulse protocol was applied to oocytes over-expressing $G\beta_1\gamma_2$ and either the wild type $Ca_V2.2$, the palmitoylation motif $Ca_V2.2$ or the mutated palmitoylation motif $Ca_V2.2$ (in all cases the auxiliary subunits of β_1b and $\alpha_2\delta$-2 were co-expressed). P2 current – P1 current was calculated, normalised and plotted against pre-pulse duration (Figure 4.5A). A Boltzmann function was fit to the curves and a

time constant for each curve found. The time constant of the facilitation kinetics of the palmitoylation motif $Ca_V2.2$ was smaller in value than that for the wild type $Ca_V2.2$ and the mutated palmitoylation motif $Ca_V2.2$, which were similar in value to each other (Figure 4.5B), as was the case when a_2A-Gαo was over-expressed and clonidine was applied.

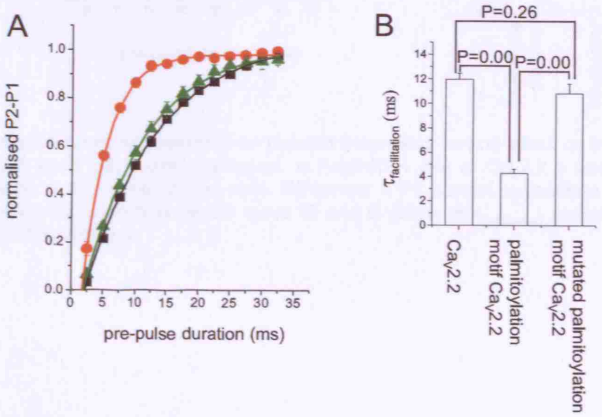

Figure 4.5. Palmitoylation motif $Ca_V2.2$ had a faster rate of facilitation than wild type $Ca_V2.2$ and mutated palmitoylation motif $Ca_V2.2$ when $G\beta_1\gamma_2$ was over-expressed. ***A*** Facilitation rate of $Ca_V2.2$ (black squares, n=13), palmitoylation motif $Ca_V2.2$ (red circles, n=9) and mutated palmitoylation motif $Ca_V2.2$ (green triangles, n=5). P2 current – P1 current, normalised and plotted against pre-pulse duration. An exponential curve fit and ***B*** graph of $\tau_{facilitation}$ comparing wild type $Ca_V2.2$, palmitoylation motif $Ca_V2.2$ and mutated palmitoylation motif $Ca_V2.2$.

4.2.2 Including cDNA coding for the isolated N-terminus in the injection mixture had no effect on facilitation rate of $Ca_V2.2$ when $G\beta_1\gamma_2$ was over-expressed.

Currents recorded from the oocytes that were injected with cDNA coding for the isolated N-terminus, along with the $Ca_V2.2\alpha_1$, β_1b, $\alpha_2\delta$-2 and $G\beta_1\gamma_2$ had the same rate of facilitation as that when cDNA coding for the isolated N-terminus was replaced with empty vector cDNA (Figure 4.6A). The time constants of facilitation

were very similar for currents with and without the isolated N-terminus (Figure 4.6B).

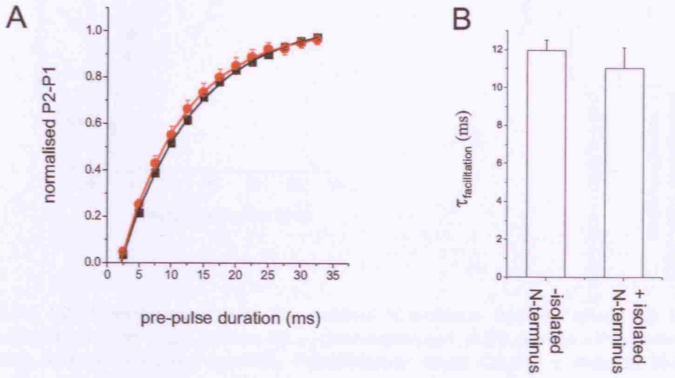

Figure 4.6. Over-expression of an isolated N-terminus had no effect on facilitation rate of wild type $Ca_V2.2$ when $G\beta_1\gamma_2$ over-expressed. ***A*** Facilitation rate of $Ca_V2.2$ ± isolated N-terminus (- black squares, n=13, + red circles, n=6). P2 current – P1 current, normalised and plotted against pre-pulse duration. An exponential curve fit and ***B*** graph of $\tau_{facilitation}$ comparing wild type $Ca_V2.2$ ± isolated N-terminus.

4.2.3 Including cDNA coding for the isolated N-terminus in the injection mixture had no effect on facilitation rate of palmitoylation motif $Ca_V2.2$ when $G\beta_1\gamma_2$ was over-expressed.

Currents recorded from the oocytes that were injected with cDNA coding for the isolated N-terminus, along with the palmitoylation motif $Ca_V2.2\alpha_1$, β_1b, $\alpha_2\delta$-2 and $G\beta_1\gamma_2$ had the same rate of facilitation as that when cDNA coding for the isolated N-terminus was replaced with empty vector cDNA (Figure 4.7A). The time constants of facilitation were very similar for currents with and without the isolated N-terminus (Figure 4.7B).

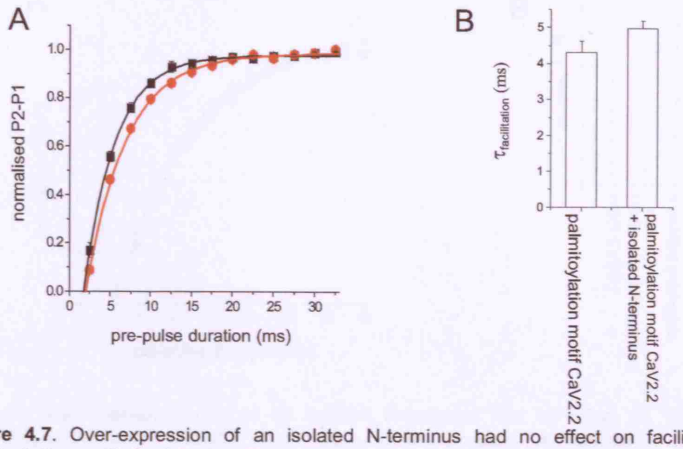

Figure 4.7. Over-expression of an isolated N-terminus had no effect on facilitation rate of palmitoylation motif $Ca_V2.2$ when $G\beta_1\gamma_2$ over-expressed. ***A*** P2 current – P1 current, normalised and plotted against pre-pulse duration. Palmitoylation motif $Ca_V2.2$ ± isolated N-terminus (- black squares, n=9, + red circles, n=8). An exponential curve was fitted. ***B*** Graph comparing $\tau_{facilitation}$ of palmitoylation motif $Ca_V2.2$ ± isolated N-terminus.

4.2.4 Including cDNA coding for the isolated N-terminus in the injection mixture had no effect on facilitation rate of mutated palmitoylation motif $Ca_V2.2$ when $G\beta_1\gamma_2$ was over-expressed.

Currents recorded from the oocytes that were injected with cDNA coding for the isolated N-terminus, along with the mutated palmitoylation motif $Ca_V2.2\alpha_1$, β_1b, $\alpha_2\delta$-2 and $G\beta_1\gamma_2$ had the same rate of facilitation as that when cDNA coding for the isolated N-terminus was replaced with empty vector cDNA (Figure 4.8A). The time constants of facilitation were very similar for currents with and without the isolated N-terminus (Figure 4.8B).

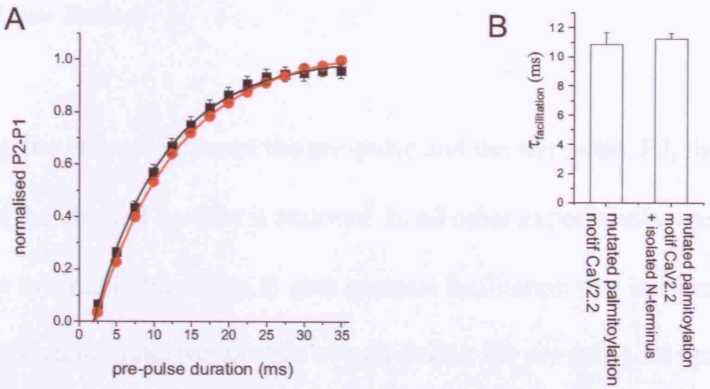

Figure 4.8. Over-expression of an isolated N-terminus had no effect on facilitation rate of palmitoylation motif $Ca_V2.2$ when $G\beta_1\gamma_2$ over-expressed. ***A*** Facilitation rate of mutated palmitoylation motif $Ca_V2.2$ ± isolated N-terminus (- black squares, n=5, + red circles, n=9). P2 current – P1 current, normalised and plotted against pre-pulse duration. An exponential curve fit and ***B*** Graph comparing $\tau_{facilitation}$ of mutated palmitoylation motif $Ca_V2.2$ ± isolated N-terminus.

4.3 Re-inhibition Rate

During the interval between the pre-pulse and the test pulse, P2, the modulation of the channel by Gβγ is restored. In all other experiments, the interval was been kept to a minimum value to give greatest facilitation that is minimally masked by the channel inactivation that occurs during the pre-pulse. In order to examine the kinetics of re-inhibition, the duration of the interval between the pre-pulse and test pulse, P2, was varied between 0.2 – 140ms (Figure 4.9A). The current trace shows that as the interval between the pre-pulse and the test pulse, P2, was increased, the P2 current decreased (Figure 4.9B).

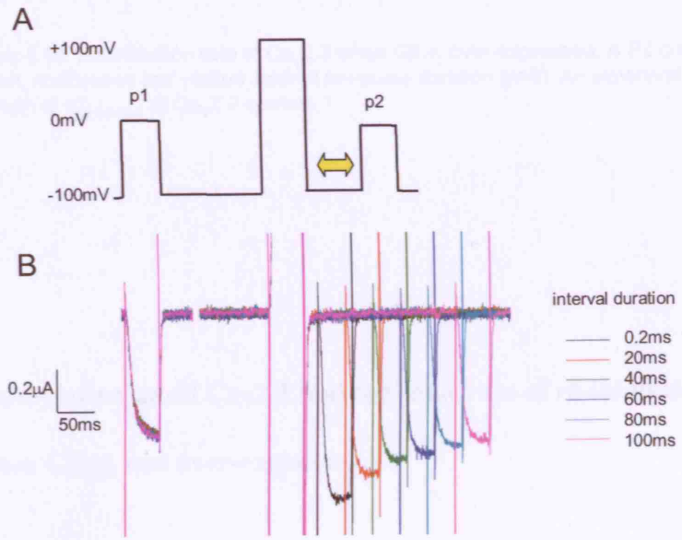

Figure 4.9. Re-inhibition rate of $Ca_V2.2$ when α_2A-Gαo over-expressed and clonidine applied. ***A*** Modified three pulse protocol, duration of the interval between pre-pulse and test pulse P2 is varied. ***B*** Corresponding current trace for $Ca_V2.2$ shows P2 current decreases as interval duration increases.

The difference between P1 current and P2 current was calculated, normalised and plotted against interval duration (Figure 4.10A). A single exponential could be fit, to give a time constant of re-inhibition (Figure 4.10B).

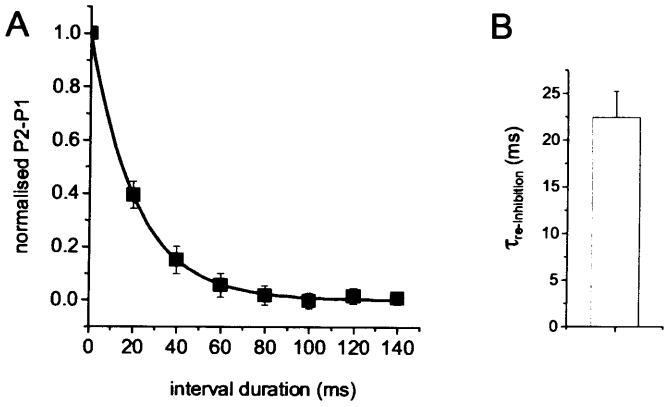

Figure 4.10. Re-inhibition rate of $Ca_V2.2$ when $G\beta_1\gamma_2$ over-expressed. ***A*** P2 current – P1 current, normalised and plotted against pre-pulse duration (n=3). An exponential curve fit. ***B*** Graph of $\tau_{reinhibition}$ of $Ca_V2.2$ current.

4.3.1 Palmitoylation motif $Ca_V2.2$ had the same rate of re-inhibition as wild type $Ca_V2.2$ when $G\beta_1\gamma_2$ was over-expressed.

The difference between P2 and P2 currents was calculated and normalised for the palmitoylation motif $Ca_V2.2$ and plotted against interval duration with that of the wild type $Ca_V2.2$ (Figure 4.11A). My results did not show a significant difference

between the time constants for the re-inhibition rates of palmitoylation motif $Ca_V2.2$ and wild type $Ca_V2.2$ (Figure 4.11B).

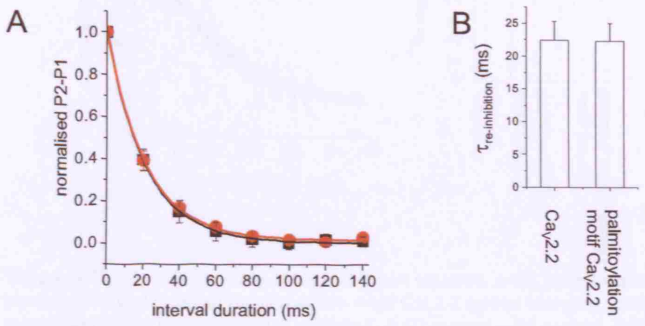

Figure 4.11. There was no difference in the re-inhibition rate of $Ca_V2.2$ (black squares, n=3) and palmitoylation motif $Ca_V2.2$ (red circles, n=4) when $G\beta_1\gamma_2$ over-expressed. ***A*** P2 current – P1 current, normalised and plotted against pre-pulse duration. An exponential curve fit and ***B*** histogram of $\tau_{reinhinition}$ comparing wild type $Ca_V2.2$ and palmitoylation motif $Ca_V2.2$.

4.3.2 Palmitoylation motif $Ca_V2.2$ and mutated palmitoylation motif $Ca_V2.2$ had the same rate of re-inhibition as wild type $Ca_V2.2$ when α_2A-Gαo was over-expressed and clonidine applied.

The difference between P2 and P2 currents was calculated and normalised for wild type $Ca_V2.2$, palmitoylation motif $Ca_V2.2$ and mutated palmitoylation motif $Ca_V2.2$ when α_2A-Gαo over-expressed and clonidine applied. These were plotted against interval duration (Figure 4.12A). My results did not show a significant difference between the time constants for the re-inhibition rates of wild type $Ca_V2.2$, palmitoylation motif $Ca_V2.2$ and mutated palmitoylation motif $Ca_V2.2$ (Figure 4.12B).

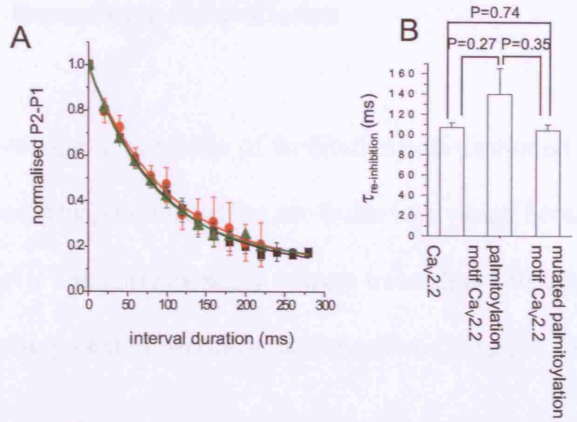

Figure 4.12. Re-inhibition rate of $Ca_V2.2$ (black squares, n=3), palmitoylation motif $Ca_V2.2$ (red circles, n=3) and mutated palmitoylation motif $Ca_V2.2$ (green triangles, n=3) when α_2A-R over-expressed and in the presence of clonidine. ***A*** P2 current – P1 current, normalised and plotted against pre-pulse duration. An exponential curve fit and ***B*** histogram of $\tau_{reinhibition}$.

4.4 Voltage-Dependence of Facilitation

The voltage-dependence of facilitation was examined by a modified three-pulse protocol. The potential of the pre-pulse was varied between -60 - +160mV (Figure 4.13A). The corresponding current trace shows that the P2 current increases as the pre-pulse potential becomes more positive (Figure 4.13B).

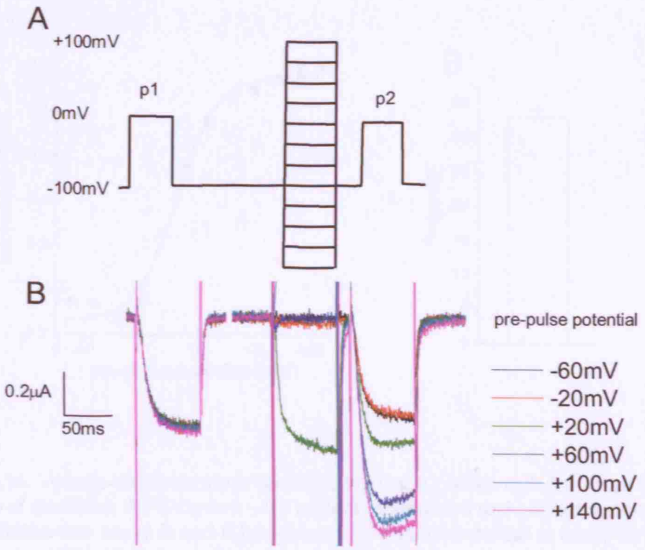

Figure 4.13. Voltage-dependence of facilitation. ***A*** Modified three pulse protocol. Potential of pre-pulse is varied between -60 and +60 mV. ***B*** Corresponding current trace for $Ca_V2.2$ shows P2 current increases as pre-pulse potential becomes more positive.

The modified three-pulse protocol was applied to channels expressing $Ca_V2.2\alpha_1$, β_1b, $\alpha_2\delta$-2 and α_2A-Gαo during clonidine application. The difference between P1 current and P2 current was calculated, normalised and plotted against pre-pulse potential (Figure 4.14A). A Boltzmann function (Equation 4.2) was fit, to

give the pre-pulse potential at which 50% facilitation was achieved ($V_{facilitation50}$, Figure 4.14B).

$$y = \frac{A_1 - A_2}{1 + e^{(x-x0)/dx}}$$ Equation 4.2

Where A_1 is the minimum current, A_2 is the maximum current, x0 is the pre-pulse potential at which 50% facilitation is achieved.

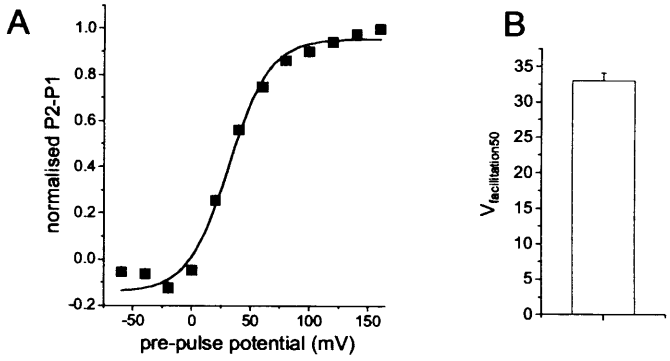

Figure 4.14. Voltage-dependence of facilitation of $Ca_V2.2$ when α_2A-Gαo over-expressed and in the presence of clonidine. ***A*** P2 current – P1 current, normalised and plotted against pre-pulse duration (n=3). A Boltzmann curve fit and ***B*** histogram of pre-pulse potential at which 50% of maximum facilitation is achieved, $V_{facilitation50}$.

4.4.1 There was no difference in the voltage-dependence of facilitation for wild type $Ca_V2.2$, palmitoylation motif $Ca_V2.2$ and mutated palmitoylation motif $Ca_V2.2$ when α_2A-Gαo was over-expressed and clonidine applied.

The voltage-dependence of facilitation was compared for wild type $Ca_V2.2$, palmitoylation motif $Ca_V2.2$ and mutated palmitoylation motif $Ca_V2.2$. The curves of

the normalised difference between P2 and P1 currents plotted against pre-pulse potential look very similar (Figure 4.15A). The curve for the palmitoylation motif $Ca_V2.2$ look slightly different at pre-pulse potentials of -60mV to +20mV. This may be due to differences in inactivation properties of the channels, affecting the degree of inactivation that is reached during the pre-pulse. Chapter 5 addresses inactivation differences between the channels formed using the different $Ca_V2.2\alpha_1$ constructs. There was no significant difference in the pre-pulse potential that is required for 50% of maximum facilitation to be reached between the wild type $Ca_V2.2$, palmitoylation motif $Ca_V2.2$ and mutated palmitoylation motif $Ca_V2.2$ (Figure 4.15B).

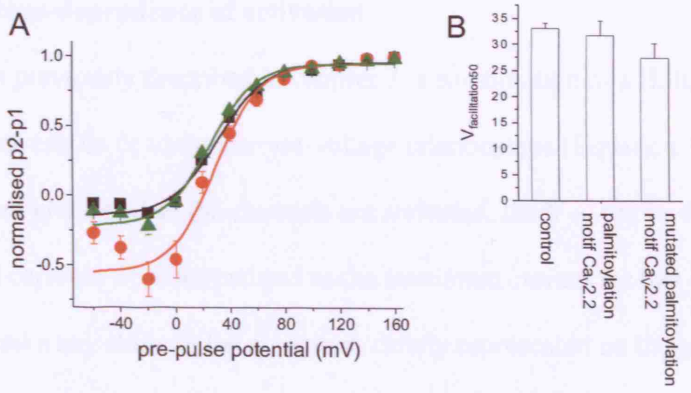

Figure 4.15. Voltage-dependence of facilitation of $Ca_V2.2$ (black squares, n=3), palmitoylation motif $Ca_V2.2$ (red circles, n=4) and mutated palmitoylation motif $Ca_V2.2$ (green triangles, n=3) when α_2A-Gαo over-expressed and in the presence of clonidine. ***A*** P2 current – P1 current, normalised and plotted against pre-pulse duration. A Boltzmann curve fit and ***B*** histogram of $V_{facilitation50}$.

Chapter 5. Results 3. Activation and Inactivation

In order to confirm that the previous comparisons were valid, the activation and inactivation characteristics for $Ca_V2.2$, palmitoylation motif $Ca_V2.2$ and mutated palmitoylation motif $Ca_V2.2$ were examined. The data for the voltage dependence of activation included in this chapter are the same as the data in chapter 3.

5.1 Activation

5.1.1 Voltage-dependence of activation

As previously described in chapter 3, a combination of a Boltzmann and a straight line can be fit to the current-voltage relationships (Equation 3.1) and the potential at which half of the channels are activated, the V_{50}, can be found. In these graphs all currents were normalised to the maximum current for that condition in order to make any shifts in the activation clearly represented on the graph.

5.1.2 Voltage dependence of activation was the same for wild type $Ca_V2.2$ and palmitoylation motif $Ca_V2.2$ when α_2A-Gαo was over-expressed.

The activation phase of the current-voltage relationship was very similar for wild type $Ca_V2.2$ and palmitoylation motif $Ca_V2.2$ when α_2A-Gαo over-expressed and clonidine not applied (Figure 5.1A). The V_{50}s of wild-type $Ca_V2.2$ and palmitoylation motif $Ca_V2.2$ were not significantly different in the absence of

clonidine (Figure 5.1B). In the presence of clonidine the activation phase of the current-voltage relationship and V_{50}s were not significantly different either (Figure 5.1C and D).

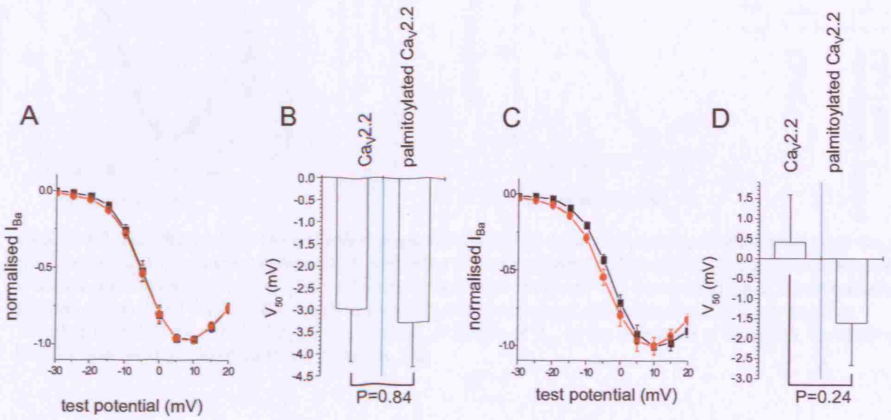

Figure 5.1. No difference in the activation phase of the IV of $Ca_V2.2$ (n=6) and palmitoylation motif $Ca_V2.2$ (n=9) when α_2A-Gαo over-expressed. ***A*** Activation phase in absence of clonidine ($Ca_V2.2$ black squares, palmitoylation motif $Ca_V2.2$ red circles). ***B*** Graph of control V_{50}, comparing $Ca_V2.2$ and palmitoylation motif $Ca_V2.2$ in the absence of clonidine. ***C*** Activation phase in the presence of clonidine ($Ca_V2.2$ black squares, mutated palmitoylation motif $Ca_V2.2$ red circles. ***D*** Graph of V_{50} in presence of clonidine, comparing $Ca_V2.2$ and palmitoylation motif $Ca_V2.2$.

The activation phase of the current-voltage relationship and the V_{50} of mutated palmitoylation motif $Ca_V2.2$ were also not significantly different from those of wild type $Ca_V2.2$ in the absence of clonidine (Figure 5.2A and B). In the presence of clonidine there were no significant differences in the activation phase of the current-voltage relationships or the V_{50}s between $Ca_V2.2$ and mutated palmitoylation motif $Ca_V2.2$ either (Figure 5.2C and D).

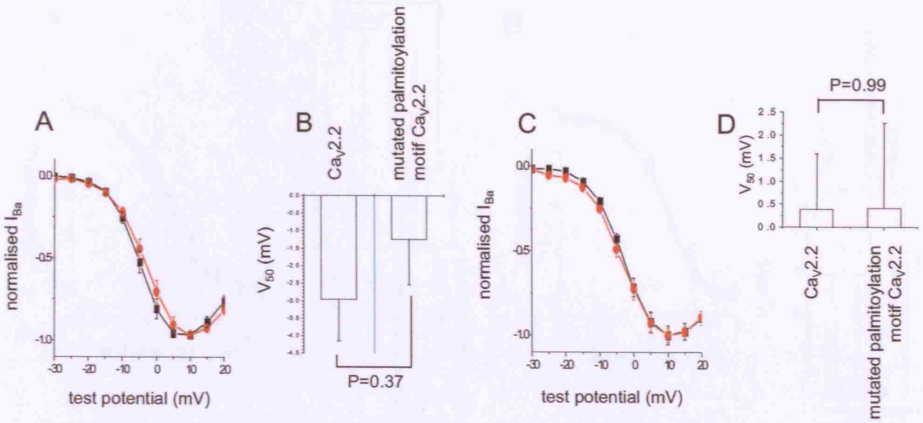

Figure 5.2. No difference in the activation phase of $Ca_V2.2$ (n=6) and mutated palmitoylation motif $Ca_V2.2$ (n=8) when α_2A-Gαo over-expressed. ***A*** Activation phase in absence of clonidine ($Ca_V2.2$ black squares, mutated palmitoylation motif $Ca_V2.2$ red circles). ***B*** Graph of control V_{50}, comparing $Ca_V2.2$ and mutated palmitoylation motif $Ca_V2.2$. ***C*** Activation phase in the presence of clonidine ($Ca_V2.2$ black squares, mutated palmitoylation motif $Ca_V2.2$ red circles). ***D*** Graph of V_{50} in the presence of clonidine, comparing $Ca_V2.2$ and mutated palmitoylation motif $Ca_V2.2$.

5.1.3 Over-expression of Gβγ

When Gβγ was over expressed, the V_{50} of the palmitoylation motif $Ca_V2.2$ and the mutated palmitoylation motif $Ca_V2.2$ were significantly hyperpolarised when compared to wild type $Ca_V2.2$ (Figure 5.3A). Following pre-pulse, however, the V_{50}s of the palmitoylation motif $Ca_V2.2$ and mutated palmitoylation motif $Ca_V2.2$ were not significantly different from wild type $Ca_V2.2$ (P=0.29 and 0.70, respectively) (Figure 5.3B). This suggests that the difference in V_{50}s without pre-pulse is due to differing Gβγ modulation and not intrinsic biophysical properties of the channels.

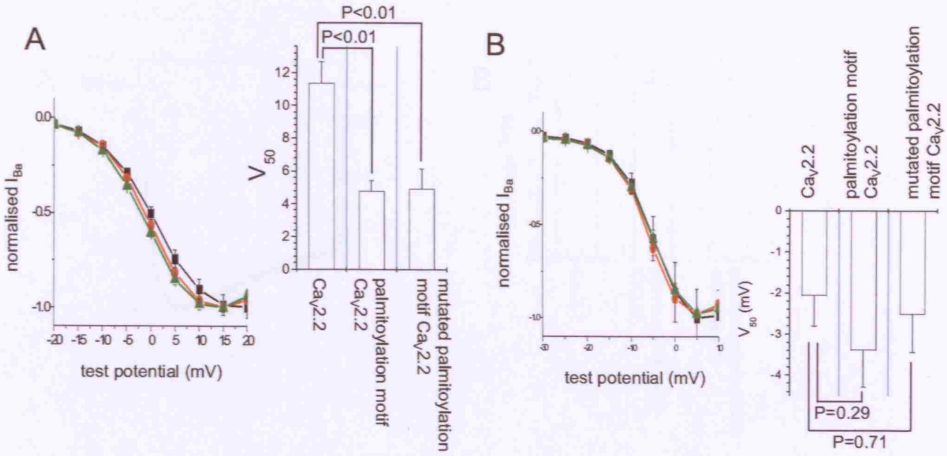

Figure 5.3. Activation phase of palmitoylation motif $Ca_V2.2$ and mutated palmitoylation motif $Ca_V2.2$ are depolarised compared to wild type $Ca_V2.2$ when Gβγ over expressed. ***A*** Activation phase without pre-pulse. $Ca_V2.2$ (black squares, n=15), palmitoylation motif $Ca_V2.2$ (red circles, n=19) and mutated palmitoylation motif $Ca_V2.2$ (green triangles, n=12). ***B*** Graph of V_{50} without pre-pulse, comparing $Ca_V2.2$, palmitoylation motif $Ca_V2.2$ and mutated palmitoylation motif $Ca_V2.2$. ***C*** Activation phase with pre-pulse. $Ca_V2.2$ (black squares), palmitoylation motif $Ca_V2.2$ (red circles) and mutated palmitoylation motif $Ca_V2.2$ (green triangles). ***D*** Graph of V_{50} with pre-pulse, comparing $Ca_V2.2$, palmitoylation motif $Ca_V2.2$ and mutated palmitoylation motif CaV2.2.

5.1.4 Kinetics of activation

A sample trace shows the fast activation kinetics of the channel when not modulated by Gβγ (Figure 5.4A). A single exponential (Equation 4.1) was fit to the activation curves of $Ca_V2.2$, palmitoylation motif $Ca_V2.2$ and mutated palmitoylation motif $Ca_V2.2$ in the absence of Gβγ modulation, i.e. without over-expressing $G\beta_1\gamma_2$ or applying clonidine. The time constant for these exponentials, $\tau_{activation}$, was equal for all three constructs in the absence of clonidine and without over-expression of $G\beta_1\gamma_2$ (Figure 5.4B).

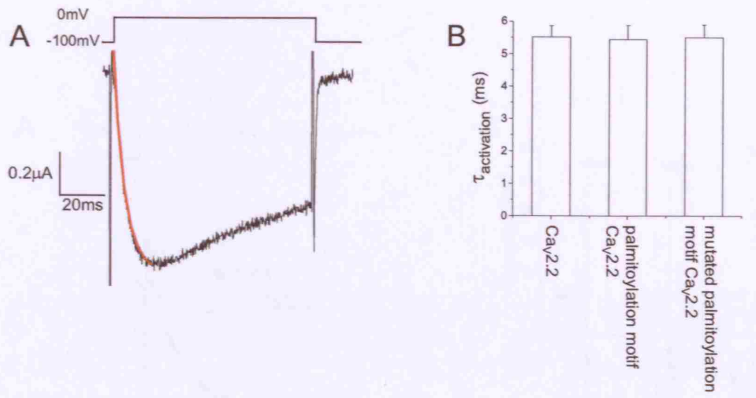

Figure 5.4. No difference in activation kinetics of $Ca_V2.2$, palmitoylation motif $Ca_V2.2$ and mutated palmitoylation motif $Ca_V2.2$ in absence of Gβγ modulation. ***A*** An example trace of activation of $Ca_V2.2$ with a first order exponential curve fitted in red. ***B*** $\tau_{activation}$ for $Ca_V2.2$ (n=7), palmitoylation motif $Ca_V2.2$ (n=5) and mutated palmitoylation motif $Ca_V2.2$ (n=9).

A sample trace shows the slower, biphasic activation of the channel when Gβγ is over-expressed (Figure 5.5A). When $G\beta_1\gamma_2$ is over-expressed, a double exponential can be fit (Equation 5.1).

$$y = y_0 + A_1e^{-x/\tau}{}_1 + A_2e^{-x/\tau}{}_2 \qquad \text{Equation 5.1}$$

Where y_0 is the offset, A_1 is the amplitude of the fast component, τ_1 is the time constant of the fast component, A_2 is the amplitude of the slow component, and τ_2 is the time constant of the slow component.

The fast component had a similar time constant to that of the unmodulated channel (Figure 5.5B). The slow component was about 5 fold slower than the fast

component, but each of the three constructs had a similar fast and slow time constants.

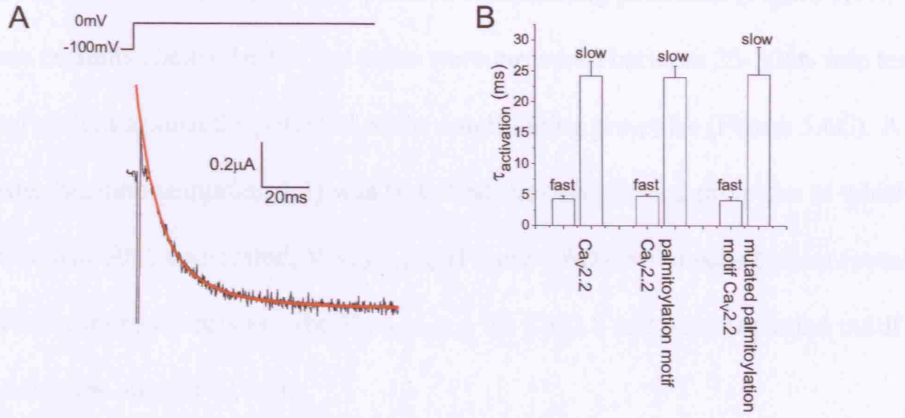

Figure 5.5. No difference in activation kinetics of $Ca_V2.2$, palmitoylation motif $Ca_V2.2$ and mutated palmitoylation motif $Ca_V2.2$ when Gβγ over-expressed. ***A*** An example trace of $Ca_V2.2$ activation with a second order exponential curve fitted in red. ***B*** τ_{fast} and τ_{slow} of second order exponential fit. of $Ca_V2.2$ (n=4), palmitoylation motif $Ca_V2.2$ (n=20), and mutated palmitoylation motif $Ca_V2.2$ (n=9).

5.2 Inactivation

Inactivation experiments were performed on oocytes that were not over-expressing $G\beta_1\gamma_2$ and in the absence of clonidine. This was to ensure that any differences in the activation of the channels when they are modulated by Gβγ did not affect the inactivation. All oocytes were injected with cDNA coding for the auxiliary subunits β_1b and $\alpha_2\delta$-2 along with either wild type $Ca_V2.2$, palmitoylation motif $Ca_V2.2$ or mutated palmitoylation motif $Ca_V2.2$.

5.2.1 Voltage-dependence of inactivation

The voltage-dependence of inactivation of $Ca_V2.2$ and palmitoylation motif $Ca_V2.2$ was examined using a modified three-pulse protocol (Figure 5.6A). Test

pulses to 0mV were preceded by a conditioning pre-pulse to a range of potentials between -110mV and -20mV. The sample traces show the current in response to the test pulse decreased with increasingly positive conditioning potentials (Figure 5.6B). The mean currents elicited by the test pulse were measured between 25-30ms into test pulse and plotted against the potential of the conditioning pre-pulse (Figure 5.6C). A Boltzmann function (Equation 4.2) was fit to find the conditioning pre-pulse at which the current was 50% inactivated, $V_{50\ inactivation}$ (Figure 5.6D). My results did not reveal a significant difference between the $V_{50\ inactivation}$ for $Ca_V2.2$ and palmitoylation motif $Ca_V2.2$ using the student's t-test.

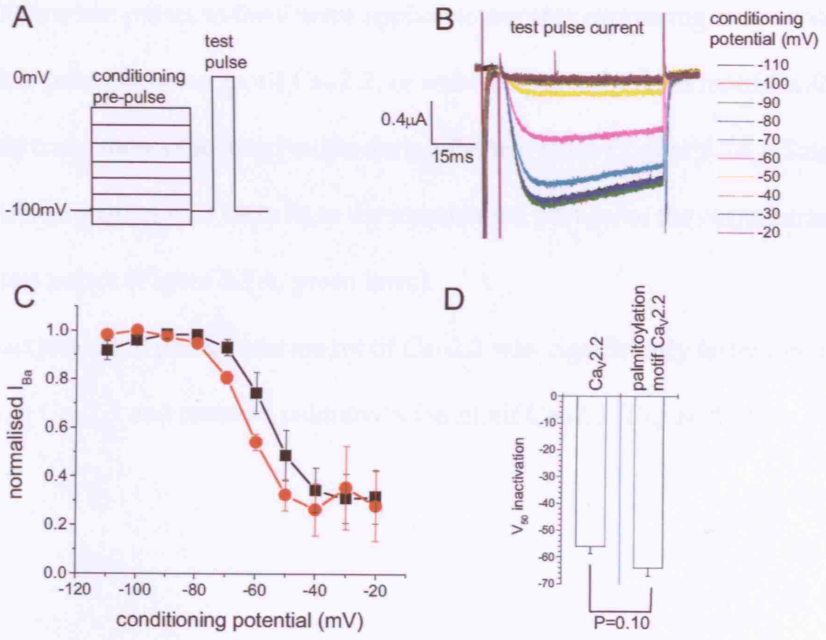

Figure 5.6. Steady state inactivation of $Ca_V2.2$ and palmitoylation motif $Ca_V2.2$. ***A*** Pulse protocol. Test pulse is preceded by a conditioning pre-pulse to between -110mV and -20mV. ***B*** Current trace in response to test pulse. ***C*** Normalised current plotted against conditioning potential. $Ca_V2.2$ black squares (n=4), Palmitoylation motif $Ca_V2.2$ red circles (n=3). ***D*** Graph of $V_{50inactivation}$ of $Ca_V2.2$ and palmitoylation motif $Ca_V2.2$.

There does appear to be some subtle differences in the voltage dependence of inactivation (Figure 5.6C) and the degree of inactivation at a conditioning potential of -60mV is significantly different for palmitoylation motif $Ca_V2.2$ and wild type $Ca_V2.2$. At a conditioning potential of -60mV, palmitoylation motif $Ca_V2.2$ exhibits a 19 ± 0.03 % reduction in current due to inactivation during the conditioning pre-pulse. At this potential wild type $Ca_V2.2$ only exhibits a 7 ± 0.03 % reduction in current due to inactivation during the conditioning pre-pulse. This difference in degree of inactivation at a potential of -60mV is significant (P=0.04).

5.2.2 Kinetics of inactivation

1000ms test pulses to 0mV were applied to oocytes expressing either wild-type $Ca_V2.2$, palmitoylation motif $Ca_V2.2$, or mutated palmitoylation motif $Ca_V2.2$. The sample trace shows the inactivation during the test pulse (Figure 5.7A). Single exponentials (Equation 4.1) were fit to the inactivation portion of the current trace for the 0mV test pulses (Figure 5.7A, green lines).

Inactivation of palmitoylation motif $Ca_V2.2$ was significantly faster that that of wild-type $Ca_V2.2$ and mutated palmitoylation motif $Ca_V2.2$ (Figure 5.7B).

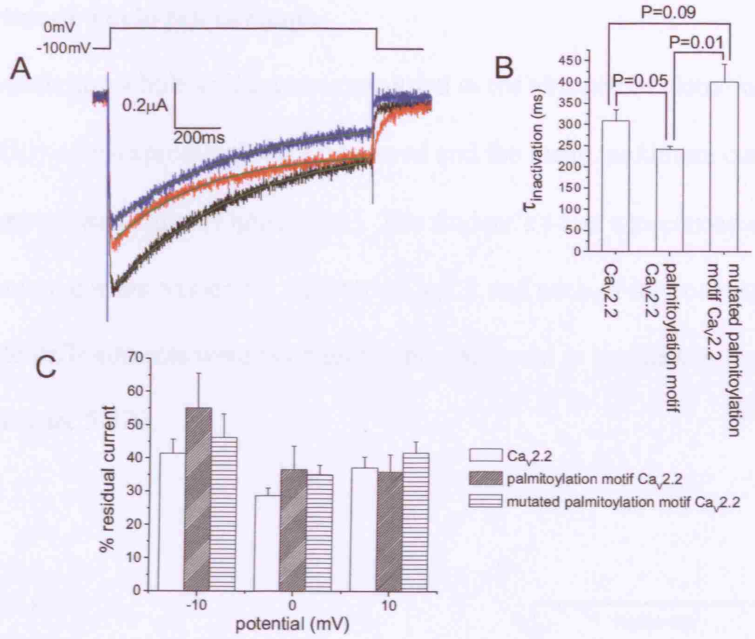

Figure 5.7. Kinetics of inactivation. *A* Pulse protocol and examples of corresponding current traces. Wild type $Ca_V2.2$ (black), palmitoylation motif $Ca_V2.2$ (red), mutated palmitoylation motif $Ca_V2.2$ (blue). Single exponential fits in green. *B* $\tau_{inactivation}$ for $Ca_V2.2$ (n=6), palmitoylation motif $Ca_V2.2$ (n=6) and mutated palmitoylation motif $Ca_V2.2$ (n=8). *C* Residual current at end of 1000ms pulse as a % of maximum current.

The percentage of residual current at the end of each of the 1000ms test pulses was calculated with respect to the peak current to that test pulse (Equation 5.2).

$$\% \text{ residual current} = \frac{\text{current at end of pulse}}{\text{peak current}} \times 100 \qquad \text{Equation 5.2}$$

There were no significant differences in the residual currents of the different constructs (Figure 5.7C). This suggests that the extent of inactivation for the different constructs was not altered i.e. the non-inactivating component was unchanged in palmitoylation motif $Ca_V2.2$ and mutated palmitoylation motif $Ca_V2.2$ compared to wild type $Ca_V2.2$.

5.3 Maximum whole-cell currents

Maximum whole-cell currents recorded in the absence of clonidine and without Gβγ over-expression, were measured and the mean maximum current for each construct was found (Figure 5.8A). The student's t-test was carried out between the maximum current values for wild type $Ca_V2.2$ and each of the constructs to show that whole-cells currents were not significantly different in magnitude from wild type $Ca_V2.2$ (Figure 5.8B).

A

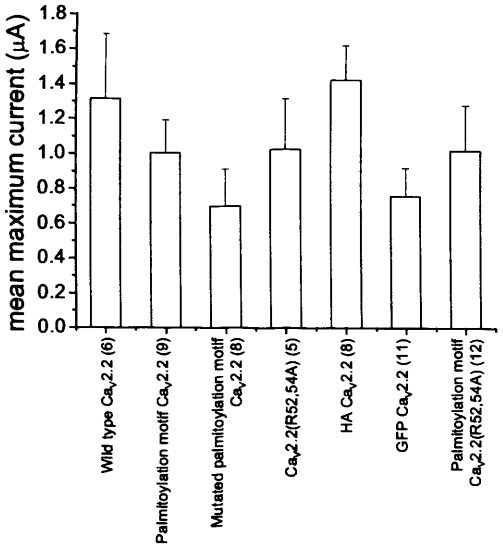

B

Construct	P value
Palmitoylation motif $Ca_V2.2$	0.43
Mutated palmitoylation motif CaV2.2	0.15
$Ca_V2.2$(R52,54A)	0.57
HA tagged $Ca_V2.2$	0.79
GFP tagged $Ca_V2.2$	0.52
Palmitoylation motif $Ca_V2.2$(R52,54A)	0.13

Figure 5.8. Maximum whole cell currents. ***A*** Mean maximum whole cell currents of each of the $Ca_V2.2$ constructs expressed. N numbers are in brackets. ***B*** P values calculated between wild type $Ca_V2.2$ and each construct show that the maximum current of each of the constructs is not significantly different to that of wild type $Ca_V2.2$.

Chapter 6. Results 4. Inhibiting Palmitoylation

If the differences in facilitation between the wild type $Ca_V2.2$ and the palmitoylation motif $Ca_V2.2$ are due to palmitoylation, then these effects should be reversed by inhibition of palmitoylation.

6.1 Inhibiting Palmitoylation Methods

Current-voltage relationships and pre-pulse facilitation rates were recorded from oocytes expressing palmitoylation motif $Ca_V2.2$, β_1b, $\alpha_2\delta$-2 and $G\beta_1\gamma_2$. Oocytes were then injected with 4.9nl of 2-bromohexdecanoic palmitate (2BP). This solution was made up by dissolving 2BP in DMSO (DiMethane Sulphonic Acid), initially to give a concentration of 500mM. This was then diluted in H_2O to give a concentration of 50mM 2BP and 10% DMSO. Injecting 4.9nl of this solution into each oocyte gave an intracellular concentration of approximately 100μM. This concentration has been shown previously to inhibit protein palmitoylation (Webb et al. 2000).

After being injected with 2BP, oocytes were incubated at 18°C for 1-2 hours before recording current-voltage relationships and pre-pulse facilitation rates again.

The same treatment was given to oocytes expressing wild type $Ca_V2.2$ instead of palmitoylation motif $Ca_V2.2$ as controls.

6.2 Inhibiting Palmitoylation Results

Three pulse protocols were applied to oocytes expressing either $Ca_V2.2$, or palmitoylation motif $Ca_V2.2$, and β_1b, $\alpha_2\delta$-2 and $G\beta_1\gamma_2$, before and after injection of 2BP.

6.2.1 2BP did not affect $Ca_V2.2$ current-voltage relationships when $G\beta_1\gamma_2$ was over-expressed

Injecting 2BP had no effect on the current-voltage relationship of oocytes over-expressing $Ca_V2.2$, β_1b, $\alpha_2\delta$-2 and $G\beta_1\gamma_2$ (Figure 6.1A). My results did not show a significant shift in the V_{50} of these currents by injecting 2BP (Figure 6.1B). Injecting 2BP did not affect these currents after a pre-pulse either (Figure 6.1C), and the V_{50} was unchanged by injecting 2BP (Figure 6.1D).

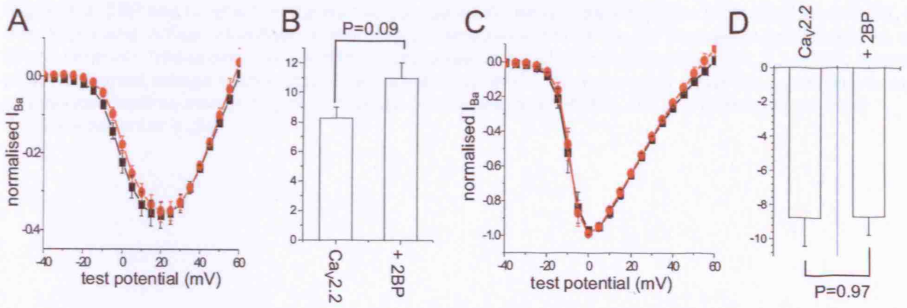

Figure 6.1. 2BP had no effect on the current-voltage relationship of $Ca_V2.2$ when $G\beta_1\gamma_2$ over-expressed. ***A*** Current-voltage relationship of $Ca_V2.2$ in absence (black squares, n= 4) and presence (red circles, n=4) of 2BP, no pre-pulse. ***B*** V_{50} of $Ca_V2.2$ ± 2BP, no pre-pulse. ***C*** Current-voltage relationship of $Ca_V2.2$ + pre-pulse when $G\beta_1\gamma_2$ over-expressed in absence (black squares, n= 4) and presence (red circles, n=4) of 2BP. ***D*** V_{50} of $Ca_V2.2$ + pre-pulse ± 2BP.

6.2.2 Injection of 2BP did not affect palmitoylation motif $Ca_V2.2$ current-voltage relationships when $G\beta_1\gamma_2$ was over-expressed

Injecting 2BP had no effect on the current-voltage relationship of oocytes over-expressing palmitoylation motif $Ca_V2.2$, β_1b, $\alpha_2\delta$-2 and $G\beta_1\gamma_2$ (Figure 6.2A). My results did not show a significant shift in the V_{50} of these currents by injecting 2BP (Figure 6.2B). Injecting 2BP did not affect these currents after a pre-pulse either (Figure 6.2C), and the V_{50} was unchanged by injecting 2BP (Figure 6.2D).

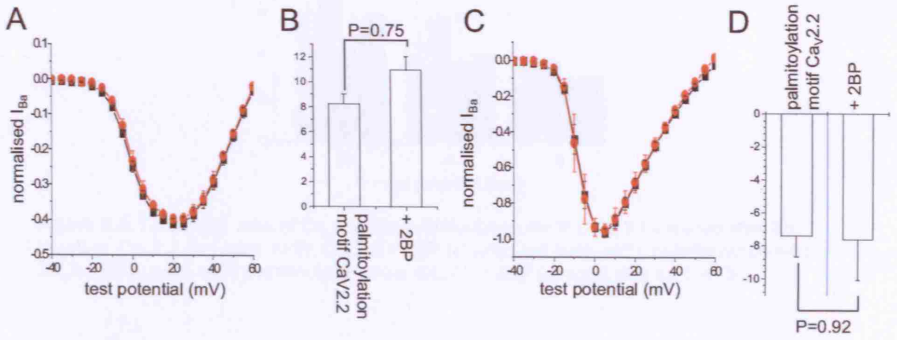

Figure 6.2. 2BP had no effect on the current-voltage relationship of palmitoylation motif $Ca_V2.2$ when $G\beta_1\gamma_2$ over-expressed. ***A*** Current-voltage relationship of palmitoylation motif $Ca_V2.2$ in absence (black squares, n= 4) and presence (red circles, n=4) of 2BP, no pre-pulse. ***B*** V_{50} of palmitoylation motif $Ca_V2.2$ ± 2BP, no pre-pulse. ***C*** Current-voltage relationship of palmitoylation motif $Ca_V2.2$ + pre-pulse when $G\beta_1\gamma_2$ over-expressed in absence (black squares, n= 4) and presence (red circles, n=4) of 2BP. ***D*** V_{50} of palmitoylation motif $Ca_V2.2$ + pre-pulse ± 2BP.

6.2.3 Injection of 2BP increased the facilitation ratio of $Ca_V2.2$ and palmitoylation motif $Ca_V2.2$ when $G\beta_1\gamma_2$ was over-expressed

Pre-pulse facilitation was observed after injection of 2BP for both $Ca_V2.2$ currents and palmitoylation motif $Ca_V2.2$ currents (Figure 6.3). There was a slight increase in facilitation ratio of $Ca_V2.2$ and palmitoylation motif $Ca_V2.2$ currents after injection of 2BP.

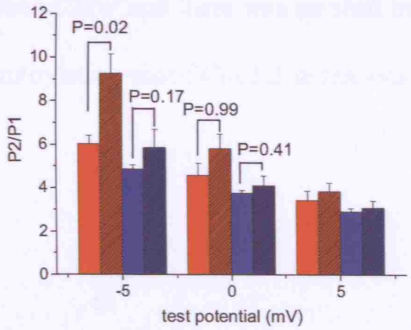

Figure 6.3. Facilitation ratio of $Ca_V2.2$ and palmitoylation motif $Ca_V2.2$ increased after 2BP injection. $Ca_V2.2$ (red bars, n=6), $Ca_V2.2$ + 2BP (shaded red bars, n=6), palmitoylation motif $Ca_V2.2$ (blue bars, n=7) palmitoylation motif $Ca_V2.2$ + 2BP (shaded blue bars, n=3).

6.2.4 Injection of 2BP had no effect on the facilitation rates of either $Ca_V2.2$ currents or palmitoylation motif $Ca_V2.2$ currents.

The modified three pulse protocol (Figure 6.4A) was applied to oocytes expressing $Ca_V2.2$ or palmitoylation motif $Ca_V2.2$ and β_1b, $\alpha_2\delta$-2 and $G\beta_1\gamma_2$ before and after injection of 2BP so that facilitation rates could be recorded before and after injection of 2BP for $Ca_V2.2$ currents and palmitoylation motif $Ca_V2.2$ currents (Figure 6.4B). The facilitation rate of $Ca_V2.2$ currents was unchanged by injection of 2BP. The facilitation rate of palmitoylation motif $Ca_V2.2$ currents was also unchanged by the injection of 2BP and there was no shift in the $\tau_{facilitation}$ for either wild type $Ca_V2.2$ or palmitoylation motif $Ca_V2.2$ in response to 2BP injection (Figure 6.4C).

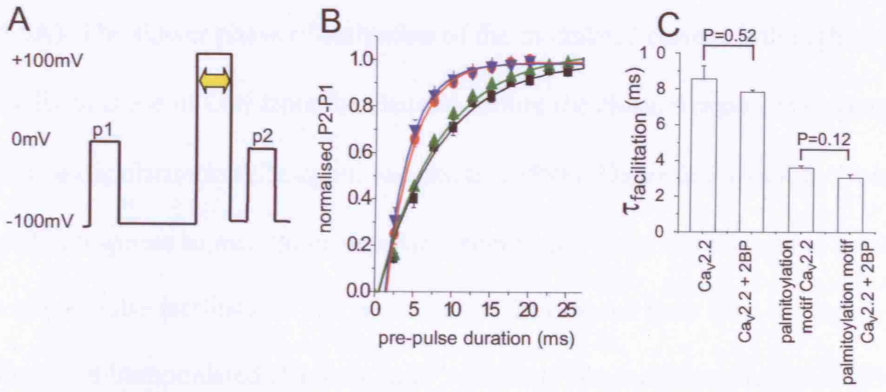

Figure 6.4. Injection of 2BP did not affect facilitation rate of $Ca_V2.2$ of palmitoylation motif $Ca_V2.2$. ***A*** Modified three-pulse protocol. Duration of pre-pulse was varied. ***B*** Normalised P2-P1 plotted against pre-pulse duration. $Ca_V2.2$ (black squares, n=6), $Ca_V2.2$ + 2BP (green triangles, n=3), palmitoylation motif $Ca_V2.2$ (red circles, n=5), palmitoylation motif $Ca_V2.2$ + 2BP (blue inverted triangles, n=3). ***C*** Graph of $\tau_{facilitation}$ comparing $Ca_V2.2$ ± 2BP and palmitoylation motif $Ca_V2.2$ ± 2BP.

Chapter 7. Discussion

As described in the introduction, Gβγ modulation of Ca_V2 family channels has several distinguishing characteristics. With respect to my work, these characteristics are a reduction in current amplitude, slowing of activation kinetics, pre-pulse facilitation, and a depolarising shift in the voltage-dependence of activation.

The slow activation kinetics are clear when Gβγ is over-expressed (Figure 3.2A), and when α_2A-Gα_o is expressed and clonidine is perfused (Figure 3.13A). The biphasic nature of the activation is thought to be due to two populations of channel being present; Gβγ-modulated and Gβγ-unmodulated. The initial fast phase of activation is due to the opening of Gβγ-unmodulated channels and thus has a similar time constant of activation as when there is no Gβγ modulation present (Figures 5.4A and 5.5A). The slower phase of activation of the modulated current is thought to be due to dissociation of Gβγ from the channel, before the channel opens, in response to membrane depolarisation (Zamponi and Snutch, 1998). Dissociation of Gβγ from the channel in response to membrane depolarisation is also generally thought to be the basis of pre-pulse facilitation. The two states of the channel have been termed "willing," for unmodulated channels, and "reluctant," for modulated channels (Bean, 1989). Reluctant channels are converted to willing channels upon depolarisation of the membrane; the channel's affinity for Gβγ becomes weaker as the channel nears the open state and Gβγ dissociates (Zamponi and Snutch, 1998; Colecraft et al., 2000). The "willing/reluctant" model also provides an explanation for the

depolarising shift in the voltage-dependence of activation of currents when modulated by Gβγ compared to control (Figure 5.1).

The present study builds on previous work that identified the N-terminal tail of $Ca_V2.2$ as being essential for Gβγ modulation of the channel (Page et al., 1998; Canti et al., 1999). The previous work had identified two arginine residues in the N-terminal tail, at positions 52 and 54, situated roughly between the N-terminus and the start of the first transmembrane segment. I have confirmed in my system that mutation of these two arginine residues to alanines, abolishes Gβγ modulation of the channel, either by over-expression of $G\beta_1\gamma_2$ or by stimulation of over-expressed α_2A-$G\alpha_o$, to provide a pathway for activation of endogenous Gβγ (Figure 3.3).

Initially, it was hypothesised that the two arginine residues might be involved in binding to PIP_2 and thus tethering the N-terminal tail of $Ca_V2.2$ to the membrane and allowing Gβγ to modulate the channel (Dolphin, 2003). Protein palmitoylation regulates protein activity by facilitating membrane interactions and trafficking, and can modulate protein-protein interactions (for review see Smotrys and Linder, 2004). The PIP_2 binding hypothesis was tested by attempting to mimic membrane tethering of the N-terminal tail by adding a palmitoylation site onto the N-terminus of the $Ca_V2.2$(R52,54A). However, this construct did not display pre-pulse facilitation when Gβγ was over-expressed, indicating that modulation could not be restored in this way. This result is not conclusive though because I cannot be sure that the channel has incorporated a lipid modification and even if it had, the site of the modification may

not be in close enough proximity to the position of the two arginines, that may be involved in PIP_2 binding, to mimic this membrane association effectively. Thus, the hypothesis of membrane association of the N-terminal tail via PIP_2 interaction cannot be confidently rejected because of this result.

Interestingly, when the palmitoylation site was added to the N-terminus of the wild type $Ca_V2.2$ (the construct termed palmitoylation motif $Ca_V2.2$) both clonidine mediated inhibition and pre-pulse facilitation were reduced compared to wild type $Ca_V2.2$ (Figures 3.7, 3.16, and 3.17).

This result led to a new hypothesis: that the two essential arginine residues in the N-terminal tail of $Ca_V2.2$ may be involved in forming a binding pocket for $G\beta\gamma$, such as in the $G\beta\gamma$ modulation of GIRK channels, in which both the N-terminal tail and the C-terminal tail of the channel subunits contain essential residues for $G\beta\gamma$ binding (He et al., 2002). As no direct binding between $G\beta\gamma$ and the N-terminal tail of $Ca_V2.2$ had been demonstrated at the time of these experiments, it seemed possible that the N-terminal tail binds to another part of the channel, possibly on the $Ca_V2.2\alpha_1$-subunit, and this interaction might help to form part of the $G\beta\gamma$ docking site. If this were the case, one can imagine that tethering the N-terminal tail to the membrane, via palmitoylation, could oppose the formation of this docking site by reducing mobility of the N-terminal tail, thus rendering the channel less sensitive to $G\beta\gamma$ modulation.

The reduced modulation of the mutated palmitoylation motif $Ca_V2.2$, in which the putative palmitoylation sites of the palmitoylation motif $Ca_V2.2$ have been mutated to prevent palmitoylation, does not support the hypothesis that reducing the mobility of the N-terminal tail by palmitoylation is the mechanism by which modulation is reduced (Figure 3.8, 3.18, and 3.19).

If the reduction in modulation is not due to the palmitoylation site, what is the mechanism for the observed reduction in modulation of both the palmitoylation motif $Ca_V2.2$ and the mutated palmitoylation motif $Ca_V2.2$?

The sequence of amino acids that was added to the palmitoylation motif $Ca_V2.2$ was copied from the first 11 amino acids of $G\alpha_q$. $G\alpha_q$ has two cysteines at amino acid positions 9 and 10 that are palmitoylated (Thiyagarajan et al., 2002). The first six amino acids of $G\alpha_q$ are highly conserved among $G\alpha_q$- and $G\alpha_{11}$-subunits and are not present in other Gα-subunits. There is some evidence that this extreme N-terminal region of $G\alpha_{q/11}$ is involved in modulating the fidelity of Gα-subunit – GPCR recognition (Kostenis et al., 1998). The mechanism of this is unknown but considering the evidence for the involvement of this sequence of amino acids in G-protein signalling, it is not inconceivable that the introduction of this region could be affecting G-protein signalling in my system.

Another, rather less complicated explanation, is that adding anything on to the N-terminus of $Ca_V2.2$ would disrupt the function of the N-terminal tail region enough to reduce modulation.

To explore this hypothesis, I examined the clonidine mediated inhibition and pre-pulse facilitation of two other constructs of $Ca_V2.2$ that had additional amino acid sequences fused to the N-terminus. These constructs were the GFP-$Ca_V2.2$ and the HA tagged $Ca_V2.2$. The GFP fused to $Ca_V2.2$ consisted of 203 amino acids and the HA tag consisted of 9 amino acids. Both of these constructs had reduced clonidine mediated inhibition and pre-pulse facilitation compared to wild type $Ca_V2.2$, supporting the hypothesis that adding anything onto the N-terminus of $Ca_V2.2$ would disrupt aspects of Gβγ modulation of the channel (Figures 3.9, 3.10, 3.20, and 3.21). Taking into consideration the different sizes of the GFP and the HA tag, it is unlikely that the reduction in modulation is due to a simple steric hindrance.

Previous studies, which have drawn, later disproved, conclusions about mechanisms of Gβγ modulation of Ca_V2 family channels, have highlighted that need to look at multiple aspects of Gβγ when screening for conditions that may affect interactions between Gβγ and the channel. For instance, the controversy surrounding the involvement of the calcium channel β-subunits in G-protein modulation, described in section 1.7.5 in the introduction, was due to consideration of isolated aspects of Gβγ modulation, rather than the whole picture. In an effort to avoid making similar mistakes in my work, I have used a modified three-pulse protocol to examine the kinetics of pre-pulse facilitation and re-inhibition of the palmitoylation site $Ca_V2.2$ and the mutated palmitoylation site $Ca_V2.2$ and compare them to wild type $Ca_V2.2$.

The increased rate of pre-pulse facilitation of palmitoylation motif $Ca_V2.2$, compared to wild type $Ca_V2.2$ and mutated palmitoylation motif $Ca_V2.2$, indicates that there is an additional effect of the palmitoylation site on Gβγ modulation, that is not seen with the mutated palmitoylation site $Ca_V2.2$ (Figures 4.4 and 4.5). Previously, it has been demonstrated that the facilitation rate of Gβγ during the pre-pulse, thought to be the rate of dissociation of Gβγ from the channel, is not dependent on the concentration of Gβγ and therefore it is assumed that Gβγ dimers do not re-associate with the channel during the pre-pulse (Stephens et al., 1998a).

A possible explanation for the reduction in facilitation ratio of the palmitoylation motif CaV2.2 is that the affinity of the palmitoylation motif CaV2.2 for Gbg is reduced compared to that of wild type CaV2.2. The difference in the facilitation rate of the palmitoylation motif CaV2.2 and the mutated palmitoylation motif CaV2.2 may be due to the binding of Gbg to the palmitoylation motif CaV2.2 having greater voltage-dependency than that of the mutated palmitoylation motif CaV2.2, thus depolarisation of the membrane has a stronger effect on Gbg binding to the palmitoylation motif CaV2.2 channel than to either the wild type CaV2.2 channel or the mutated palmitoylation motif CaV2.2 channel.

Thus, at -100mV, the affinities of the palmitoylation motif $Ca_V2.2$ and the mutated palmitoylation motif $Ca_V2.2$ are similar, and at 0mV, the affinity of the mutated palmitoylation motif for Gβγ has not reduced to as great an extent as that of the

palmitoylation motif $Ca_V2.2$. Similar results to those I have observed for the mutated palmitoylation motif $Ca_V2.2$ have been obtained by mutation of an isoleucine residue at position 49 in the N-terminal tail of $Ca_V2.2$ (Canti et al., 1999). The construct, $Ca_V2.2$(I49A), displayed reduced inhibition and pre-pulse facilitation on stimulation of a dopamine D2 receptor, compared to wild type $Ca_V2.2$, but did not display an increase in the facilitation rate compared to wild type $Ca_V2.2$. If the affinity of the palmitoylation motif $Ca_V2.2$ for Gβγ were reduced at all potentials, I would expect the slow component of activation in the presence of Gβγ modulation to be faster for the palmitoylation motif $Ca_V2.2$ than the wild type $Ca_V2.2$. This is because the slow component of activation of modulated currents is though to be due to the dissociation of Gβγ from the channel. The slow component of activation is not increased for the palmitoylation motif $Ca_V2.2$ compared to the wild type $Ca_V2.2$ and the mutated palmitoylation motif $Ca_V2.2$ at a test potential of 0mV, indicating that the difference in sensitivity of Gβγ dissociation from the channel occurs at more depolarised potentials (Figure 5.5).

The hyperpolarising effect of the palmitoylation motif and the mutated palmitoylation motif on the current-voltage relationship in the presence of Gβγ modulation, compared to that of wild type $Ca_V2.2$ in the presence of Gβγ modulation, may indicate that Gβγ does not have the same effect on the channels with these motifs as it does on the wild type $Ca_V2.2$ (Figure 5.3). For instance, the binding of Gβγ to the palmitoylation motif $Ca_V2.2$ channel or the mutated palmitoylation motif $Ca_V2.2$ channel may have less of a stabilising effect on the closed state of those channels than Gβγ does by binding to the wild type channel. This may mean that the

palmitoylation motif $Ca_V2.2$ channel and the mutated palmitoylation motif $Ca_V2.2$ channel can open before Gβγ has completely dissociated.

The possible change in the voltage-dependency of the Gβγ modulation of the palmitoylation motif $Ca_V2.2$ was explored by varying the potential of the pre-pulse in the three pulse protocol between -40 and +60mV. These results did not show a difference in the voltage-dependence of facilitation, with 50% of the maximum facilitation achieved by a test potential of approximately +30mV. It is difficult to compare the different conditions due to the apparent increase in the inactivation of the currents of the palmitoylation motif $Ca_V2.2$ compared to the wild type $Ca_V2.2$ and the mutated palmitoylation motif $Ca_V2.2$ (Figure 4.15). Comparison of the inactivation of the channels showed that the palmitoylation motif $Ca_V2.2$ channels had an increase in the kinetics of inactivation and may show a small shift in the voltage-dependence of inactivation (Figures 5.6 and 5.7). My experiments did not show the shift in the conditioning potential at which half the current is inactivated to be significant between wild type $Ca_V2.2$ and palmitoylation motif $Ca_V2.2$, but the palmitoylation motif $Ca_V2.2$ current was significantly more inactivated than the wild type $Ca_V2.2$ current at a conditioning potential of -60mV (Figure 5.7). The difference in the voltage-dependent inactivation may explain why the palmitoylation motif $Ca_V2.2$ channels did not display any difference in the voltage-dependence of facilitation when the pre-pulse potential was varied, even if there is a difference in the voltage-dependence of facilitation.

The N-terminal tail has previously been implicated in the control of the kinetics of inactivation (Stephens et al., 2000). When the N-terminal tail of $Ca_V2.2$ was truncated to amino acid 55, the retardation of inactivation caused by over-expression of the β_1b-subunit was opposed. This effect was even more prominent when the truncated channel was co-expressed with the β_2a-subunit instead of the β_1b-subunit. The β_2a-subunit has more pronounced effects on inactivation kinetics than the β_1b-subunit and it would be interesting to see what the effects of the palmitoylation motif and the mutated palmitoylation motif would have on the retardation of inactivation kinetics caused by co-expression of the β_2a-subunit. In agreement with the literature (Page et al., 1998), artificial manipulations of the N-terminal tail did not affect any other intrinsic biophysical properties of the channel in the absence of G$\beta\gamma$ modulation. The voltage-dependence and kinetics of activation were not altered for the palmitoylation motif $Ca_V2.2$ and the mutated palmitoylation motif $Ca_V2.2$ compared to the wild type $Ca_V2.2$ channel (Figures 5.1, 5.2 and 5.4).

Are these differences in modulation between the palmitoylation motif $Ca_V2.2$ and the mutated palmitoylation motif $Ca_V2.2$ actually due to the palmitoylation status of the N-terminal tail?

I tried to inhibit palmitoylation of the palmitoylation motif $Ca_V2.2$ channel by injecting 2-bromohexadecanoic palmitate (2BP) into oocytes, in order to find out whether this would eliminate the effects of the palmitoylation motif on modulation. Injecting 2BP did not significantly increase the facilitation ratio of palmitoylation motif $Ca_V2.2$, nor did it affect the facilitation rate of palmitoylation motif $Ca_V2.2$

(Figures 6.1-6.4). This does not provide evidence to support the theory that palmitoylation of the palmitoylation motif $Ca_V2.2$ is what is causing the differences in $G\beta\gamma$ modulation of this channel. Injection of 2BP did seem to increase pre-pulse facilitation of wild type $Ca_V2.2$. This may be due to effects of 2BP on lipid modifications of other proteins. Both $G\alpha$ and $G\beta\gamma$ usually incorporate lipid modifications, and these are important for signalling functions of the G-proteins (for review see (Wedegaertner et al., 1995). In attempt to demonstrate that injecting 2BP into oocytes is able to inhibit palmitoylation of over-expressed proteins, I tried to show that injection of 2BP into oocytes could inhibit palmitoylation of over-expressed β_2a-subunits. The advantage of using β_2a-subunits as a positive control for effectiveness of 2BP application is that there has already been demonstrated a clear difference in the inactivation kinetics of channels containing palmitoylated β_2a-subunits and non-palmitoylated β_2a-subunits (see section 1.3.12). Unfortunately, I was unable to finish these experiments so I cannot draw conclusion from them.

I do not know whether the palmitoylation motif $Ca_V2.2$ is in fact palmitoylated. A variety of different sequences result in palmitoylation of proteins (for review see Smotrys and Linder, 2004), and in the absence of a known consensus sequence, I cannot assume that the palmitoylation motif $Ca_V2.2$ is palmitoylated without some direct evidence, particularly in the light of experiments showing that palmitoylation is a dynamic protein modification (Hurley et al., 2000). I tried to show that the palmitoylation motif $Ca_V2.2$ was palmitoylated by incorporating labelled palmitic acid into the protein, but the results of these experiments were inconclusive.

I have included the details of these preliminary experiments in the appendix. There are other compounds in addition to 2BP that can be used to inhibit protein palmitoylation. Cerulenin and tunicamycin are both antibiotic compounds that have been used experimentally to inhibit protein palmitoylation (Resh, 2006). Unfortunately, I was unable to try either of these compounds.

The Isolated N-terminal Tail

My experiments did not show the injection of cDNA coding for the isolated N-terminal tail as a discrete protein fragment to have any effect on Gβγ modulation of currents, either by stimulation of the α_2A-Gα_o tandem and applying clonidine, or by over-expressing Gβγ (Figures 3.4, 3.5, 3.22, and 3.33). This is in stark contrast to the results published during the course of my research (Agler et al., 2005). In this paper, it is demonstrated that over-expressing the isolated N-terminal tail with $Ca_V2.2$ channels in HEK293 cells results in constitutively inhibited channels when Gβγ are provided either by over-expressing Gβγ or by stimulating an over-expressed muscarinic receptor. It is shown, using yeast 2-hybrid, that a peptide of the N-terminal tail of $Ca_V2.2$ is able to bind to $G\beta_1$-subunits, but $G\beta_1$-subunit positive interaction was also found between $G\beta_1$ and N-terminal tail peptides of both $Ca_V1.2$ and $Ca_V2.1$. Therefore, the binding of $G\beta_1$ to the N-terminal tail of $Ca_V2.2$ cannot explain the unique role of the N-terminal tail of this channel subtype in the modulation by Gβγ.

Using both yeast 2-hybrid and FRET it is demonstrated that the N-terminal tail of $Ca_V2.2$ is able to bind to the I-II loop of $Ca_V2.2$. This binding was not seen

between the N-terminal tail of $Ca_V1.2$ and either the I-II loop of $Ca_V2.2$ or $Ca_V1.2$. Thus it is suggested that the interaction between the N-terminal tail and the I-II loop of $Ca_V2.2$ is the basis for the Gβγ modulation of $Ca_V2.2$ channels. However, the N-terminal tail of $Ca_V2.2$ was not able to bind to the I-II loop of $Ca_V1.2$, which does not explain why a chimeric channel, in which the N-terminal tail of $Ca_V1.2$ is replaced by the N-terminal tail of $Ca_V2.2$, is modulated (Canti et al., 1999).

Interestingly the main site of interaction between the I-II loop and the N-terminal tail was found to be within amino acids 56-95 of the N-terminal tail, which does not include the two arginines that are essential for Gβγ modulation (these are at positions 52 and 54) and deletion of this region of the $Ca_V2.2$ channel, amino acids 56-95, renders it insensitive to Gβγ modulation.

A modified version of the model that has been proposed (Agler et al., 2005) is shown (Figure 7.1). This model incorporates the essential determinants that have been accepted as part of the Gβγ modulation of $Ca_V2.2$ channels. I suggest that a complex is formed between the N-terminal tail and the I-II loop of $Ca_V2.2$. This complex between the N-terminal tail and the I-II loop is necessary for Gβγ dimers to interact with the channel and modulate its function. When the N-terminal tail, the I-II loop, and Gβγ are bound, movement of the voltage-sensor is resisted and the channel is in the "reluctant" state. If the N-terminal tail is immobilised by tethering to the membrane via a lipid modification, the complex can still form, but it is less stable and hence more responsive to changes in membrane potential and the channel is converted to the "willing" state more easily.

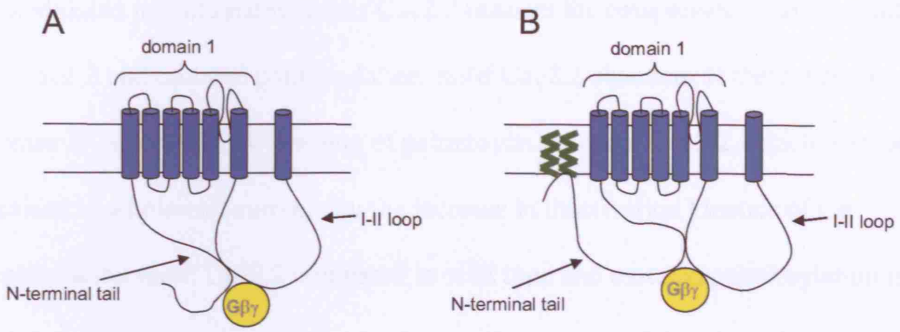

Figure 7.1 Proposed model of Gβγ interaction with the N-terminal tail and the I-II loop of the $Ca_V2.2$ channel. ***A*** The interaction of the N-terminal tail and the I-II loop form a binding pocket through which Gβγ dimers can modulate the channel. ***B*** If the N-terminal tail is tethered to the membrane via lipid modification, Gβγ can still bind and modulate the channel but the binding affinity is more sensitive to voltage changes across the membrane.

Ideas for further work

Additional work that I would have liked to have done to further this research was to use a mammalian expression system such as COS-7 cells, to make patch-clamp recordings of whole-cell and single-channel currents. Patch-clamp recording of COS-7 cells would have the advantages that steady-state inactivation pulse protocols are easier to record and that it would be easier to demonstrate palmitoylation of palmitoylation motif $Ca_V2.2$ using metabolic labelling techniques in a mammalian cell line. This would allow me to find out whether my palmitoylation motif $Ca_V2.2$ is palmitoylated, to give me more clues as to whether the palmitoylation status is the basis of the difference between facilitation rates of the palmitoylation motif $Ca_V2.2$ and the mutated palmitoylation motif $Ca_V2.2$.

Single channel recordings would allow further investigation into kinetics of the modulated palmitoylation motif $Ca_V2.2$ channel for comparison with the wild type $Ca_V2.2$ and mutated palmitoylation motif $Ca_V2.2$ channels. If there were a decrease in latency of first opening of palmitoylation motif $Ca_V2.2$, which may be disguised in whole-cell currents by the increase in inactivation kinetics of the palmitoylation motif $Ca_V2.2$ compared to wild type and mutated palmitoylation motif $Ca_V2.2$, it would support my hypothesis that dissociation of $G\beta\gamma$ from the palmitoylation motif $Ca_V2.2$ has a greater sensitivity than wild type $Ca_V2.2$, or mutated palmitoylation motif $Ca_V2.2$, to depolarisation of the membrane.

References

Adams SR, Harootunian AT, Buechler YV, Taylor SS, Tsien RY (1991) Fluorescence ratio imaging of cyclim AMP in single cells. Nature 349: 694-697.

Aggarwal SK, MacKinnon R (1996) Contribution of the S4 segment to gating charge in the Shaker K+ channel. Neuron 16: 1169-1177.

Agler HL, Evans J, Tay LH, Anderson MJ, Colecraft HM, Yue DT (2005) G protein-gated inhibitory module of N-type (ca(v)2.2) ca2+ channels. Neuron 46: 891-904.

Baertschi AJ, Audigier Y, Lledo PM, Israel JM, Bockaert J, Vincent JD (1992) Dialysis of lactotropes with antisense oligonucleotides assigns guanine nucleotide binding protein subtypes to their channel effectors. Mol Endocrinol 6: 2257-2265.

Bangalore R, Mehrke G, Gingrich K, Hofmann F, Kass RS (1996) Influence of L-type Ca channel alpha 2/delta-subunit on ionic and gating current in transiently transfected HEK 293 cells. Am J Physiol 270: H1521-H1528.

Barclay J, Balaguero N, Mione M, Ackerman SL, Letts VA, Brodbeck J, Canti C, Meir A, Page KM, Kusumi K, Perez-Reyes E, Lander ES, Frankel WN, Gardiner RM, Dolphin AC, Rees M (2001) Ducky mouse phenotype of epilepsy and ataxia is associated with mutations in the Cacna2d2 gene and decreased calcium channel current in cerebellar Purkinje cells. J Neurosci 21: 6095-6104.

Bean BP (1989) Neurotransmitter inhibition of neuronal calcium currents by changes in channel voltage dependence. Nature 340: 153-156.

Bean BP, Nowycky MC, Tsien RW (1984) Beta-adrenergic modulation of calcium channels in frog ventricular heart cells. Nature 307: 371-375.

Beedle AM, McRory JE, Poirot O, Doering CJ, Altier C, Barrere C, Hamid J, Nargeot J, Bourinet E, Zamponi GW (2004) Agonist-independent modulation of N-type calcium channels by ORL1 receptors. Nat Neurosci 7: 118-125.

Bell DC, Butcher AJ, Berrow NS, Page KM, Brust PF, Nesterova A, Stauderman KA, Seabrook GR, Nurnberg B, Dolphin AC (2001) Biophysical properties, pharmacology, and modulation of human, neuronal L-type (alpha(1D), Ca(V)1.3) voltage-dependent calcium currents. J Neurophysiol 85: 816-827.

Bennett MK, Calakos N, Scheller RH (1992) Syntaxin: a synaptic protein implicated in docking of synaptic vesicles at presynaptic active zones. Science 257: 255-259.

Bergsman JB, Tsien RW (2000) Syntaxin modulation of calcium channels in cortical synaptosomes as revealed by botulinum toxin C1. J Neurosci 20: 4368-4378.

Berjukow S, Marksteiner R, Sokolov S, Weiss RG, Margreiter E, Hering S (2001) Amino acids in segment IVS6 and beta-subunit interaction support distinct conformational changes during Ca(v)2.1 inactivation. J Biol Chem 276: 17076-17082.

Bernstein J (1902) Untersuchungen zur thermodynamik der bioelektrischen strome. Pflugers Arch 521-562.

Bernstein J (1912) Elektrobiologie. Braunschweig: Vieweg.

Berrow NS, Brice NL, Tedder I, Page KM, Dolphin AC (1997) Properties of cloned rat alpha1A calcium channels transiently expressed in the COS-7 cell line. Eur J Neurosci 9: 739-748.

Berrow NS, Campbell V, Fitzgerald EM, Brickley K, Dolphin AC (1995) Antisense depletion of beta-subunits modulates the biophysical and pharmacological properties of neuronal calcium channels. J Physiol 482 (Pt 3): 481-491.

Bertaso F, Ward RJ, Viard P, Milligan G, Dolphin AC (2003) Mechanism of action of Gq to inhibit G beta gamma modulation of CaV2.2 calcium channels: probed by the use of receptor-G alpha tandems. Mol Pharmacol 63: 832-843.

Bezprozvanny I, Scheller RH, Tsien RW (1995) Functional impact of syntaxin on gating of N-type and Q-type calcium channels. Nature 378: 623-626.

Bichet D, Lecomte C, Sabatier JM, Felix R, De Waard M (2000) Reversibility of the Ca(2+) channel alpha(1)-beta subunit interaction. Biochem Biophys Res Commun 277: 729-735.

Birnbaumer L, Qin N, Olcese R, Tareilus E, Platano D, Costantin J, Stefani E (1998) Structures and functions of calcium channel beta subunits. J Bioenerg Biomembr 30: 357-375.

Blackmer T, Larsen EC, Bartleson C, Kowalchyk JA, Yoon EJ, Preininger AM, Alford S, Hamm HE, Martin TF (2005) G protein betagamma directly regulates SNARE protein fusion machinery for secretory granule exocytosis. Nat Neurosci 8: 421-425.

Bogdanov Y, Brice NL, Canti C, Page KM, Li M, Volsen SG, Dolphin AC (2000) Acidic motif responsible for plasma membrane association of the voltage-dependent calcium channel beta1b subunit. Eur J Neurosci 12: 894-902.

Boland LM, Bean BP (1993) Modulation of N-type calcium channels in bullfrog sympathetic neurons by luteinizing hormone-releasing hormone: kinetics and voltage dependence. J Neurosci 13: 516-533.

Borst JG, Sakmann B (1998) Facilitation of presynaptic calcium currents in the rat brainstem. J Physiol 513 (Pt 1): 149-155.

Bourinet E, Soong TW, Stea A, Snutch TP (1996) Determinants of the G protein-dependent opioid modulation of neuronal calcium channels. Proc Natl Acad Sci U S A 93: 1486-1491.

Bourinet E, Soong TW, Sutton K, Slaymaker S, Mathews E, Monteil A, Zamponi GW, Nargeot J, Snutch TP (1999) Splicing of alpha 1A subunit gene generates phenotypic variants of P- and Q-type calcium channels. Nat Neurosci 2: 407-415.

Brody DL, Yue DT (2000) Relief of G-protein inhibition of calcium channels and short-term synaptic facilitation in cultured hippocampal neurons. J Neurosci 20: 889-898.

Butcher AJ, Leroy J, Richards MW, Pratt WS, Dolphin AC (2006) The importance of occupancy rather than affinity of CaV{beta} subunits for the calcium channel I-II linker in relation to calcium channel function. J Physiol.

Campbell V, Berrow N, Dolphin AC (1993) GABAB receptor modulation of Ca2+ currents in rat sensory neurones by the G protein G(0): antisense oligonucleotide studies. J Physiol 470: 1-11.

Campbell V, Berrow NS, Fitzgerald EM, Brickley K, Dolphin AC (1995) Inhibition of the interaction of G protein G(o) with calcium channels by the calcium channel beta-subunit in rat neurones. J Physiol 485 (Pt 2): 365-372.

Canti C, Bogdanov Y, Dolphin AC (2000) Interaction between G proteins and accessory subunits in the regulation of 1B calcium channels in Xenopus oocytes. J Physiol 527 Pt 3: 419-432.

Canti C, Davies A, Berrow NS, Butcher AJ, Page KM, Dolphin AC (2001) Evidence for two concentration-dependent processes for beta-subunit effects on alpha1B calcium channels. Biophys J 81: 1439-1451.

Canti C, Dolphin AC (2003) CaVbeta subunit-mediated up-regulation of CaV2.2 currents triggered by D2 dopamine receptor activation. Neuropharmacology 45: 814-827.

Canti C, Page KM, Stephens GJ, Dolphin AC (1999) Identification of residues in the N terminus of alpha1B critical for inhibition of the voltage-dependent calcium channel by Gbeta gamma. J Neurosci 19: 6855-6864.

Carafoli E (1992) The Ca2+ pump of the plasma membrane. J Biol Chem 267:2115-2118.

Carbone E, Lux HD (1984) A low voltage-activated calcium conductance in embryonic chick sensory neurons. Biophys J 46: 413-418.

Carbone E, Lux HD (1987) Single low-voltage-activated calcium channels in chick and rat sensory neurones. J Physiol 386: 571-601.

Castellano A, Wei X, Birnbaumer L, Perez-Reyes E (1993a) Cloning and expression of a neuronal calcium channel beta subunit. J Biol Chem 268: 12359-12366.

Castellano A, Wei X, Birnbaumer L, Perez-Reyes E (1993b) Cloning and expression of a third calcium channel beta subunit. J Biol Chem 268: 3450-3455.

Catterall WA (1988) Molecular properties of voltage-sensitive sodium and calcium channels. Braz J Med Biol Res 21: 1129-1144.

Catterall WA (2000) Structure and regulation of voltage-gated Ca2+ channels. Annu Rev Cell Dev Biol 16: 521-555.

Cavalli A, Druey KM, Milligan G (2000) The regulator of G protein signaling RGS4 selectively enhances alpha 2A-adreoreceptor stimulation of the GTPase activity of Go1alpha and Gi2alpha. J Biol Chem 275: 23693-23699.

Chang FC, Hosey MM (1988) Dihydropyridine and phenylalkylamine receptors associated with cardiac and skeletal muscle calcium channels are structurally different. J Biol Chem 263: 18929-18937.

Chaudhuri D, Chang SY, DeMaria CD, Alvania RS, Soong TW, Yue DT (2004) Alternative splicing as a molecular switch for Ca2+/calmodulin-dependent facilitation of P/Q-type Ca2+ channels. J Neurosci 24: 6334-6342.

Chen J, DeVivo M, Dingus J, Harry A, Li J, Sui J, Carty DJ, Blank JL, Exton JH, Stoffel RH, . (1995) A region of adenylyl cyclase 2 critical for regulation by G protein beta gamma subunits. Science 268: 1166-1169.

Chen S, Zheng X, Schulze KL, Morris T, Bellen H, Stanley EF (2002) Enhancement of presynaptic calcium current by cysteine string protein. J Physiol 538: 383-389.

Chien AJ, Carr KM, Shirokov RE, Rios E, Hosey MM (1996) Identification of palmitoylation sites within the L-type calcium channel beta2a subunit and effects on channel function. J Biol Chem 271: 26465-26468.

Chien AJ, Hosey MM (1998) Post-translational modifications of beta subunits of voltage-dependent calcium channels. J Bioenerg Biomembr 30: 377-386.

Clapham DE, Neer EJ (1997) G protein beta gamma subunits. Annu Rev Pharmacol Toxicol 37: 167-203.

Cole KS (1949) Dynamic electrical characteristics of the squid axon membrane. Arch Sci Physiol 3: 253-258.

Cole KS (1968) Membranes, ions and impulses. Berkeley: University of California Press.

Cole KS, Curtis HJ (1939) Electrical impedence of the squid giant axon during activity. J Gen Physiol 22: 649-670.

Colecraft HM, Patil PG, Yue DT (2000) Differential occurrence of reluctant openings in G-protein-inhibited N- and P/Q-type calcium channels. J Gen Physiol 115: 175-192.

Cooper CB, Arnot MI, Feng ZP, Jarvis SE, Hamid J, Zamponi GW (2000) Cross-talk between G-protein and protein kinase C modulation of N-type calcium channels is dependent on the G-protein beta subunit isoform. J Biol Chem 275: 40777-40781.

Cox DH, Dunlap K (1994) Inactivation of N-type calcium current in chick sensory neurons: calcium and voltage dependence. J Gen Physiol 104: 311-336.

Curtis BM, Catterall WA (1984) Purification of the calcium antagonist receptor of the voltage-sensitive calcium channel from skeletal muscle transverse tubules. Biochemistry 23: 2113-2118.

Cuttle MF, Tsujimoto T, Forsythe ID, Takahashi T (1998) Facilitation of the presynaptic calcium current at an auditory synapse in rat brainstem. J Physiol 512 (Pt 3): 723-729.

D'Ascenzo M, Martinotti G, Azzena GB, Grassi C (2002) cGMP/protein kinase G-dependent inhibition of N-type Ca2+ channels induced by nitric oxide in human neuroblastoma IMR32 cells. J Neurosci 22: 7485-7492.

De Jongh KS, Warner C, Catterall WA (1990) Subunits of purified calcium channels. Alpha 2 and delta are encoded by the same gene. J Biol Chem 265: 14738-14741.

De Waard M, Liu H, Walker D, Scott VE, Gurnett CA, Campbell KP (1997) Direct binding of G-protein betagamma complex to voltage-dependent calcium channels. Nature 385: 446-450.

De Waard M, Pragnell M, Campbell KP (1994) Ca2+ channel regulation by a conserved beta subunit domain. Neuron 13: 495-503.

De Waard M, Witcher DR, Pragnell M, Liu H, Campbell KP (1995) Properties of the alpha 1-beta anchoring site in voltage-dependent Ca2+ channels. J Biol Chem 270: 12056-12064.

Degtiar VE, Wittig B, Schultz G, Kalkbrenner F (1996) A specific G(o) heterotrimer couples somatostatin receptors to voltage-gated calcium channels in RINm5F cells. FEBS Lett 380: 137-141.

Delmas P, Abogadie FC, Buckley NJ, Brown DA (2000) Calcium channel gating and modulation by transmitters depend on cellular compartmentalization. Nat Neurosci 3: 670-678.

Delmas P, Abogadie FC, Milligan G, Buckley NJ, Brown DA (1999) betagamma dimers derived from Go and Gi proteins contribute different components of adrenergic inhibition of Ca2+ channels in rat sympathetic neurones. J Physiol 518 (Pt 1): 23-36.

Diverse-Pierluissi M, Dunlap K (1993) Distinct, convergent second messenger pathways modulate neuronal calcium currents. Neuron 10: 753-760.

Diverse-Pierluissi M, Dunlap K (1995) Interaction of convergent pathways that inhibit N-type calcium currents in sensory neurons. Neuroscience 65: 477-483.

Dolphin AC (2003) G protein modulation of voltage-gated calcium channels. Pharmacol Rev 55: 607-627.

Dolphin AC, Forda SR, Scott RH (1986) Calcium-dependent currents in cultured rat dorsal root ganglion neurones are inhibited by an adenosine analogue. J Physiol 373: 47-61.

Dolphin AC, Prestwich SA (1985) Pertussis toxin reverses adenosine inhibition of neuronal glutamate release. Nature 316: 148-150.

Dolphin AC, Scott RH (1987) Calcium channel currents and their inhibition by (-)-baclofen in rat sensory neurones: modulation by guanine nucleotides. J Physiol 386: 1-17.

Dunlap K, Fischbach GD (1978) Neurotransmitters decrease the calcium ocmponent of sensory neurone action potentials. Nature 276: 837-839.

Dunlap K, Fischbach GD (1981) Neurotransmitters decrease the calcium conductance activated by depolarization of embryonic chick sensory neurones. J Physiol 317: 519-535.

Ellis SB, Williams ME, Ways NR, Brenner R, Sharp AH, Leung AT, Campbell KP, McKenna E, Koch WJ, Hui A, . (1988) Sequence and expression of mRNAs encoding the alpha 1 and alpha 2 subunits of a DHP-sensitive calcium channel. Science 241: 1661-1664.

Elmslie KS, Jones SW (1994) Concentration dependence of neurotransmitter effects on calcium current kinetics in frog sympathetic neurones. J Physiol 481 (Pt 1): 35-46.

Ewald DA, Pang IH, Sternweis PC, Miller RJ (1989) Differential G protein-mediated coupling of neurotransmitter receptors to Ca2+ channels in rat dorsal root ganglion neurons in vitro. Neuron 2: 1185-1193.

Fatt P, Ginsborg BL (1958) The ionic requirements for the production of action potentials in crustacean muscle fibres. J Physiol 142: 516-543.

Fatt P, Katz B (1953) The electrical properties of crustacean muscle fibres. J Physiol 120: 171-204.

Fedulova SA, Kostyuk PG, Veselovsky NS (1985) Two types of calcium channels in the somatic membrane of new-born rat dorsal root ganglion neurones. J Physiol 359: 431-446.

Fitzgerald EM (2002) The presence of Ca2+ channel beta subunit is required for mitogen-activated protein kinase (MAPK)-dependent modulation of alpha1B Ca2+ channels in COS-7 cells. J Physiol 543: 425-437.

Fletcher JE, Lindorfer MA, DeFilippo JM, Yasuda H, Guilmard M, Garrison JC (1998) The G protein beta5 subunit interacts selectively with the Gq alpha subunit. J Biol Chem 273: 636-644.

Forscher P, Oxford GS, Schulz D (1986) Noradrenaline modulates calcium channels in avian dorsal root ganglion cells through tight receptor-channel coupling. J Physiol 379: 131-144.

Garcia DE, Li B, Garcia-Ferreiro RE, Hernandez-Ochoa EO, Yan K, Gautam N, Catterall WA, Mackie K, Hille B (1998) G-protein beta-subunit specificity in the fast membrane-delimited inhibition of Ca2+ channels. J Neurosci 18: 9163-9170.

Golard A, Siegelbaum SA (1993) Kinetic basis for the voltage-dependent inhibition of N-type calcium current by somatostatin and norepinephrine in chick sympathetic neurons. J Neurosci 13: 3884-3894.

Grassi F, and Lux HD (1989) Voltage-dependent GABA-induced modulation of calcium currents in chick sensory neurons. Neurosci Lett 105: 113-119.

Gurdon JB, Lane CD, Woodland HR, Marbaix G (1971) Use of frog eggs and oocytes for the study of messenger RNA and its translation in living cells. Nature 233: 177-182.

Gurnett CA, De Waard M, Campbell KP (1996) Dual function of the voltage-dependent Ca2+ channel alpha 2 delta subunit in current stimulation and subunit interaction. Neuron 16: 431-440.

Hagiwara S, Ozawa S, Sand O (1975) Voltage clamp analysis of two inward current mechanisms in the egg cell membrane of a starfish. J Gen Physiol 65: 617-644.

Hamid J, Nelson D, Spaetgens R, Dubel SJ, Snutch TP, Zamponi GW (1999) Identification of an integration center for cross-talk between protein kinase C and G protein modulation of N-type calcium channels. J Biol Chem 274: 6195-6202.

Hanlon MR, Berrow NS, Dolphin AC, Wallace BA (1999) Modelling of a voltage-dependent Ca2+ channel beta subunit as a basis for understanding its functional properties. FEBS Lett 445: 366-370.

He C, Yan X, Zhang H, Mirshahi T, Jin T, Huang A, Logothetis DE (2002) Identification of critical residues controlling G protein-gated inwardly rectifying K(+) channel activity through interactions with the beta gamma subunits of G proteins. J Biol Chem 277: 6088-6096.

Herlitze S, Garcia DE, Mackie K, Hille B, Scheuer T, Catterall WA (1996) Modulation of Ca2+ channels by G-protein beta gamma subunits. Nature 380: 258-262.

Herlitze S, Hockerman GH, Scheuer T, Catterall WA (1997) Molecular determinants of inactivation and G protein modulation in the intracellular loop connecting domains I and II of the calcium channel alpha1A subunit. Proc Natl Acad Sci U S A 94: 1512-1516.

Hermann L (1899) Zur theorie der erregungsleitung und der elektrischen errengung. Pflugers Arch 75: 574-590.

Hermann L (1905a) Beitrage zur physiologie un physik des nerven. Pflugers Arch 109: 95-144.

Hermann L (1905b) Lehrbuch der physiologie. Berlin: August Hirschwald.

Hess P, Tsien RW (1984) Mechanism of ion permeation through calcium channels. Nature 309: 453-456.

Hille B (1994) Modulation of ion-channel function by G-protein-coupled receptors. Trends Neurosci 17: 531-536.

Hilgemann DW, Nicoll DA, Philipson KD (1991) Charge movement during Na+ translocation by native and cloned Na+/Ca+ exchangers. Nature 352:715-718.

Hillman D, Chen S, Aung TT, Cherksey B, Sugimori M, Llinas RR (1991) Localization of P-type calcium channels in the central nervous system. Proc Natl Acad Sci U S A 88: 7076-7080.

Hodgkin AL (1937a) Evidence for electrical transmission in nerve. Part I. J Physiol 90: 183-210.

Hodgkin AL (1937b) Evidence for electrical transmission in nerve. Part II. J Physiol 90: 211-232.

Hodgkin AL, Huxley AF (1945) Resting and action potentials in single nerve fibres. J Physiol 104: 176-195.

Hodgkin AL, Huxley AF (1952a) A quantitative description of membrane current and its application to conduction and excitation in nerve. J Physiol 117: 500-544.

Hodgkin AL, Huxley AF (1952b) Currents carried by sodium and potassium ions through the membrane of the giant axon of Loligo. J Physiol 116: 449-472.

Hodgkin AL, Huxley AF (1952c) The components of membrane conductance in the giant axon of Loligo. J Physiol 116: 473-496.

Hodgkin AL, Huxley AF (1952d) The dual effect of membrane potential on sodium conductance in the giant axon of Loligo. J Physiol 116: 497-506.

Hodgkin AL, Huxley AF, Katz B (1949) Ionic currents underlying activity in the giant axon of the squid. Arch Sci Physiol 3: 129-150.

Hodgkin AL, Huxley AF, Katz B (1952) Measurement of current-voltage relations in the membrane of the giant axon of Loligo. J Physiol 116: 424-448.

Holz GG, Rane SG, Dunlap K (1986) GTP-binding proteins mediate transmitter inhibition of voltage-dependent calcium channels. Nature 319: 670-672.

Huang CL, Feng S, Hilgemann DW (1998) Direct activation of inward rectifier potassium channels by PIP2 and its stabilization by Gbetagamma. Nature 391: 803-806.

Hullin R, Asmus F, Ludwig A, Hersel J, Boekstegers P (1999) Subunit expression of the cardiac L-type calcium channel is differentially regulated in diastolic heart failure of the cardiac allograft. Circulation 100: 155-163.

Hurley JH, Cahill AL, Currie KPM, Fox AP (2000) The role of dynamic palmitoylation in Ca2+ channel inactivation. Proc Nat Acad Sci 97: 9293-9298.

Ikeda SR (1991) Double-pulse calcium channel current facilitation in adult rat sympathetic neurones. J Physiol 439: 181-214.

Ikeda SR (1996) Voltage-dependent modulation of N-type calcium channels by G-protein beta gamma subunits. Nature 380: 255-258.

Ikeda SR, Schofield GG (1989) Somatostatin blocks a calcium current in rat sympathetic ganglion neurones. J Physiol 409: 221-240.

Imagawa T, Smith JS, Cofonado R, Campbell KP, (1987) Purified ryanodine receptor from skeletal muscle sarcoplasmic reticulum is the Ca2+-permeable pore of the calcium release channel. J Biol Chem 262: 16636-16643.

Jarvis SE, Magga JM, Beedle AM, Braun JE, Zamponi GW (2000) G protein modulation of N-type calcium channels is facilitated by physical interactions between syntaxin 1A and Gbetagamma. J Biol Chem 275: 6388-6394.

Jay SD, Ellis SB, McCue AF, Williams ME, Vedvick TS, Harpold MM, Campbell KP (1990) Primary structure of the gamma subunit of the DHP-sensitive calcium channel from skeletal muscle. Science 248: 490-492.

Jay SD, Sharp AH, Kahl SD, Vedvick TS, Harpold MM, Campbell KP (1991) Structural characterization of the dihydropyridine-sensitive calcium channel alpha 2-subunit and the associated delta peptides. J Biol Chem 266: 3287-3293.

Jeong SW, Ikeda SR (1999) Sequestration of G-protein beta gamma subunits by different G-protein alpha subunits blocks voltage-dependent modulation of Ca2+ channels in rat sympathetic neurons. J Neurosci 19: 4755-4761.

Jones LP, Patil PG, Snutch TP, Yue DT (1997) G-protein modulation of N-type calcium channel gating current in human embryonic kidney cells (HEK 293). J Physiol 498 (Pt 3): 601-610.

Jones SW, Elmslie KS (1997) Transmitter modulation of neuronal calcium channels. J Membr Biol 155: 1-10.

Josephson IR, Varadi G (1996) The beta subunit increases Ca2+ currents and gating charge movements of human cardiac L-type Ca2+ channels. Biophys J 70: 1285-1293.

Katz B, Miledi R (1969) Tetrodotoxin-resistant electric activity in presynaptic terminals. J Physiol 203: 459-487.

Katz P, Whalen G, Kehrl JH (1994) Differential expression of a novel protein kinase in human B lymphocytes. Preferential localization in the germinal center. J Biol Chem 269: 16802-16809.

Kenakin T (1997) Differences between natural and recombinant G protein-coupled receptor systems with varying receptor/G protein stoichiometry. Trends Pharmacol Sci 18: 456-464.

Kleuss C, Hescheler J, Ewel C, Rosenthal W, Schultz G, Wittig B (1991) Assignment of G-protein subtypes to specific receptors inducing inhibition of calcium currents. Nature 353: 43-48.

Klugbauer N, Lacinova L, Marais E, Hobom M, Hofmann F (1999) Molecular diversity of the calcium channel alpha2delta subunit. J Neurosci 19: 684-691.

Kostenis E, Zeng FY, Wess J (1998) Functional characterization of a series of mutant G protein alphaq subunits displaying promiscuous receptor coupling properties. J Biol Chem 273: 17886-17892.

Kraus RL, Sinnegger MJ, Koschak A, Glossmann H, Stenirri S, Carrera P, Striessnig J (2000) Three new familial hemiplegic migraine mutants affect P/Q-type Ca(2+) channel kinetics. J Biol Chem 275: 9239-9243.

Kurachi Y, Ito H, Sugimoto T, Katada T, Ui M (1989) Activation of atrial muscarinic K+ channels by low concentrations of beta gamma subunits of rat brain G protein. Pflugers Arch 413: 325-327.

Laporte

Lee A, Scheuer T, Catterall WA (2000) Ca2+/calmodulin-dependent facilitation and inactivation of P/Q-type Ca2+ channels. J Neurosci 20: 6830-6838.

Lee A, Wong ST, Gallagher D, Li B, Storm DR, Scheuer T, Catterall WA (1999) Ca2+/calmodulin binds to and modulates P/Q-type calcium channels. Nature 399: 155-159.

Lee HK, Elmslie KS (2000) Reluctant gating of single N-type calcium channels during neurotransmitter-induced inhibition in bullfrog sympathetic neurons. J Neurosci 20: 3115-3128.

Leroy J, Richards MW, Butcher AJ, Nieto-Rostro M, Pratt WS, Davies A, Dolphin AC (2005) Interaction via a key tryptophan in the I-II linker of N-type calcium channels is required for beta1 but not for palmitoylated beta2, implicating an

additional binding site in the regulation of channel voltage-dependent properties. J Neurosci 25: 6984-6996.

Letts VA, Felix R, Biddlecome GH, Arikkath J, Mahaffey CL, Valenzuela A, Bartlett FS, Mori Y, Campbell KP, Frankel WN (1998) The mouse stargazer gene encodes a neuronal Ca2+-channel gamma subunit. Nat Genet 19: 340-347.

Lin Y, McDonough SI, Lipscombe D (2004) Alternative splicing in the voltage-sensing region of N-type CaV2.2 channels modulates channel kinetics. J Neurophysiol 92: 2820-2830.

Lin Z, Lin, Y, Schorge S, Pan JQ, Beierlein, Lipscombe D (1999) Alternative splicing of a short cassette exon in a1B generates functionally distinct N-type calcium channels in central and peripheral neurons. J Neurosci 19: 5322-5331.

Lipscombe D, Pan JQ, Gray AC (2002) Functional diversity in neuronal voltage-gated calcium channels by alternative splicing of CaValpha1. Mol Neurobiol 26: 21-44.

Liu H, De Waard M, Scott VE, Gurnett CA, Lennon VA, Campbell KP (1996) Identification of three subunits of the high affinity omega-conotoxin MVIIC-sensitive Ca2+ channel. J Biol Chem 271: 13804-13810.

Llinas R, Steinberg IZ, Walton K (1980) Transmission in the squid giant synapse: a model based on voltage clamp studies. J Physiol (Paris) 76: 413-418.

Llinas R, Sugimori M, Lin JW, Cherksey B (1989) Blocking and isolation of a calcium channel from neurons in mammals and cephalopods utilizing a toxin fraction (FTX) from funnel-web spider poison. Proc Natl Acad Sci U S A 86: 1689-1693.

Llinas R, Sugimori M, Silver RB (1992) Presynaptic calcium concentration microdomains and transmitter release. J Physiol Paris 86: 135-138.

Llinas R, Yarom Y (1981) Electrophysiology of mammalian inferior olivary neurones in vitro. Different types of voltage-dependent ionic conductances. J Physiol 315: 549-567.

Logothetis DE, Kurachi Y, Galper J, Neer EJ, Clapham DE (1987) The beta gamma subunits of GTP-binding proteins activate the muscarinic K+ channel in heart. Nature 325: 321-326.

Lopez HS, Brown AM (1991) Correlation between G protein activation and reblocking kinetics of Ca2+ channel currents in rat sensory neurons. Neuron 7: 1061-1068.

Ludwig A, Flockerzi V, Hofmann F (1997) Regional expression and cellular localization of the alpha1 and beta subunit of high voltage-activated calcium channels in rat brain. J Neurosci 17: 1339-1349.

Marmont G (1949) Studies on the axon membrane. I. A new method. J Cell Comp Physiol 34: 351-382.

McCleskey EW, Fox AP, Feldman DH, Cruz LJ, Olivera BM, Tsien RW, Yoshikami D (1987) Omega-conotoxin: direct and persistent blockade of specific types of

calcium channels in neurons but not muscle. Proc Natl Acad Sci U S A 84: 4327-4331.

McDonald TF, Pelzer S, Trautwein W, Pelzer DJ (1994) Regulation and modulation of calcium channels in cardiac, skeletal, and smooth muscle cells. Physiol Rev 74: 365-507.

McEnery MW, Snowman AM, Sharp AH, Adams ME, Snyder SH (1991) Purified omega-conotoxin GVIA receptor of rat brain resembles a dihydropyridine-sensitive L-type calcium channel. Proc Natl Acad Sci U S A 88: 11095-11099.

McFadzean I, Mullaney I, Brown DA, Milligan G (1989) Antibodies to the GTP binding protein, Go, antagonize noradrenaline-induced calcium current inhibition in NG108-15 hybrid cells. Neuron 3: 177-182.

McHugh D, Sharp EM, Scheuer T, Catterall WA (2000) Inhibition of cardiac L-type calcium channels by protein kinase C phosphorylation of two sites in the N-terminal domain. Proc Natl Acad Sci U S A 97: 12334-12338.

Meir A, Bell DC, Stephens GJ, Page KM, Dolphin AC (2000) Calcium channel beta subunit promotes voltage-dependent modulation of alpha 1 B by G beta gamma. Biophys J 79: 731-746.

Meir A, Dolphin AC (1998) Known calcium channel alpha1 subunits can form low threshold small conductance channels with similarities to native T-type channels. Neuron 20: 341-351.

Meir A, Dolphin AC (2002) Kinetics and Gbetagamma modulation of Ca(v)2.2 channels with different auxiliary beta subunits. Pflugers Arch 444: 263-275.

Menon-Johansson AS, Berrow N, Dolphin AC (1993) G(o) transduces GABAB-receptor modulation of N-type calcium channels in cultured dorsal root ganglion neurons. Pflugers Arch 425: 335-343.

Meza U, Adams B (1998) G-Protein-dependent facilitation of neuronal alpha1A, alpha1B, and alpha1E Ca channels. J Neurosci 18: 5240-5252.

Mikami A, Imoto K, Tanabe T, Niidome T, Mori Y, Takeshima H, Narumiya S, Numa S (1989) Primary structure and functional expression of the cardiac dihydropyridine-sensitive calcium channel. Nature 340: 230-233.

Milligan G and Kostenis E, (2006) Heterotrimeric G-proteins: a short history. Br J Pharmacol 147: S46-55

Mintz IM, Venema VJ, Swiderek KM, Lee TD, Bean BP, Adams ME (1992) P-type calcium channels blocked by the spider toxin omega-Aga-IVA. Nature 355: 827-829.

Mori Y, Friedrich T, Kim MS, Mikami A, Nakai J, Ruth P, Bosse E, Hofmann F, Flockerzi V, Furuichi T, . (1991) Primary structure and functional expression from complementary DNA of a brain calcium channel. Nature 350: 398-402.

Moss FJ, Viard P, Davies A, Bertaso F, Page KM, Graham A, Canti C, Plumpton M, Plumpton C, Clare JJ, Dolphin AC (2002) The novel product of a five-exon stargazin-related gene abolishes Ca(V)2.2 calcium channel expression. EMBO J 21: 1514-1523.

Natochin M, Moussaif M, Artemyev NO (2001) Probing the mechanism of rhodopsin-catalysed tansducin activation. J Neurochem 77:202-210.

Neely A, Olcese R, Wei X, Birnbaumer L, Stefani E (1994) Ca2+-dependent inactivation of a cloned cardiac Ca2+ channel alpha1 subunit expressed in Xenopus oocytes. Biophys J 66:1895-1903.

Neely A, Wei X, Olcese R, Birnbaumer L, Stefani E (1993) Potentiation by the beta subunit of the ratio of the ionic current to the charge movement in the cardiac calcium channel. Science 262: 575-578.

Neer EJ (1995) Heterotrimeric G proteins: organizers of transmembrane signals. Cell 80: 249-257.

Neher E, Sakmann B (1976) Single-channel currents recorded from membrane of denervated frog muscle fibres. Nature 260: 799-802.

Nernst W (1888) Zur kinetik der in losung befindlichen korper: Theory der diffusion. Z Phys Chem 613-637.

Nilius B (1986) Possible functional significance of a novel type of cardiac Ca channel. Biomed Biochim Acta 45: K37-45.

Nishizuka Y (1992) Intracellular signalling by hydrolysis of phosholipids and activation of protein kinase C. Science 258: 607-614.

Nowycky MC, Fox AP, Tsien RW (1985) Three types of neuronal calcium channel with different calcium agonist sensitivity. Nature 316: 440-443.

Nuss HB, Marben E (1994) Electrophysiological properties of neonatal mouse cardiac myocytes in primary culture. J Physiol 479: 265-279.

O'Connor VM, Shamotienko O, Grishin E, Betz H (1993) On the structure of the 'synaptosecretosome'. Evidence for a neurexin/synaptotagmin/syntaxin/Ca2+ channel complex. FEBS Lett 326: 255-260.

Olcese R, Qin N, Schneider T, Neely A, Wei X, Stefani E, Birnbaumer L (1994) The amino terminus of a calcium channel beta subunit sets rates of channel inactivation independently of the subunit's effect on activation. Neuron 13: 1433-1438.

Page KM, Canti C, Stephens GJ, Berrow NS, Dolphin AC (1998) Identification of the amino terminus of neuronal Ca2+ channel alpha1 subunits alpha1B and alpha1E as an essential determinant of G-protein modulation. J Neurosci 18: 4815-4824.

Page KM, Stephens GJ, Berrow NS, Dolphin AC (1997) The intracellular loop between domains I and II of the B-type calcium channel confers aspects of G-protein sensitivity to the E-type calcium channel. J Neurosci 17: 1330-1338.

Pan JQ, Lipscombe D (2000) Alternative splicing in the cytoplasmic I-II loop of the N-type Ca channel a1B subunit: Functional differences are b subunit specific. J Neurosci 20: 4769-4775.

Pardo L, Ballesteros JA, Osman R, Weinstein H (1992) On the use of the transmembrane domain of bacteriorhodopsin as a template for modeling the three-dimensional structure of guanine nucleotide-binding regulatory protein-coupled receptors. Proc Nat Acad Sci 89:4009-4012.

Patil PG, Brody DL, Yue DT (1998) Preferential closed-state inactivation of neuronal calcium channels. Neuron 20: 1027-1038.

Patil PG, de Leon M, Reed RR, Dubel S, Snutch TP, Yue DT (1996) Elementary events underlying voltage-dependent G-protein inhibition of N-type calcium channels. Biophys J 71: 2509-2521.

Perez-Reyes E, Castellano A, Kim HS, Bertrand P, Baggstrom E, Lacerda AE, Wei XY, Birnbaumer L (1992) Cloning and expression of a cardiac/brain beta subunit of the L-type calcium channel. J Biol Chem 267: 1792-1797.

Perez-Reyes E, Kim HS, Lacerda AE, Horne W, Wei XY, Rampe D, Campbell KP, Brown AM, Birnbaumer L (1989) Induction of calcium currents by the expression of the alpha 1-subunit of the dihydropyridine receptor from skeletal muscle. Nature 340: 233-236.

Peterson BZ, DeMaria CD, Adelman JP, Yue DT (1999) Calmodulin is the Ca2+ sensor for Ca2+ -dependent inactivation of L-type calcium channels. Neuron 22: 549-558.

Pragnell M, De Waard M, Mori Y, Tanabe T, Snutch TP, Campbell KP (1994) Calcium channel beta-subunit binds to a conserved motif in the I-II cytoplasmic linker of the alpha 1-subunit. Nature 368: 67-70.

Qin N, Platano D, Olcese R, Costantin JL, Stefani E, Birnbaumer L (1998) Unique regulatory properties of the type 2a Ca2+ channel beta subunit caused by palmitoylation. Proc Natl Acad Sci U S A 95: 4690-4695.

Qin N, Platano D, Olcese R, Stefani E, Birnbaumer L (1997) Direct interaction of gbetagamma with a C-terminal gbetagamma-binding domain of the Ca2+ channel alpha1 subunit is responsible for channel inhibition by G protein-coupled receptors. Proc Natl Acad Sci U S A 94: 8866-8871.

Qin N, Yagel S, Momplaisir ML, Codd EE, D'Andrea MR (2002) Molecular cloning and characterization of the human voltage-gated calcium channel alpha(2)delta-4 subunit. Mol Pharmacol 62: 485-496.

Raghib A, Bertaso F, Davies A, Page KM, Meir A, Bogdanov Y, Dolphin AC (2001) Dominant-negative synthesis suppression of voltage-gated calcium channel Cav2.2 induced by truncated constructs. J Neurosci 21: 8495-8504.

Randall A, Tsien RW (1995) Pharmacological dissection of multiple types of Ca2+ channel currents in rat cerebellar granule neurons. J Neurosci 15: 2995-3012.

Restituito S, Cens T, Barrere C, Geib S, Galas S, De Waard M, Charnet P (2000) The [beta]2a subunit is a molecular groom for the Ca2+ channel inactivation gate. J Neurosci 20: 9046-9052.

Rettig J, Sheng ZH, Kim DK, Hodson CD, Snutch TP, Catterall WA (1996) Isoform-specific interaction of the alpha1A subunits of brain Ca2+ channels with the presynaptic proteins syntaxin and SNAP-25. Proc Natl Acad Sci U S A 93: 7363-7368.

Reuter H (1967) The dependence of slow inward current in Purkinje fibres on the extracellular calcium-concentration. J Physiol 192: 479-492.

Reuter H (1983) Calcium channel modulation by neurotransmitters, enzymes and drugs. Nature 301: 569-574.

Richards MW, Butcher AJ, Dolphin AC (2004) Ca2+ channel beta-subunits: structural insights AID our understanding. Trends Pharmacol Sci 25: 626-632.

Roche JP, Treistman SN (1998) The Ca2+ channel beta3 subunit differentially modulates G-protein sensitivity of alpha1A and alpha1B Ca2+ channels. J Neurosci 18: 878-886.

Rousset M, Cens T, Restituito S, Barrere C, Black JL, III, McEnery MW, Charnet P (2001) Functional roles of gamma2, gamma3 and gamma4, three new Ca2+ channel subunits, in P/Q-type Ca2+ channel expressed in Xenopus oocytes. J Physiol 532: 583-593.

Ruiz-Velasco V, Ikeda SR (2000) Multiple G-protein betagamma combinations produce voltage-dependent inhibition of N-type calcium channels in rat superior cervical ganglion neurons. J Neurosci 20: 2183-2191.

Ruth P, Rohrkasten A, Biel M, Bosse E, Regulla S, Meyer HE, Flockerzi V, Hofmann F (1989) Primary structure of the beta subunit of the DHP-sensitive calcium channel from skeletal muscle. Science 245: 1115-1118.

Sandoz G, Lopez-Gonzalez I, Grunwald D, Bichet D, Altafaj X, Weiss N, Ronjat M, Dupuis A, De Waard M (2004) Cavbeta-subunit displacement is a key step to induce the reluctant state of P/Q calcium channels by direct G protein regulation. Proc Natl Acad Sci U S A 101: 6267-6272.

Scott RH, Dolphin AC (1986) Regulation of calcium currents by a GTP analogue: potentiation of (-)-baclofen-mediated inhibition. Neurosci Lett 69: 59-64.

Sheng ZH, Rettig J, Cook T, Catterall WA (1996) Calcium-dependent interaction of N-type calcium channels with the synaptic core complex. Nature 379: 451-454.

Shi C, Soldatov NM (2002) Molecular determinants of voltage-dependent slow inactivation of the Ca2+ channel. J Biol Chem 277: 6813-6821.

Singer D, Biel M, Lotan I, Flockerzi V, Hofmann F, Dascal N (1991) The roles of the subunits in the function of the calcium channel. Science 253: 1553-1557.

Smotrys JE, Linder ME (2004) Palmitoylation of intracellular signaling proteins: regulation and function. Annu Rev Biochem 73: 559-587.

Snow BE, Krumins AM, Brothers GM, Lee SF, Wall MA, Chung S, Mangion J, Arya S, Gilman AG, Siderovski DP (1998) A G protein gamma subunit-like domain shared between RGS11 and other RGS proteins specifies binding to Gbeta5 subunits. Proc Natl Acad Sci U S A 95: 13307-13312.

Sokolov S, Weiss RG, Timin EN, Hering S (2000) Modulation of slow inactivation in class A Ca2+ channels by beta-subunits. J Physiol 527 Pt 3: 445-454.

Stanley EF (1993) Single calcium channels and acetylcholine release at a presynaptic nerve terminal. Neuron 11: 1007-1011.

Stanley EF, Atrakchi AH (1990) Calcium currents recorded from a vertebrate presynaptic nerve terminal are resistant to the dihydropyridine nifedipine. Proc Natl Acad Sci U S A 87: 9683-9687.

Stanley EF, Mirotznik RR (1997) Cleavage of syntaxin prevents G-protein regulation of presynaptic calcium channels. Nature 385: 340-343.

Stea A, Soong TW, Snutch TP (1995) Determinants of PKC-dependent modulation of a family of neuronal calcium channels. Neuron 15: 929-940.

Stephens GJ, Brice NL, Berrow NS, Dolphin AC (1998a) Facilitation of rabbit alpha1B calcium channels: involvement of endogenous Gbetagamma subunits. J Physiol 509 (Pt 1): 15-27.

Stephens GJ, Canti C, Page KM, Dolphin AC (1998b) Role of domain I of neuronal Ca2+ channel alpha1 subunits in G protein modulation. J Physiol 509 (Pt 1): 163-169.

Stephens GJ, Page KM, Bogdanov Y, Dolphin AC (2000) The alpha1B Ca2+ channel amino terminus contributes determinants for beta subunit-mediated voltage-dependent inactivation properties. J Physiol 525 Pt 2: 377-390.

Stephens GJ, Page KM, Burley JR, Berrow NS, Dolphin AC (1997) Functional expression of rat brain cloned alpha1E calcium channels in COS-7 cells. Pflugers Arch 433: 523-532.

Stephens L, Smrcka A, Cooke FT, Jackson TR, Sternweis PC, Hawkins PT (1994) A novel phosphoinositide 3 kinase activity in myeloid-derived cells is activated by G protein beta gamma subunits. Cell 77: 83-93.

Sternweis PC, Smrcka A (1992) Regulation of phospholipase C by G proteins. Trends Biochem Sci 17:502-506.

Stotz SC, Hamid J, Spaetgens RL, Jarvis SE, Zamponi GW (2000) Fast inactivation of voltage-dependent calcium channels. A hinged-lid mechanism? J Biol Chem 275: 24575-24582.

Stotz SC, Jarvis SE, Zamponi GW (2004) Functional roles of cytoplasmic loops and pore lining transmembrane helices in the voltage-dependent inactivation of HVA calcium channels. J Physiol 554: 263-273.

Strauss O, Mergler S, Wiederholt M (1997) Regulation of L-type calcium channels by protein tyrosine kinase and protein kinase C in cultured rat and human retinal pigment epithelial cells. FASEB J 11: 859-867.

Sunahara RK, Dessauer CW, Whisnant RE, Kleuss C, Gilman AG (1997) Interaction of Gsalpha with the cytosolic domains of mammalian adenylyl cyclase. J Biol Chem 272: 22265-22271.

Swartz KJ (1993) Modulation of Ca2+ channels by protein kinase C in rat central and peripheral neurons: disruption of G protein-mediated inhibition. Neuron 11: 305-320.

Swartz KJ, Merritt A, Bean BP, Lovinger DM (1993) Protein kinase C modulates glutamate receptor inhibition of Ca2+ channels and synaptic transmission. Nature 361: 165-168.

Swick AG, Janicot M, Cheneval-Kastelic T, McLenithan JC, Lane MD (1992) Promoter-cDNA-directed heterologous protein expression in Xenopus laevis oocytes. Proc Natl Acad Sci U S A 89: 1812-1816.

Takahashi M, Catterall WA (1987) Identification of an alpha subunit of dihydropyridine-sensitive brain calcium channels. Science 236: 88-91.

Takahashi T, Kajikawa Y, Tsujimoto T (1998) G-Protein-coupled modulation of presynaptic calcium currents and transmitter release by a GABAB receptor. J Neurosci 18: 3138-3146.

Tanabe T, Takeshima H, Mikami A, Flockerzi V, Takahashi H, Kangawa K, Kojima M, Matsuo H, Hirose T, Numa S (1987) Primary structure of the receptor for calcium channel blockers from skeletal muscle. Nature 328: 313-318.

Tang S, Mikala G, Bahinski A, Yatani A, Varadi G, Schwartz A (1993) Molecular localization of ion selectivity sites within the pore of a human L-type cardiac calcium channel. J Biol Chem 268: 13026-13029.

Tang WJ, Krupinski J, Gilman AG (1991) Expression and characterization of calmodulin-activated (type I) adenylylcyclase. J Biol Chem 266: 8595-8603.

Tareilus E, Roux M, Qin N, Olcese R, Zhou J, Stefani E, Birnbaumer L (1997) A Xenopus oocyte beta subunit: evidence for a role in the assembly/expression of

voltage-gated calcium channels that is separate from its role as a regulatory subunit. Proc Natl Acad Sci U S A 94: 1703-1708.

Thaler C, Gray AC, Lipscombe D (2004) Cumulative inactivation of N-type CaV2.2 Calcium channels modified by alternative splicing. Proc Nat Acad Sci 101; 5675-5679.

Thiyagarajan MM, Bigras E, Van Tol HH, Hebert TE, Evanko DS, Wedegaertner PB (2002) Activation-induced subcellular redistribution of G alpha(s) is dependent upon its unique N-terminus. Biochemistry 41: 9470-9484.

Tottene A, Moretti A, Pietrobon D (1996) Functional diversity of P-type and R-type calcium channels in rat cerebellar neurons. J Neurosci 16: 6353-6363.

Van Petegem F, Clark KA, Chatelain FC, Minor DL, Jr. (2004) Structure of a complex between a voltage-gated calcium channel beta-subunit and an alpha-subunit domain. Nature 429: 671-675.

Wakamori M, Mikala G, Mori Y (1999) Auxiliary subunits operate as a molecular switch in determining gating behaviour of the unitary N-type Ca2+ channel current in Xenopus oocytes. J Physiol 517 (Pt 3): 659-672.

Walker D, Bichet D, Geib S, Mori E, Cornet V, Snutch TP, Mori Y, De Waard M (1999) A new beta subtype-specific interaction in alpha1A subunit controls P/Q-type Ca2+ channel activation. J Biol Chem 274: 12383-12390.

Walker D, De Waard M (1998) Subunit interaction sites in voltage-dependent Ca2+ channels: role in channel function. Trends Neurosci 21: 148-154.

Wedegaertner PB, Wilson PT, Bourne HR (1995) Lipid modifications of trimeric G proteins. J Biol Chem 270: 503-506.

West JW, Patton DE, Scheuer T, Wang Y, Goldin AL, Catterall WA (1992) A cluster of hydrophobic amino acid residues required for fast Na(+)-channel inactivation. Proc Natl Acad Sci U S A 89: 10910-10914.

Westenbroek RE, Hell JW, Warner C, Dubel SJ, Snutch TP, Catterall WA (1992) Biochemical properties and subcellular distribution of an N-type calcium channel alpha 1 subunit. Neuron 9: 1099-1115.

Westenbroek RE, Sakurai T, Elliott EM, Hell JW, Starr TV, Snutch TP, Catterall WA (1995) Immunochemical identification and subcellular distribution of the alpha 1A subunits of brain calcium channels. J Neurosci 15: 6403-6418.

Wheeler DB, Randall A, Tsien RW (1994) Roles of N-type and Q-type Ca2+ channels in supporting hippocampal synaptic transmission. Science 264: 107-111.

Williams SR, Toth TI, Turner JP, Hughes SW, Crunelli V (1997) The 'window' component of the low threshold Ca2+ current produces input signal amplification and bistability in cat and rat thalamocortical neurones. J Physiol 505 (Pt 3): 689-705.

Witcher DR, De Waard M, Sakamoto J, Franzini-Armstrong C, Pragnell M, Kahl SD, Campbell KP (1993) Subunit identification and reconstitution of the N-type Ca2+ channel complex purified from brain. Science 261: 486-489.

Wu L, Bauer CS, Zhen XG, Xie C, Yang J (2002) Dual regulation of voltage-gated calcium channels by PtdIns(4,5)P2. Nature 419: 947-952.

Yassin M, Zong S, Tanabe T (1996) G-protein modulation of neuronal class E (alpha 1E) calcium channel expressed in GH3 cells. Biochem Biophys Res Commun 220: 453-458.

Yasui B, Fuchs F, Briggs FN (1968) The role of the sulfhydryl groups of tropomyosin and troponin in the calcium control of actomyosin contractility. J Biol Chem 243: 735-742.

Yokoyama CT, Sheng ZH, Catterall WA (1997) Phosphorylation of the synaptic protein interaction site on N-type calcium channels inhibits interactions with SNARE proteins. J Neurosci 17: 6929-6938.

Zamponi GW, Bourinet E, Nelson D, Nargeot J, Snutch TP (1997) Crosstalk between G proteins and protein kinase C mediated by the calcium channel alpha1 subunit. Nature 385: 442-446.

Zamponi GW, Snutch TP (1998) Decay of prepulse facilitation of N type calcium channels during G protein inhibition is consistent with binding of a single Gbeta subunit. Proc Natl Acad Sci U S A 95: 4035-4039.

Zhang H, He C, Yan X, Mirshahi T, Logothetis DE (1999) Activation of inwardly rectifying K+ channels by distinct PtdIns(4,5)P2 interactions. Nat Cell Biol 1: 183-188.

Zhang JF, Ellinor PT, Aldrich RW, Tsien RW (1994) Molecular determinants of voltage-dependent inactivation in calcium channels. Nature 372: 97-100.

Zhang JF, Ellinor PT, Aldrich RW, Tsien RW (1996) Multiple structural elements in voltage-dependent Ca2+ channels support their inhibition by G proteins. Neuron 17: 991-1003.

Appendix

Methods

Oocytes were injected with the following combinations of cDNA:

Wild type $Ca_V2.2$, β_1b, $\alpha_2\delta$-2

Palmitoylation motif $Ca_V2.2$, β_1b, $\alpha_2\delta$-2

Mutated palmitoylation motif $Ca_V2.2$, β_1b, $\alpha_2\delta$-2

Wild type $Ca_V2.2$, β_2a, $\alpha_2\delta$-2

Concentrations and ratios of subunits were as in the Methods section of this thesis.

Injected cells were used immediately in metabolic labelling experiments.

Metabolic labelling

L-^{35}S Met/Cys

Batches of 20 oocytes were injected with one of the cDNA combinations shown above and then incubated for 24 hours at 18°C in 995µl ND96 and 5µl PRO-MIX (L-^{35}S Met/Cys 1000Ci/mmol, 10mCi/ml, Amersham, UK). This yielded a final radioactive concentration of 50µCi/ml.

[^{3}H] palmitic acid

Batches of 20 oocytes were injected with one of the cDNA combinations as above were incubated for 18hrs @ 18°C in ND96 buffer and then for a further 6 hours in 0.6ml 2mCi/ml [^{3}H] palmitic acid. This solution was made from a [^{3}H]

palmitic acid stock, (48Ci/mmol, 1mCi/ml in 5ml ethanol (GE Healthcare, UK). The ethanol was removed by evaporation under nitrogen gas and the resultant solid palmitic acid was re-dissolved in 125µl 100% ethanol and made up to 2.5ml with ND96. This yielded a final radioactive concentration of 2mCi/ml and 5% (v/v) ethanol.

Immunoprecipitation

Each batch of 20 oocytes were washed with phosphate buffered saline (PBS, Sigma, UK) and re-suspended in 1ml RIPA buffer (50mM Tris, pH8.0, 150mM NaCl, 5mM EDTA, 1% Igepal, 0.25% deoxycholic acid, 0.1% SDS (all Sigma-Aldrich), and Incomplete Protease Inhibitor Cocktail (1 tablet per 50ml buffer, Roche Mannheim, Germany). Oocytes were lysed by up and down passage through a pipette tip and sonicated in a bath sonicator for 2 mins. Samples were centrifuged twice at 12000 x *g* for 10 mins at 4°C and the supernatant transferred to fresh tubes to which the relevant antibodies were added. 20µl of $Ca_V2.2$ I-II loop antibody (500µg/ml) (Raghib et al., 2001) was added to all samples not containing β_2a. To the samples containing β_2a, 25µl of β_2a antibody (400µg/ml). To each tube 25µl protein G-sepharose (a 50% slurry pre-equilibrated with RIPA buffer) was added and they were incubated at 4°C overnight with constant mixing. Beads were washed three times with 1ml RIPA buffer and immunocomplexes were eluted from the sepharose beads in 30µl SDS-PAGE sample buffer (Sigma-Aldrich). Samples were cenrifuged (1000 x *g*, 2mins) to pellet the sepharose beads and then 30µl of each sample was electrophoresed on 3-8% Tris-acetate gels, one for the L-^{35}S Met/Cys and one for the

[^{3}H] palmitic acid. Markers used were Trichrome Ranger markers (Perbio, Cheshire, UK).

The proteins were fixed in the gels by incubation for 30 mins in isopropanol:water:acetic acid 25:65:10, and rinsed with water twice. For the detection [^{3}H] palmitic acid incorporation, the gels were incubated for 30 mins in Amplify reagent (GE Healthcare). Gels were mounted onto filter paper, overlaid with Saran wrap and dried under vacuum for 2 hours at 80°C. The Saran wrap was removed and the gels were mounted on a sheet of hyperfilm (GE Healthcare) in a film cassette. The hyperfilm for the [^{3}H] palmitic acid gel was preflashed to increase sensitivity (Laskey and Mills, 1975). The gels were then placed at -70°C for either 72 hours (L-^{35}S Met/Cys) or 3 weeks ([^{3}H] palmitic acid).

The films were then developed using an automated film developer.

Results

Incorporation of [^{35}S] Met/Cys

In each lane there was a doublet band representing $Ca_V2.2$ (Figure A1*A*). There was no band in the β_{2a} lane at 55kDa, where we would expect β_{2a} to be. This suggests either that the oocytes did not express β_{2a}, or that β_{2a} was not efficiently immunoprecipitated with the β_{2a} antibody.

Incorporation of [^{3}H] palmitic acid

There were no bands corresponding in size to α_1B detected in any lanes (Figure A1*B*). This may be due to the lack of palmitoylation of the palmitoylation motif $Ca_V2.2$, or due to the poor incorporation [^{3}H] palmitic acid. Without the confirmation of the [^{3}H] palmitic acid labelling of the β_{2a}, which is known to be palmitoylated in oocytes, then it is impossible to say whether this result is because the palmitoylation motif $Ca_V2.2$ is not palmitoylated or because the labelling conditions were not adequate to identify protein palmitoylation.

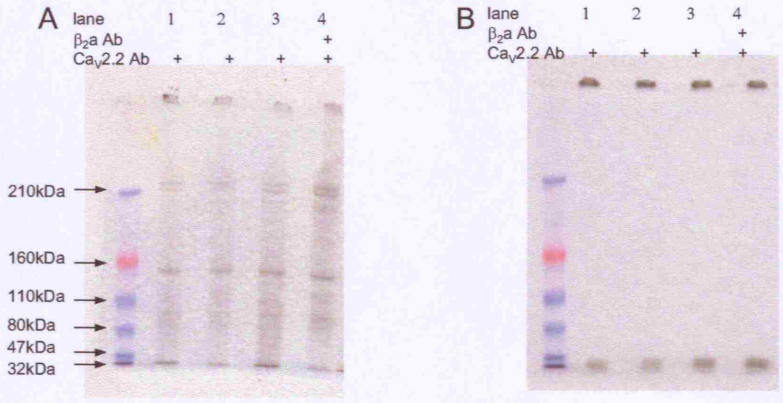

Figure A1. Autoradiography of immunoprecipitated, labelled proteins. ***A*** Proteins labelled with L-^{35}S Met/Cys. Lane 1: wild type $Ca_V2.2$ and β_2a, lane 2: palmitoylation motif $Ca_V2.2$ and β_1b, lane 3 mutated palmitoylation motif $Ca_V2.2$ and β_1b, lane 4: wild type $Ca_V2.2$ and β_2a. Band around 200kDa represents $Ca_V2.2$ (indicated by arrow). ***B*** No visible bands labelled with [^{3}H] palmitic acid.